Introduction of PEM Fuel Cells on Inland Ships

Gert-Jan Nuij

TU Delft Delft University of Technology

Report: SDPO.21.001.m

Thesis for the degree of MSc in Marine Technology in the specialization of Ship Design

Introduction of PEM Fuel Cells on Inland Ships

By

Gert-Jan Nuij

Performed at

Delft University of Technology

This thesis (SDPO.21.001.m) is classified as non-confidential in accordance with the general conditions for projects performed by the TUDelft

February 23, 2021

Supervisors

Responsible supervisor: Dr.Ir. R. G. Hekkenberg

E-mail: R.G.Hekkenberg@tudelft.nl

Thesis exam committee

Chair/Responsible Professor: Dr.Ir. R. G. Hekkenberg

Staff Member: Dr.Ir. L. van Biert

Staff Member: Dr. V. Reppa

Author Details

Studynumber: 4396316

E-mail: gjn.ducinaltum@gmail.com

An electronic version of this thesis is available at *http://repository.tudelft.nl/*.

Summary

When emission regulations become more strict for ships, the demand for alternative fuels rises. These regulations apply to inland shipping as well. In 2050, the CCNR wants to have an emission-free inland shipping sector. This prospect suggests looking at fuel options with zero emissions. One of these options is hydrogen. However, storing hydrogen might impose issues on an inland ship regarding space requirements. A sea-going ship can be adjusted freely in its dimensions to provide extra space for the hydrogen storage. Inland ships are bound to the restrictions of the inland waterways. Therefore, the solution for the inland ship is not the same as the sea-going vessel. The new space requirements impose issues on the inland ship design. These issues could change the total cost and the earning potential of the inland ship. Also, the conventional engine cannot run on hydrogen. Therefore, this Thesis investigates the inland ship's performance when outfitted with a PEM fuel cell system running on hydrogen.

Research Question

The research goal is to study inland ships with a PEM fuel cell (FC) system running on hydrogen. This system will affect the design and performance in the required freight rate (RFR). The hydrogen storage density is lower than the diesel density, but its energy density is higher. These characteristics increase the fuel tank size, which creates a challenge fitting such a tank on an inland ship. The design is affected, which results in a different total cost and cargo space capacity. The following research question is created based on these challenges:

- ***How does an inland ship with a PEM FC system running on hydrogen perform in terms of the required freight rate?***

Several aspects need to be identified to evaluate the question. The inland ship's power needs to be determined in its environmental condition, which is shallow water. The PEM fuel cell supplies this power, which has a specific system behaviour. The inland ship design needs to be adjusted to fit the new components. Based on these aspects, these sub-questions have been established:

1. What is the resistance of inland ships in shallow water?
Inland ships operate in shallow waters. In these water depths the resistance and the power demand rises. It is important to include these conditions in the calculations.

2. What does the system efficiency of a PEM FC look like?
The PEM FC system efficiency has a different trend than a diesel engine. The PEM FC has a high efficiency at a low power load and it decreases for higher power loads. It is important to include this behaviour to determine the hydrogen fuel consumption.

3. What circumstances define the sections of the cases in ship speed and water depth?
The inland ship performance is determined for a general approach and two cases. The general approach will determine the relations of the new system with respect to the ship speed and range. This knowledge will help evaluate two cases.

4. Which design implications are imposed on the inland ships by the PEM FC system and different hydrogen storage systems?
The hydrogen storage is voluminous. This aspect changes the inland ship design. The new system requires more components and they replace a few others from the conventional design. Therefore, the design is adjusted to cope with the new weights and volumes.

5. What are the cargo space losses and costs of the inland ships?
The previous considerations are combined to determine the cargo capacity losses and the total cost of the PEM FC inland ships. The new cargo capacity and total cost will provide the information to calculate the performance in terms of the required freight rate.

This research performs its calculations in Matlab. It only considers PEM FC systems. The liquid and compressed hydrogen storage are considered. The three different inland ships considered are dry bulk inland ships sailing at design draught in shallow water.

Calculation Model

The calculation model is divided into several sections to answer the sub-questions and the research question. The first section handles the resistance calculations. The inland ships considered are 85, 110, and 135-meter long ships. The deep water resistance is calculated with Holtrop & Mennen (1982). The shallow water resistance is determined with the method proposed by Karpov. The large-bladed propellers considered for the inland ships are three from the Wageningen B-series and four from the Kaplan-series.

The second part is the combination of the shallow water model and the propeller model. The ship speed, shallow water resistance, and propulsion efficiency lead to the inland ship's propulsion power. The propulsion power divided by a transmission and electric motor efficiency each of 95% results in the PEM FC's brake power.

The third section contains the fuel cell model to determine the system efficiency of the fuel cell. The cell in the PEM FC system has three types of losses: the activation, ohmic, and mass concentration loss. The cell potential and these losses result in the cell voltage. Combining multiple cells results in the stack power. The stack is conditioned by auxiliary systems to stop it from degenerating. Subtracting these system's power from the stack power results in the net power and system efficiency. Combining multiple stacks covers the ship's brake power.

The fourth part combines the previous sections. A general overview and two cases are calculated. The overview is a evaluation of the PEM FC inland ships with a set of ship speeds and ranges on a fixed water depth. The two cases are a short trip of 466 km, and a long trip of 1686 km. The trips consist of multiple sections, each having its current and water depth. The calculation is performed in low and high water depths. The installed power is increased to raise the system efficiency, decrease fuel consumption, and save costs during the trips. The hydrogen storage size is large due to the trip's range. The refuelling frequency is increased to decrease the hydrogen storage size and save costs.

Design Implications

Designing inland ships with a PEM FC system with hydrogen imposes issues regarding cost, design, and regulation. A cost overview is established to calculate the investment cost and operational cost. Furthermore, a factor is calculated accounting for the hydrogen storage types, because of casing, insulation material, and shape. The design assumptions for the bulk carrier and the container carrier are different. The required fuel storage space for the bulk carrier is subtracted from the cargo hold. For a container carrier, one TEU is subtracted from the capacity every time the hydrogen storage exceeds one TEU's volume.

The regulation, regarding the use of fuel hydrogen, is not yet finished. Therefore, assumptions are made based on the statement that hydrogen fuel regulation should be as strict as LNG fuel regulation (Tronstad, Åstrand, Haugom, & Langfeldt, 2017). This statement has led to assuming that both storage options can be stored in the cargo hold, below deck separated from the engine room and cargo. Three design option are considered, from which one is chosen that carries out the design assumptions. A design is chosen with all new components in the foreship and the crew residence in the foreship moved to the aftship. This design includes extra fuel storage on deck in the foreship. First, the tanks on deck are used for hydrogen storage and afterwards volume from the cargo hold.

Results

Now the calculation model is applied to the design assumptions. The general overview shows the liquid and compressed hydrogen storage being around five and nine times higher than diesel storage. It shows that hydrogen has a significant impact on the volumetric capacity, but tonnage capacity as well. Applying the costs shows that the PEM FC inland ship has a larger investment cost than the conventional inland ship without considering the expensive hydrogen storage. Also, operational costs are higher than conventional inland ships. Combining the higher cost and tonnage loss showed that the ship's RFR is higher than the conventional ship. The combination results in a low optimal ship speed around 10 km/h, lower than a conventional ship. The ship speed has a large effect on the RFR due to the strong relationship with fuel consumption, while the range's impact is small. The hydrogen fuel price has a significant influence on the RFR. Higher prices lead to lower optimal ship speeds and vice versa.

The cases show room for improving the inland ship's RFR. Increasing the installed power and refuelling frequency both show promise in reducing the RFR. The inland ships sailing the short trip obtain the optimal refuelling frequency earlier compared to the long ones. When the inland ship is built for short trips the new system does not influence the design as much as it would for inland ships fit for long trajectories.

Conclusion & Recommendation

The conclusions drawn from the calculations show several items. Liquid hydrogen displays a better performance for inland ships than compressed hydrogen. The difference in performance becomes small when their storage costs become similar. The hydrogen price has a significant impact on the RFR because fuel cost is a large cost component. The optimal ship speed for the PEM FC ships is low. These speeds are not available sailing upstream because strong currents result in extensive cargo delivery times. The trip case evaluation shows a reduction in the RFR for increasing the installed power and refuelling frequency. Increasing the frequency shows values for the RFR of the liquid and compressed hydrogen options close to each other. The storage types become similar in size, decreasing the differences in cost and size. Still, liquid hydrogen remains the better option.

This research recommends looking into several other aspects. Only two hydrogen storage options are considered, while others might be a better option. Designing inland ships with the PEM FC system can be performed more thoroughly to create better design assumptions. This approach could decrease the new system's influence. The shallow water is included only influencing the resistance and shipapeed. However, it also affects the inland ship's draught. The last aspect is to look into other inland ship dimensions and types because only a part of the spectrum is considered here.

Contents

List of Figures

List of Tables

List of Symbols

Physics Symbols Ship

$1 + k_1$ Form factor ship

ΔC_r Change in Residual Resistance coefficient due to river/channel dimensions

η_H Hull efficiency

η_O Open-water efficiency

η_R Relative Rotative efficiency

η_{EM} Electric motor efficiency

η_{TRM} Transmission efficiency

ρ_w Fresh water density of 1000 kg/m^3

a^* Correction factor for the ship speed in shallow water (Frictional Resistance)

a^{**} Correction factor for the ship speed in shallow water (Residual Resistance)

C_A Model-Ship Correlation Resistance coefficient

C_F Frictional Resistance coefficient

C_r Residual Resistance coefficient

C_{stern} Stern coefficient of ship

$f_{V,comp}$ Volume fraction of compressed hydrogen storage

$f_{V,liquid}$ Volume fraction of liquid hydrogen storage

Fr Froude number

Fr_h Froude depth number

n_{prop} Number of propellers

P/D Pitch over Diameter ratio of propeller

P_B Brake Power of ship

P_D Propulsion Power of ship

R_A Model-Ship Correlation Resistance

R_B Added Resistance of Bulb

R_F Frictional Resistance

R_W Wave Resistance

R_{App} Frictional Resistance of Appendages

$R_{shallow}$ Shallow Water Resistance

R_{total} Total Ship Resistance

R_{TR} Transom Resistance

v_1 Adjusted Ship speed for frictional resistance in shallow water

v_2 Adjusted Ship speed for residual resistance in shallow water

V_{box} Volume of rectangular box shape where hydrogen tank could reside

V_{fuel} Volume of fuel on board of ship

S Wetted area of ship

Physics Symbols Fuel Cell

α_a Transfer coefficient anode

α_c Transfer coefficient cathode

ΔG^0 Gibbs free energy of reaction in fuel cell

$\dot{m}_{H_2}$ Mass flow of hydrogen fuel

$\dot{V}_{air}$ Air flow

η Efficiency

a_a Activity of gas at anode

a_c Activity of gas at cathode

A_{cell} Area of cell

E Fuel cell potential at operating conditions

E^0 Ideal fuel cell potential

F Faraday's constant

f_{comp} Factor for compressor power calculation

H_2 Hydrogen

i Current density

$i_{0,a}$ Exchange current density of anode

$i_{0,c}$ Exchange current density of cathode

i_{lim} Limiting current density

i_{loss} Current density loss

LHV_{H_2} Lower Heating Value of hydrogen

N_{cell} Number of cells per stack

O_2 Oxygen

p_{drop} Pressure drop

p_{H_2} Partial pressure of hydrogen

p_{O_2} Partial pressure of oxygen

R Universal gas constant

r_{el} Electronic resistance of cell

r_{ion} Ionic resistance of cell

T_{amb} Ambient temperature

T_{FC} Operating temperature of PEM FC

V_{act} Activation voltage loss of cell

V_{conc} Mass concentration voltage loss of cell

V_{ohmic} Ohmic voltage loss of cell

Other Symbols

h_w Water depth

B Breadth

DE Diesel Engine

EM Electric Motor

ER Engine Room

FC Fuel Cell

GA General Arrangement

HW High water

L Length

LNG Liquid Natural Gas

LT Low Temperature

LW Low Water

O&M Operation & Maintenance

P Power

PEM Polymer Electrolyte Membrane or Proton-Exchange Membrane

RFR Required Freight Rate

T Draught

TEU Twenty Foot Equivalent container

Chapter 1

Introducion

1.1 Background

The International Maritime Organisation (IMO) wants to reduce all greenhouse gas (GHG) emissions produced by the maritime industry by 50% in 2050 (IMO, 2019). The Central Commission of the Navigation of the Rhine (CCNR) is taking the IMO guidelines to the next level by setting the goal to eliminate GHG and local emissions in inland shipping by 2050 (CCNR, 2019). This goal requires alternative fuels since conventional marine gas oil will not suffice with these new regulations. At the moment, new build inland ships need to comply with the stage V regulation. This regulation enforces a steep reduction in the inland ship's local emissions. It forces the industry to look at other options than conventional diesel engines. Stage V regulation does not enforce a limit on greenhouse gasses (GHGs). The new systems within stage V limits sometimes reduce GHG emissions. However, this reduction is not significant. In the end, the shipowners need to take a step towards a fuel that emits zero emissions. Future inland ships have to adjust to comply with the new GHG emission goals of the CCNR. Therefore, it is decided to look at a fuel that has no harmful emissions. Few fuels remain an option for ships if harmful emissions are not permitted. These options are batteries, hydrogen, ammonia, and nuclear fuel. Nuclear fuel is has a very high density, but it requires extreme safety measures and techniques for someone to employ it on an inland ship. Batteries as the primary energy source would need a lot of space to store it due to a low volumetric energy density. It will also be heavy, which harms the tonnage capacity of inland ships. The harmful emissions are zero when one feds ammonia to a fuel cell. Ammonia itself is very toxic and should be stored carefully. Pure hydrogen as a fuel in a modified internal combustion engine or a fuel cell has the benefit to emit water, which is not a harmful substance to emit. However, it is very voluminous, even in their storage units.

These new fuels might impose difficulties regarding the design of inland ships. Generally, alternative fuels and their storage systems are more voluminous and or weigh more. These characteristics create issues for inland ship design. Inland ships tend to require as much space as possible for carrying cargo within their limits of the inland rivers. The solution for a sea-going ship might not be the same as for an inland ship. A sea-going ship can often be designed with a greater length to have more space available for the lesser power-dense alternative fuel system, but this does not hold for an inland ship. The design restriction of an inland ship arises from the characteristics of the inland waterways. It will affect the cargo capacity rather than the overall ship dimensions. Research is key to check the implications the new system can have on the ship design. The new system will have different characteristics of weight and volume. The hydrogen storage is also voluminous and has a certain weight to it. The difference in volume and weight requirement between the conventional and new system can result in cargo capacity reductions. This reduction impacts earning potential. Aside from the cargo capacity

reductions, the new system and fuel will cost more than the conventional arrangement. This cost increase and cargo capacity reduction mean that the inland ship has to earn more per ton of cargo transported per kilometre sailed. Therefore, the research needs to investigate the inland ship sailing on hydrogen.

1.2 Research gap

Several similar types of research have been conducted around the subject of hydrogen fuel and inland ships. Panteia (2019) researched the transition from conventional to alternative fuels for inland ships in short-, mid- and long-term. They looked into several alternative fuels such as biofuels, diesel-electric, battery-electric, and hydrogen-electric. They concluded that the hydrogen-electric drive is the best option as inland ship fuel from a long-term perspective. However, this research did not go in great depth on the inland ship's performance with hydrogen concerning design or earning potential. Biert, Godjevac, Visser & Purushothaman Vellayani (2016) wrote a review article regarding a review of fuel cell systems for maritime applications. The conclusion from Biert et al. (2016) shows that a LT-PEM FC system with cryogenic stored hydrogen can be the most compact system overall. This system could be compact when decreasing the refuelling interval time, so increasing the bunker frequency. This relevant trade-off comes to mind here, and this Thesis should address it. There exist a gap looking at these two pieces of research. It showed that hydrogen could be a proper solution in the long-term transition to alternative fuels. It did not look into adjusting the ship design and how hydrogen impacts the earning potential in greater depth. Also, the specific application of the LT-PEM FC on inland ships is yet to be investigated. This research will go into the direction of inland ships with a LT-PEM FC system with hydrogen fuel based on these gaps found.

1.3 Research Question

The research goal is to study inland ships with Low-Temperature (LT) PEM fuel cells (FCs) running on hydrogen fuel. This new system will affect the design, and impact the inland ship performance in their required freight rate. Hydrogen has a low density in its gas form under standard conditions. Therefore, the industry uses different storage techniques to increase this density. Still, the fuel remains low in density compared to diesel. It does have a higher energy density compared to diesel. These two characteristics result in a different volume of consumed fuel compared to diesel. Inland ships cannot be changed freely in their dimensions, because of the inland waterway restrictions. Therefore, it becomes a challenge to fit the low-density hydrogen on board of the ship. The conventional design needs to be adjusted for hydrogen fuel. There exist a triangular relation between the ship speed, ship range, and cargo capacity for a ship sailing on hydrogen fuel. This research will address this relation. This relation will result in the required freight rate of the inland ships. This research also explores how one could save costs because of the voluminous characteristic and high fuel price of hydrogen. It is known that the efficiency of a PEM FC system is high in low power load conditions. It will be evaluated if installing more power could reduce the power load far enough to increase efficiency. The fuel consumption reduces when the PEM FC efficiency increases. Lower fuel consumption results in less stored fuel but installing more power results in more costs. The refuelling frequency is also a variable capable of saving costs for the PEM FC ship. Biert et al. (2016) mentioned the importance of this variable. If the ship is refuelled more often, the expensive, heavy, and voluminous hydrogen tanks can become smaller. However, this increase results in larger trip completion times for the inland ship. This Thesis will investigate these two cost-saving methods.

The following research question is created based on the challenges of this research:

- ***How does an inland ship with a PEM FC system running on hydrogen perform in terms of the required freight rate?***

This research needs to identify several aspects before it can answer the research question. The inland ships operate in shallow water, and in these conditions the resistance increases. This aspect results in more significant power demands by the ship. The power supply comes from a PEM FC system. This system behaves differently from a diesel engine. Therefore, this research includes this behaviour to calculate fuel consumption. Ship speed and range calculations will explain more on the general characteristics of the PEM FC inland ship. This research uses a case to evaluate how design considerations can reduce the total cost. Some design assumptions have to be established to combine these aspects with inland ships. As mentioned earlier, the inland ship cannot just become slightly larger. Therefore, some design considerations have to be evaluated. This process of calculations is translated into a calculation model. The calculation model can determine the results based on the input. This process is displayed in figure 1.1. This figure shows how this Thesis is built up and how it will reach the research question's answer. This research has to make a resistance approximation for the inland ships. This approximation makes it possible to determine the inland ship's propeller and power demand for different ship speeds. The PEM FC model will provide the inland ship's power. One can calculate the power load on the PEM FC based on the installed power and ship speed. This power load is needed to calculate the fuel consumption. Different design assumptions need to be included to evaluate how the PEM FC system impacts the design. The fuel consumption leads a hydrogen tank size which needs to fit on the ships. Other components will be outfitted on the inland ships as well. All PEM FC components make the ship heavier, and they are voluminous. Therefore, these components will decrease the cargo capacity of inland ships. The following sub-questions are set-up based on this process:

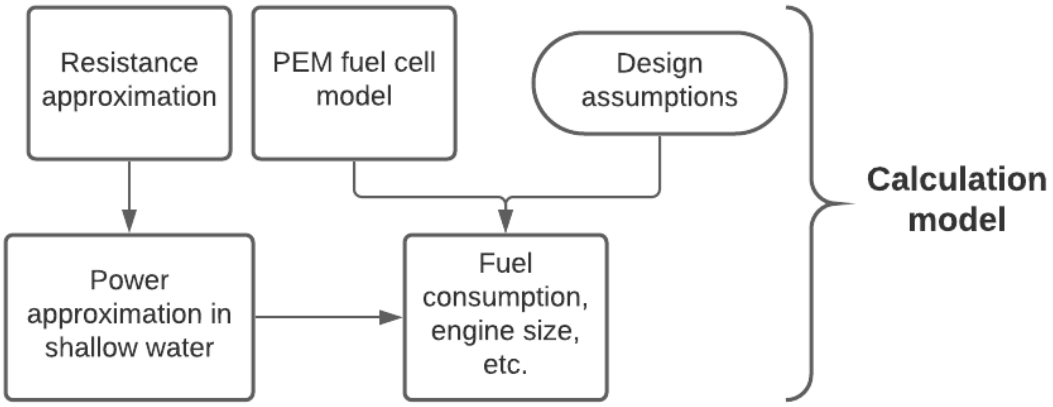

Figure 1.1: The calculation process

1. ***What is the resistance of inland ships in shallow water?***
   Inland ships operate in a challenging environment where the cargo has to be shipped as fast and inexpensive as possible. However, shallow water poses a problem to both desires, because it can limit the cargo carried and limit the ship speed. It is believed that the maximum power demands occur in fully loaded condition with limited water clearance below the ships. Therefore water depths that do not allow fully loaded conditions are not evaluated. The shallow water performance will provide the information to compute the installed power and the power demand under certain conditions. The shallow water calculations will provide the information to determine hydrogen fuel consumption and the

PEM FC size.

2. ***What does the system efficiency of a Low-Temperature Proton-Exchange Membrane Fuel Cell look like?***
   The PEM FC will provide the power supply. The system efficiency behaviour of the PEM FC is different from that of a conventional diesel engine. The PEM FC behaviour has to be evaluated and taken into consideration in the design of inland ships. This evaluation provides the PEM FC's system efficiency, which will be needed to calculate the hydrogen fuel consumption. This information will give an elaboration on the optimal operating conditions of the PEM FC.

3. ***What circumstances define the sections of the cases in ship speed and water depth?***
   This research will formulate a general approach and two cases to evaluate the inland ship's performance. This research performs calculations to determine the triangular relation of the PEM FC system. This relation exists between the ship speed, range and cargo capacity. It can show the link to performance indicators such as fuel consumption, hydrogen storage size, cargo capacity loss, total cost, and the required freight rate. The circumstances in these calculations are several ship speeds and ranges on a fixed water depth. This research will formulate two cases based on river data. The circumstances in these cases will vary. The cases consist of sections, and each section has its water current and water depth. The ship speed varies along the sections depending on the water current and water depth. The two cases consist of a short and long trip. The short trip is approximately 466 kilometres long and the long one around 1686 kilometres long. The same performance indicators from the general approach are used to evaluate the cases.

4. ***Which design implications are imposed on the inland ships by the PEM FC system and different hydrogen storage systems?***
   The behaviour of the PEM FC is not the only aspect that the design needs to consider. The storage of hydrogen fuel imposes some challenges in the design of the inland ship. The hydrogen fuel is known to be very light and voluminous, and techniques are used to increase the hydrogen storage density. In this research liquid hydrogen and hydrogen under a pressure of 700 bar are considered possible storage options onboard of inland ships. The PEM FC itself uses quite a lot of space, because of the auxiliary equipment that is needed to run the engine smoothly. With the PEM FC system, the design should include electric motor(s) (EMs) and batteries as well. The PEM FC and the hydrogen fuel characteristics have to be dealt with in the design to evaluate the ship's performance properly.

5. ***What are the cargo space losses and costs of the inland ships?***
   The answers to the previous questions have to be combined to evaluate the triangular relation. The new cargo capacity of the inland ship will be a function of the ship speed and range. The ship speed and range will determine the amount of hydrogen fuel and the new system components' sizes. The cargo capacity can be calculated based on the design assumptions, the weights and the volumes of the new system components. These new components also determine the total cost's magnitude. The cargo capacity, total cost and ship range together will result in the required freight rate. Afterwards, this research can evaluate the inland ship's performance.

1.4 Methodology and Scope

The method that is used in this research is to perform calculations based on theories and approximation methods. This research performs the calculations in MATLAB. Based on other

research, these theories and approximation methods are used to determine the different parts of the research goal. The outcomes of these theories and approximation methods are verified and validated with data from research and data from practice to make this a quantitative study.

The focus of this research is to determine the influence the proposed system has on inland ships. Several subjects are in-and outside of the scope of this research, which are:

- Only the LT PEM FC system is considered as the energy provider of the inland ships. This research does not evaluate other types of FC systems.
- Two hydrogen storage options are taken into account: liquid hydrogen and compressed hydrogen under 700 bar. Other storage options are not considered, such as 350 bar pressurized hydrogen or solids. This research examines liquid and 700 bar compressed hydrogen because they significantly increase the hydrogen density.
- The shallow water limitations are bound to limit the speed, not the total cargo carried by ship. The cases studied include water depths large enough to enable the inland ships to sail in full cargo load conditions.
- The trips consist of different sections. For each section, the bottom of the river is assumed even.
- In this research, three different inland ships are modelled, and two inland ship types are evaluated. The three ships have the following length, width, and draught (L x B x T):
  - Ship 1: 85 $\times$ 9.5 $\times$ 3.0 metre
  - Ship 2: 110 $\times$ 11.45 $\times$ 3.6 metre
  - Ship 3: 135 $\times$ 11.45 $\times$ 3.6 metre

  These three ships cover most of the fleet. Bulk and container carrying inland ships are taken into consideration since these two types are considered dry bulk carriers and cover most of the dutch fleet (IVR, 2018).

1.5 Structure

The report structure is outlined as follows. The second chapter of the report describes the calculation model. The methodology is translated into this calculation model to obtain the goal of this research. The calculation model consists of a few model parts. These parts are:

- A model of the deepwater ship resistance approximation.
- A model for the determination of the propeller and its characteristics.
- A model to predict the power demand in shallow water.
- A model to determine the system efficiency of a PEM FC.
- The main model in which the trip conditions and design assumptions are given. This model uses the other model parts to determine the performance indicators.

The third chapter describes the design implications the PEM FC and hydrogen storage system have on the ship. The cost of the new system and the conventional system are given in an overview. The chapter will describe how they are applied to the model. Furthermore, it will discuss how the loss of cargo space comes about. This aspect requires a description of the design assumption and an evaluation of how the new system would fit properly on the inland ships.

Chapter 4 and 5 contain the results obtained from applying the case descriptions on the calculation model and design assumptions. Chapter 4 discusses the general relations of the PEM FC inland ships and 5 the case results. The final chapter gives the conclusion and recommendation of this research.

Chapter 2

Calculation model

This chapter elaborates on the calculation model that will calculate the performance indicators of the inland ships. The model consists of several sub-models as figure 1.1 displays. The first paragraph describes the first sub-model, which contains the resistance and propeller calculations. The resistance model is determined for deepwater and for shallow water conditions. Afterwards, the propeller model determines the propeller type fit for each inland ship. The second paragraph describes the power prediction of the inland ships. In the third section, the calculation model for the PEM fuel cell (FC) is established and evaluated. The fourth section contains the trip model. This paragraph explains the general model and two cases. The two different trips are created to be able to determine power demands during the different sections. Together with all the model parts, the entire calculation model can be finalised. The calculation model will then be able to evaluate the inland ships with PEM FC systems.

2.1 Resistance & Propeller model

In this paragraph, the model for the deepwater, shallow water and the propeller is determined. Each sub-model is verified and validated.

2.1.1 Deep water resistance

Model

A prediction method for the deepwater ship resistance is chosen to make a resistance approximation of the inland ships. This research uses this prediction to determine a load which the propeller should be able to handle. The deepwater resistance approximation also forms the basis of the shallow water resistance calculation. It is chosen to do this calculation for deepwater instead of the shallow because it is believed a higher speed in deepwater will provide a sufficient load on the propeller. This way the propeller performance will not fall behind in shallow water. In this Thesis, the method of Holtrop & Mennen (1982) is used for deepwater resistance. This method is well known and able to make a good approximation of the resistance in deep water. It is also used for inland ship research which has been seen in a paper by Hekkenberg, Dorsser and Scheighofer (2017) about modelling sailing time and cost of inland ships. Although inland ships have high block coefficients that lie at the end of the ship spectrum for Holtrop & Mennen, the method still predicts a fairly good resistance. As it is common in practice, this research will approximate the resistance in deep water first. Afterwards, the resistance is corrected for the waterway conditions (Hekkenberg, Dorsser, & Schweighofer, 2017).

The individual components have to be determined to determine the total resistance as is

displayed in equation 2.1.

$$R_{total} = (1 + k_1) \cdot R_F + R_{App} + R_W + R_B + R_{TR} + R_A \tag{2.1}$$

R_F is the frictional resistance, displayed in equation 2.2, and it is multiplied with the form factor of the ship. S is the water surface of the ship, ρ_w the water density of the river, C_F the frictional coefficient, and v_{ship} the ship speed relative to the water.

$$R_F = 0.5\rho_w S \cdot C_F \cdot v_{ship}^2 \tag{2.2}$$

R_{App} is the additional frictional resistance created by the appendages. The rudders, propeller shaft(s) and the bow thruster openings are considered for the appendages resistance. R_W is the wave-making and breaking resistance of the ship. This Thesis further addresses it as wave resistance. R_B is the additional resistance created by the bulb of the ship. This resistance component is zero for the inland ship since a bulb is not present on inland ships. R_{TR} is the additional pressure resistance of the immersed transom and the R_A is the model-ship correlation resistance. The model-ship correlation resistance, the appendage resistance, and the transom resistance are calculated similarly as the frictional coefficient. The frictional coefficient is replaced with the respective coefficients of those resistances.

Table 2.1 shows the parameters needed for the resistance approximation. These input values are required to use the Holtrop & Mennen method (1982).

Parameter	**Ship 1**	**Ship 2**	**Ship 3**	**Unit**
Length	86	110	135	m
Width	9.5	11.45	11.45	m
Draught	3.0	3.6	3.6	m
Displacement	2150	4050	4990	m^3
Propeller diameter	1.4	1.85	1.7	m
Transom area (immersed)	3.0	5.0	5.0	m^2
Bilge radius	0.5	0.5	0.5	m
Waterplane coefficient	0.92	0.93	0.93	-
Center of buoyancy forward of $\frac{1}{2}$L	1.0	1.0	1.0	% of L
C_{stern} (V-shape)	-10	-10	-10	-
Number of propellers	1	1	2	-

Table 2.1: Inland ship parameters

This research bases the waterplane coefficient on an empirical formula for tankers and bulkers by Schneekluth (1998). The other values are based on their knowledge of inland ships. With this information, the Holtrop & Mennen method can be used to determine the resistance in the deepwater condition.

Verification

Part one of the verification is checking whether the approximation method for the resistance of ships by Holtrop & Mennen (1982) is implemented well in Matlab. The viscous resistance should dominate the total ship resistance for the lower Froude numbers. Wave resistance becomes more important when the speed (Froude number) becomes larger. The Froude number is calculated in equation 2.3.

$$Fr = \frac{v_{ship}}{\sqrt{g \cdot L}} \tag{2.3}$$

g Is the gravitational acceleration and L the ship's length. Figures 2.1 shows the resistance of ship 1, 2 and 3 calculated via the Holtrop & Mennen method. The appendage resistance is included in the frictional resistance in this figure.

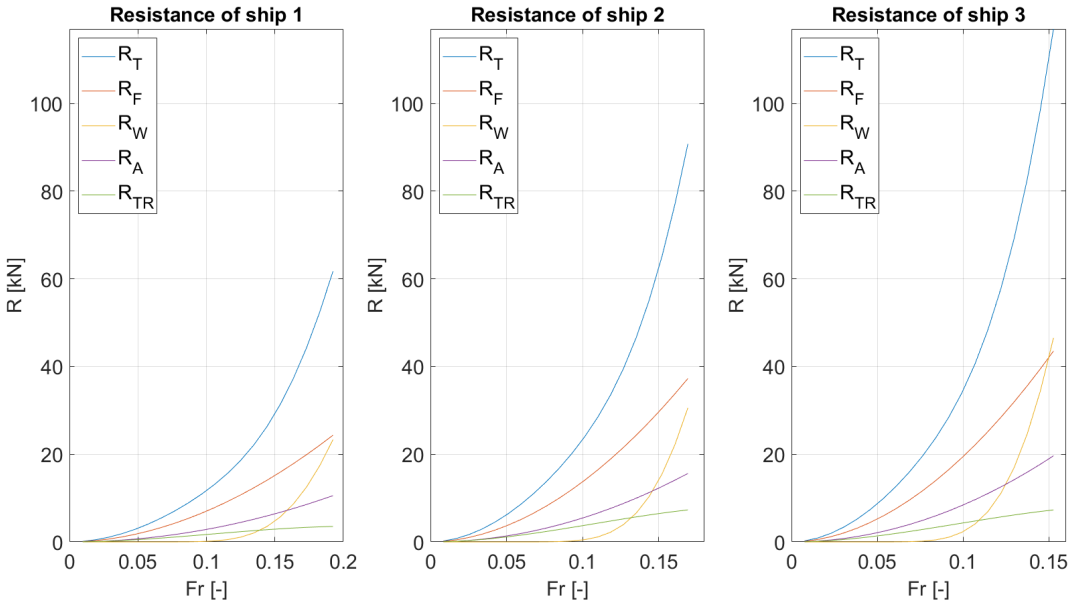

Figure 2.1: Resistance approximation

Figure 2.1 reflects the resistance in the way that it should. The wave resistance is low at lower ship speeds compared to the viscous resistance. The model-ship correlation resistance is a correction for the roughness of the hull and the still-air resistance, which is, in fact, a part of the frictional resistance. This figure shows for the ship speeds chosen that the major contributor to the total resistance is the viscous resistance. Figure 2.2 shows the individual contributions of the different resistance components.

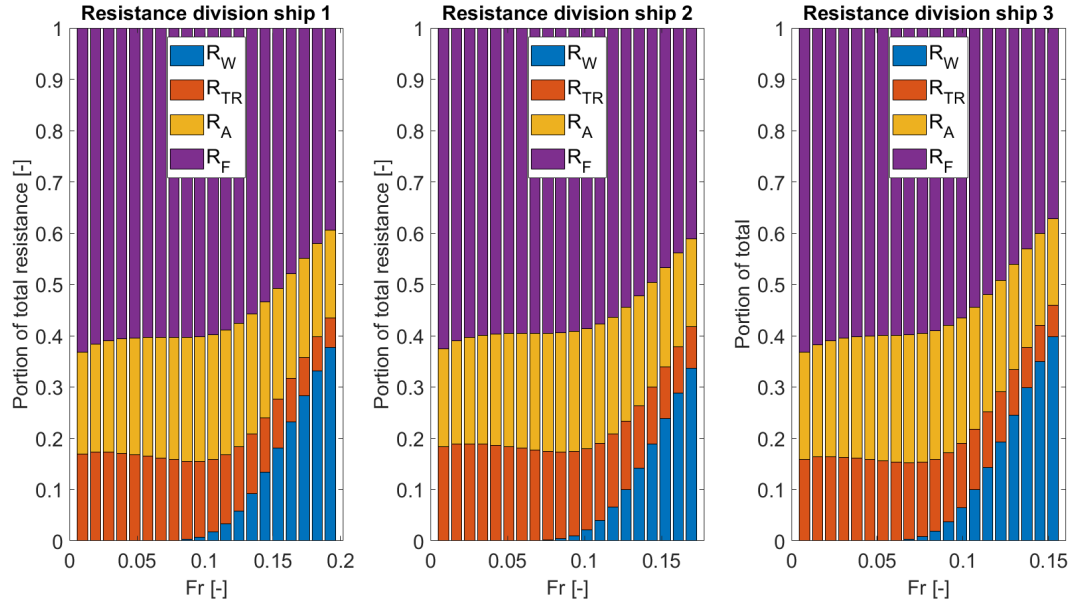

Figure 2.2: Resistance division

Figure 2.2 displays clearly that the wave resistance contributes more to the total resistance for higher Froude numbers. Still, the majority of the total resistance consists of frictional resistance.

Validation

The values given in figure 2.1 should give realistic values. Therefore, the values are compared to ones from other research to validate them. Pompée (2015) researched modelling inland ship resistance and showed in several figures different methods to describe the resistance in restricted waterways of an inland ship with a LxBxT of 110x11.4x2.8 meters. The ship is similar to ship 2 used in this research. The open water resistance in figure 7.6 from the article by Pompée is compared to the resistance of the ships in this Thesis in table 2.2 (Pompée, 2015).

Ship [−]	**Ship speed** [km/h]	**Resistance** [kN]
Ship 2 Thesis	14	33.6
	16	46.7
	18	65.3
Ship Pompée	14	45
	16	62
	18	88

Table 2.2: Open deepwater resistance comparison (Pompée, 2015)

Comparing the ship resistances from table 2.2 with one another shows that the model can produce realistic values. The order size is inline between the ship resistances. The resistance of ship 2 is lower than the Pompée ship, while the Pompée ship has a smaller draught and zero transom area. The resistance estimation by Holtrop & Mennen is highly dependent on its detailed input. Small changes in the input values affect the resistance approximation significantly because inland ships reside on the edge of the spectrum. This characteristic could be the explanation of the differences in the deepwater resistance.

2.1.2 Shallow water resistance

Model

The deepwater resistance in paragraph 2.1.1 is corrected to account for the shallow water effect. The correction method is from Karpov[1]. This method is also used in the dissertations of Hekkenberg (2013) and Van Dorsser (2015). The diagrams of Karpov, posted in the paper of Pompée (2015), are used to determine correction factors for the frictional resistance and the residual resistance. Karpov bases these correction factors on the Froude depth number (Fr_h) and the water depth over draught ratio (h_w/T). The Fr_h calculation is similar to equation 2.3 where the ship's length is replaced with the water depth, h_w. This research uses equations from the Karpov diagrams based on the ship speed, draught, and water depth (Hassel, 2011). The paper of Hassel (2011) provides equations for each h_w/T ratio with the Fr_h as the input value. They represent the curves from the Karpov diagrams. This research uses these equations and interpolates between them to create a dependency on the h_w/T ratio. In the paper of Pompé (2015) the correction on the river width versus the ship width from Artjuskov (1968) is presented. This correction is added to the resistance calculation. Since the trips used in this research follow the rivers Waal and Rhine mostly, a ship width over river width ratio of 0.04 is assumed.

[1]Hekkenberg (2013, p.36) note that: "The original paper by Karpov, (Karpov, A.B., "Calculation of Ship resistance in restricted waters", TRUDY GII T. IV, Vol. 2, 1946) is written in Russian and no longer available".

Verification

This section will elaborate on the verification of the shallow water resistance model. According to Karpov, the resistance in shallow water consists of a corrected frictional resistance and corrected residual resistance, see equation 2.4.

$$\begin{aligned} R_{shallow} &= 0.5\rho_w S[(C_F + C_A)v_1^2 + (C_r(\frac{v_\infty}{v_\prime})^2 + \Delta C_r)v_2^2] \\ v_1 &= v_\infty / a^* \\ v_2 &= v_\infty / a^{**} \end{aligned} \tag{2.4}$$

This correction factors a^* and a^{**} are determined with the Fr_h and the h_w/T in the graphs presented by Pompée (2015). The increase of the residual resistance, shown as $\frac{v_\infty}{v_\prime}$ and ΔC_r in equation 2.4, are determined with the tables of Artjushkov (1968) also given in the paper of Pompée (2015). These corrections should lead to an increase in the resistance of deepwater resistance. Figure 2.3 shows the resistance of each ship in different water depths.

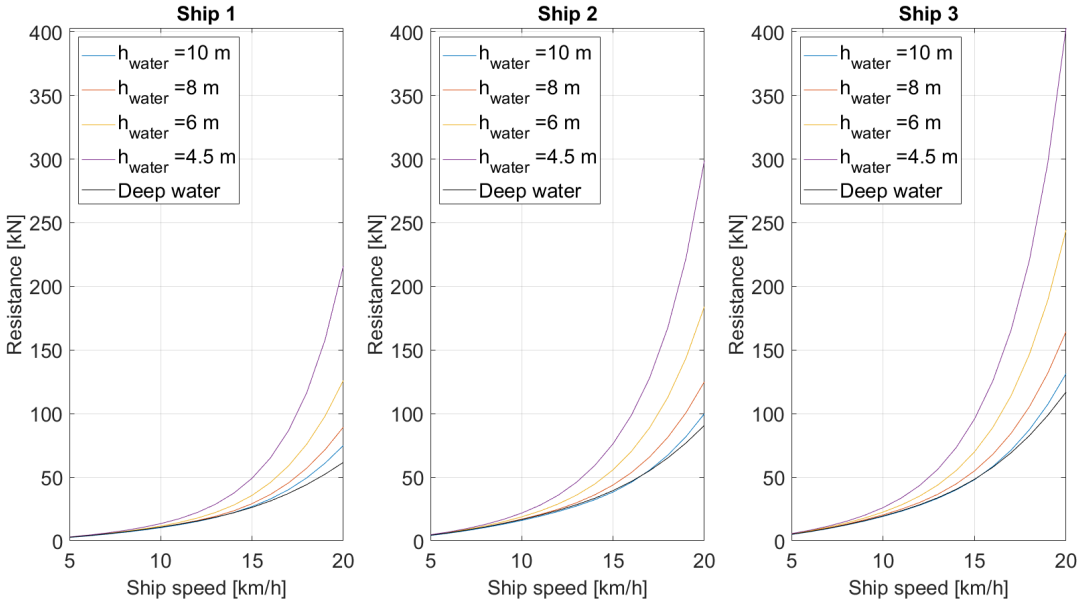

Figure 2.3: Resistance in shallow water

The figure shows an increase in resistance for lower water depth and higher ship speeds, which one expects in shallow water. The resistance rises significantly with the ship speed due to the correction factors a^* and a^{**}. These factors become smaller for higher F_h and smaller water depth ratios. The speed squared and the decrease of the correction factors result in significant increases in the resistance. The resistance becomes much harder to overcome in lower water depth ratios due to the limited speed in shallow waters.

Validation

The resistance curves in figure 2.3 should be validated. Therefore, this research compares ship 2 with the ship in figure 7.8 of the paper by Pompé (2015). The ship dimensions are changed to those of the Pompée ship and the water depth is set to 4.5 meters in the calculation model.

Ship [−]	**Ship speed** [km/h]	**Shallow water resistance** [kN]
Ship 2 Thesis	12	26.2
	14	44.5
	16	77.8
Ship Pompée	12	40
	14	72
	16	150

Table 2.3: Shallow water resistance comparison (Pompée, 2015)

Comparing the values in table 2.3 shows that the shallow water resistance in this calculation model is lower than the resistance from Pompé. This difference could be explained by the base method that determines deepwater resistance. The resistance approximation of Holtrop & Mennen (1982) is sensitive to the ship's input parameters. Inland ships lie on the edge of the spectrum of applicability for Holtrop & Mennen method. Apart from this, the resistance seems to take on realistic values compared to the values found by Pompée.

2.1.3 Propeller

Model

An extension is made on the deepwater resistance model from paragraph 2.1.1 to determine the inland ship's propeller. Two scripts are written containing the calculations for each propeller type, the Wageningen B-series and the Wageningen Kaplan-series.

First, the model calculates the blade area ratio with Keller's formula based on the ship resistance at a design speed. The wake fraction and the thrust deduction factor are determined via the formulas of Papmel as presented by Pompée (2015). These formulas are used in the work of Hekkenberg (2013) as well. These factors are assumed constant throughout the calculations. The blade area ratio from Keller's formula shows which propellers remain an option to carry the propeller load in the given condition. The number of blades can be altered to adjust the required blade area ratio. These two parameters decide which propeller is the best fit for the inland ship. Two propeller types are considered in this research: the Wageningen B-series and the Wageningen Kaplan series. The model can choose between three large blade area ratio propellers from the Wageningen B-series: B4-70, B4-85, and B4-100 (Oosterveld & van Oossanen, 1975). Four propellers can be chosen from the Wageningen Kaplan-series: K_a3-65, K_a4-55, K_a4-70, and K_a5-75 (Oosterveld, 1970). The function script calculates which type of propeller is the best fit based on the blade area ratio and the number of propeller blades. The sub-model calculates the propeller polynomials based on a range of pitch/diameter (P/D) ratios and an advance, J. Five common P/D ratios are chosen to calculate the Kaplan series polynomials, namely 0.6, 0.8, 1.0, 1.2 and 1.4 (Oosterveld, 1970). A range of P/D ratios from 0.5 until 1.4 with a step size of 0.1 is used for the Wageningen B-series (Oosterveld & van Oossanen, 1975). The propeller model calculates the efficiency of the chosen propeller for each P/D ratio and advance. Afterwards, the optimal P/D ratio is chosen by the model that associates with the highest open water efficiency. This way results in a propeller fit to carry the thrust load required for propelling the ship. The propeller curves are used throughout the model to determine other operational points of the inland ships. This way, the open water efficiency changes for the different sailing conditions of the inland ships.

Verification

The polynomials implemented have to generate the curves of the Wageningen-K_a propellers with nozzles and the Wageningen B-series propellers. This verification will compare the propeller curves generated by the model with the original propeller curves. After this process, the propeller is matched to the ship to obtain the optimal value for the P/D ratio.

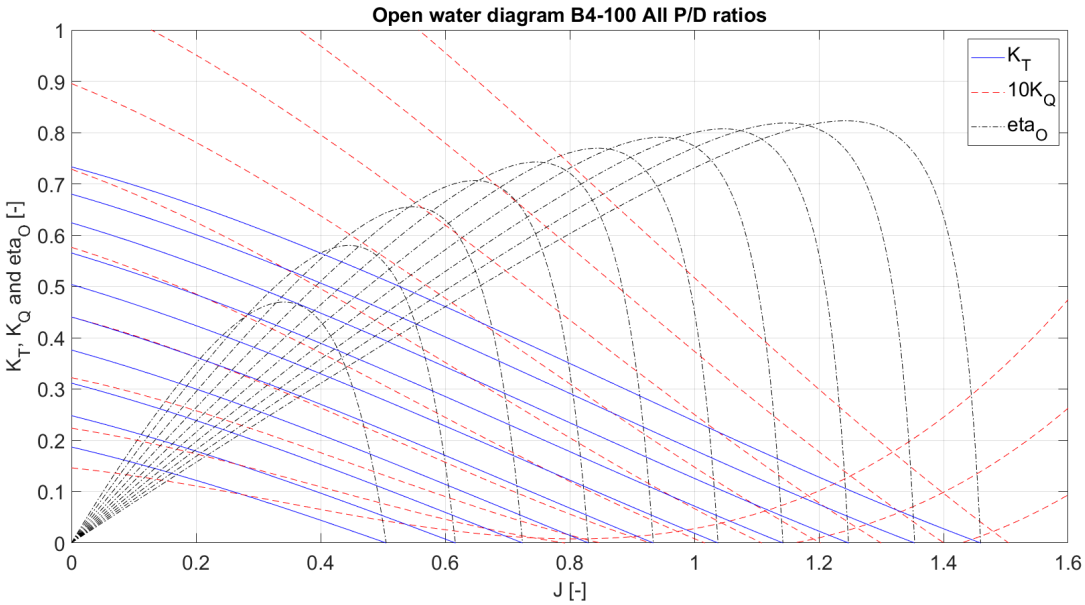

Figure 2.4: Wageningen B4-100

Figure 2.5 shows the polynomial of the Wageningen K_a5-75 and figure 2.4 the polynomial of the B4-100. The script can produce the propeller curves for a given range of advance and pitch over diameter ratio. With the thrust demand curves, the model determines the optimal P/D ratio by checking which P/D ratio the open water efficiency is maximum in the deepwater condition. Figures A.3, A.4, 2.5, and A.5 are compared to the figures of determined by Oosterveld (1970). The comparison shows that the figures are the same for each propeller and P/D ratio. This similarity means the propeller model works and that it uses the correct calculations for the open water efficiency determination.

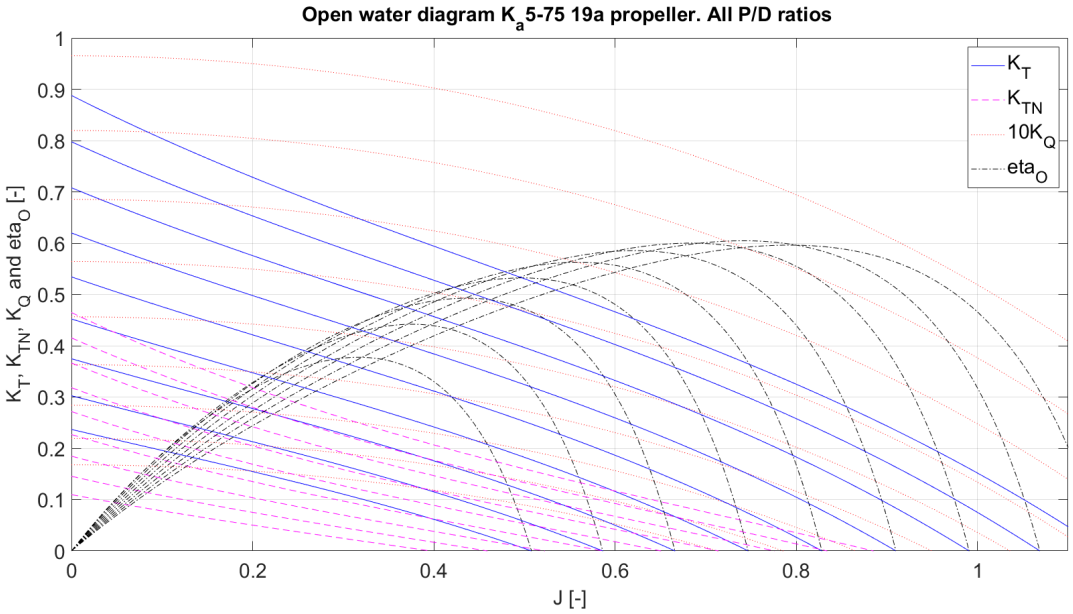

Figure 2.5: Wageningen K_a5-75

Validation

Validating the propeller for inland ships is performed by checking whether the implemented propeller characteristics are realistic and if the propeller results match those found in practice. The deepwater resistance and these polynomials determine which propeller at which P/D ratio gives the best open water efficiency. The resistance calculation with shallow water correction results in a new thrust demand curve. This new curve results in different open-water efficiencies of the propeller. The sub-model has determined the following propellers for the inland ships:

- Ship 1: Wageningen B4-100
- Ship 2: Wageningen B4-100
- Ship 3: Wageningen Ka5-75

The high thrust load did not allow ship 1 and 2 to have a ducted propeller, like ship 3, because the blade area ratio had to be higher for ship 1 and 2. The two propeller arrangement of ship 3 results in lower thrust load per propeller. This lower load results in the ducted propeller. The required blade area ratio is too high when ship 3 has a one propeller arrangement. The open water efficiency of ship 1, ship 2 and ship 3 takes on values respectively around 0.37, 0.35 and 0.56 in deep water at the design speed. The open water efficiencies tend to be low for inland ships, between values of 0.2 to 0.55 (Pompée, 2015). So the value for ship 1 and 2 are more realistic compared to ship 3. The efficiency of ship 3 is significantly higher compared to the other ships. This effect occurs, because of the two propeller propulsion configuration and because the propellers are ducted. Ducted propellers increase the efficiency of the propulsion system for heavy loaded propellers (Oosterveld, 1970).

2.2 Power prediction

2.2.1 Model

The power prediction is the third model part which predicts the power needed of the inland ships. The water depth, the draught, and the desired speed are the primary input of this sub-

model. The model uses the shallow water resistance and the propeller model from paragraph 2.1 to determine the power demand of the inland ships. The current is subtracted or added to the desired ship velocity depending on upstream or downstream sailing. The power prediction model uses this corrected velocity. The propeller polynomials from the deepwater condition are used to determine a new matching point based on the corrected resistance and different ship speeds. The matching points lead to different propulsion performances on each trajectory of the trip. Furthermore, this research assumes a transmission efficiency and electric motor efficiency of respectively 95% and 95%. The transmission of power through the gearbox and the shaft to the propeller contains losses. The transmission efficiency accounts for these losses. The efficiency of an electric motor could reach values of 92% to 98% (Klein Woud & Stapersma, 2012). Therefore, this Thesis assumes an efficiency of 95% for the electric. The efficiencies, the corrected speed and shallow water resistance result in the brake power of the ship, see equation 2.5.

$$P_B = \frac{R_{shallow} \cdot v_{ship}}{\eta_H \cdot \eta_R \cdot \eta_O \cdot \eta_{TRM} \cdot \eta_{EM}} \tag{2.5}$$

η_R is the relative rotative efficiency, η_H the hull efficiency, η_O the open-water efficiency, η_{TRM} the transmission efficiency, and η_{EM} the electric motor efficiency. $R_{shallow}$ is the shallow water resistance that depends on the water depth and the ship speed. This way the calculation predicts the power demand of a ship sailing up or down a river in limited water depths. This power equals the power demanded from the fuel cell for each section of the trip. Since the ship will be driven by the fuel cells completely, the cells will have to generate all electricity demand onboard the inland ships, not only the main engines. It is assumed that the auxiliary equipment and other systems on board the inland ship account for around 5 kW during the trip. The fuel cell system replaces the generator sets on board of the ships. Therefore, the diesel generator power is added to the maximum power demand to determine the ship´s installed power.

2.2.2 Verification

Two items have to be checked to verify the power prediction model. One part is the change in the propulsion efficiency due to the resistance increase. The second part is the power increase in shallow water.

The wake fraction and the thrust deduction factor result in the hull efficiency. The relative rotative efficiency remains constant since it is dependent on the parameters of the ships. The open-water efficiency changes due to the variations in the thrust demand. The shallow water resistance induces these variations. The propulsion efficiency is the multiplication of the hull, relative rotative, and the open-water efficiency. Therefore, the propulsion efficiency varies in shallow water due to the changes in the open-water efficiency. The shallow water resistance is based on Karpov[2]. This method corrects the ship speed in shallow water for the frictional part and the residual part of the resistance, which results in higher resistances. Figure 2.6 shows the propulsion power per ship for different water depths. The propulsion power is calculated with equation 2.6.

$$P_D = \frac{R_{shallow} \cdot v_{ship}}{\eta_H \cdot \eta_R \cdot \eta_O} \tag{2.6}$$

[2]Hekkenberg (2013, p.36) note that: "The original paper by Karpov, (Karpov, A.B., "Calculation of Ship resistance in restricted waters", TRUDY GII T. IV, Vol. 2, 1946) is written in Russian and no longer available".

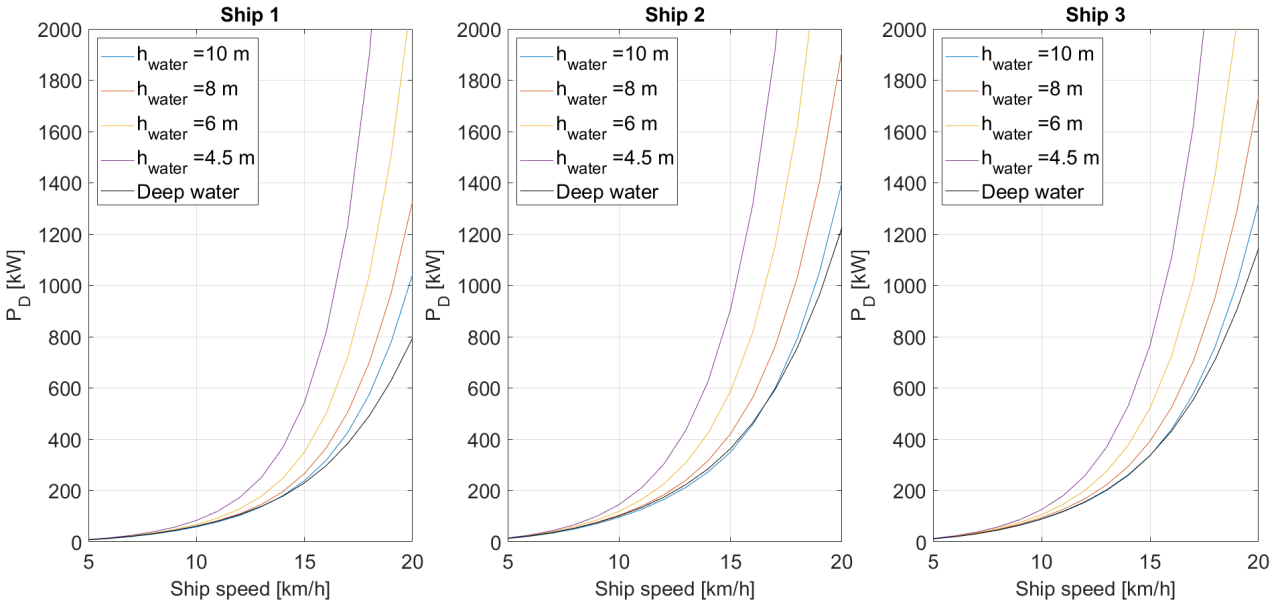

Figure 2.6: Power calculation for multiple water depths

The propulsion power rises significantly for higher ship speeds. This rise happens due to the decrease in propulsion efficiency for higher resistances in shallow waters and the higher shallow water resistance. Other researches show that in shallow water the power increase is similar to figure 2.6. In Appendix C table C.1 is given with the calculated propulsion efficiencies per h_w/T and ship speed. This table shows that the propulsion efficiency becomes lower for lower water depths and higher ship speeds.

Figure 2.6 shows an unexpected effect happening in all sub-figures, but most noticeable in the second sub-figure, which is that of ship 2. The deepwater power is higher compared to the shallow water power at high water depths and low ship speeds. This effect is rather peculiar since the resistance should become higher in shallow water compared to deep water. What happens is a difference in resistance definition in the deep water and the shallow water resistance approximation. In the approximation of the resistance by Holtrop & Mennen (1982) the resistance is determined with equation 2.1. The shallow water resistance is approximated with the formula from Karpov in equation 2.4. The key difference between the deepwater and shallow water resistance is the form factor, $1 + k_1$. In the deepwater resistance, the form factor is multiplied with the frictional resistance coefficient to include viscous pressure resistance. The formula for the shallow water resistance does not include the form factor. Since the effect happens at lower ship speeds, where frictional resistance dominates the total resistance, the higher deep water resistance compared to the shallow water resistance is likely to be caused by this form factor. Looking back at the deepwater resistance determination, the form factor of ship 1 to 3 are respectively 1.297, 1.326 and 1.274. The form factor of ship 2 is higher than the other ships. This aspect is visible in the figure because the effect is more noticeable for ship 2. This effect is also visible in figure 2.3.

2.2.3 Validation

To validate the power calculations, the model must predict powers comparable to power demands of actual inland ships sailing on the Rhine. Hekkenberg (2013) made a comparison between the resistance by the model of Hekkenberg and the DST (Zigic, 2007). The resistance from the model of Hekkenberg (2013) is based on Holtrop & Mennen and Van Terwisga (1990), together with a shallow water correction based on Karpov. DST determined the resistance with

CFD calculations. It showed that the resistance increases significantly for lower water depths. The shallow water correction of Karpov is based on a speed correction for different h_w/T ratios. This correction increases the speed in lower water depths resulting in higher values for the resistance at the given ship speed. Pompée (2015) shows this large increase in resistance in various comparisons between different shallow and confined water correction methods. This model does represent shallow water effects, which lead to a significant increase in resistance and power. Table 2.4 shows the comparison between the propulsion powers.

Ship [−]	**Length** [m]	**Ship speed** [km/h]	**Propulsion power** [kN]
Ship 2 Thesis	110	12	200
		14	416
		16	902
Ship Pompée	110	12	275
		14	460
		16	840
Ship 3 Thesis	135	12	202
		14	421
		16	896
Ship Hekkenberg	135	12	350
		14	640
		16	1160

Table 2.4: Propulsion power comparison (Hekkenberg, 2013), (Pompée, 2015)

Ship 2 from this Thesis is compared to the ship in the research of Pompée (2015). Ship 3 is compared to the ship from the research of Hekkenberg (2013). The presented values of Hekkenberg (2013) and Pompée (2015) compared to the values from the model in table 2.4 proves the statement from earlier. Ship 2 shows similar values for the propulsion power as the ship's values from Pompée (2015). The propulsion power of ship 3 seems to be a bit on the low side compared to the ship from Hekkenberg (2013). Comparing figure 2.6 to the power determination in shallow water from another paper of Hekkenberg (2015) also shows many similarities in these power determination.

Table 2.5 shows the brake power required on board of the ships for each trip calculated by the model. The table shows the maximum power required that the model chose between the low water (LW) or high water (HW) depths.

$P_{required}$	**Trip 1**	**Trip 2**	**Unit**
Ship 1	687	1004	kW
Ship 2	925	1487	kW
Ship 3	805	1363	kW

Table 2.5: Highest power demands of ships in either LW or HW depth

Table 2.5 shows that trip 2 will determine the minimum required power due to the highest power demand. The required power of ship 3 is low compared to ship 2. Although ship 3 is the largest, the power demand seems to be lower than ship 2. This lower power occurs due to the propulsion arrangement of ship 3. It has a better efficiency due to a two-propeller arrangement which allows the ship to have propellers with nozzles. The nozzled propellers result in higher propulsion efficiency than open propellers under high load conditions. The propellers fit for ship 1 and 2 are open propellers and lead to lower propulsion efficiencies compared to ship 3.

The propulsion efficiency becomes even lower for the ships in shallow water.

Also, inland ships tend to be overpowered (Geest & Menist, 2019). It is insightful to compare the values computed by the model with the power demands of inland ships. Data has been acquired from one skipper to compare their power requirements to those obtained by the model, see table 2.6. The table displays the ship speed with respect to the river bottom.

Trajectory [−]	**Section(s)** [−]	**Ship speed** $[km/h]$	T **ship skipper** $[m]$	P_B **ship skipper** $[kW]$	P_B **ship model** $[kW]$
Mannheim-Duisburg	10-6	17.4	1.65	320	256
Rotterdam-Basel	1-14	10	2.7	799	697
Gambsheim-Rotterdam	13-1	17	3.6	400	296
Millingen-Duisburg	5	10	3.0	799	685
Bingen-Mannheim	10	10	2.7	512	886
Bingen-Mannheim	10	10	3.0	671	886

Table 2.6: Power comparison in LW inland ship skipper vs ship model

From the values of table 2.6 between the 135 meter inland ship and the model's ship, it becomes clear that the model calculated power demands slightly lower compared to the values of the skipper overall. This effect is expected since the resistance estimation from Karpov is known to underestimate the resistance in shallow. The power predictions are close. However, the ship from the skipper does not sail fully loaded in 5 of the 6 cases, while the ship in the model does. The power prediction of ship 3 is also low due to good propulsion efficiency. All previous comparisons considered, the model gives a valid prediction of the power in shallow water. However, the last two rows of the table show that the model exceeds the power demands of the skipper. This difference is expected since the ship in the model is fully loaded while the inland ship from the skipper is not.

Another validation check is added in the form of a comparison with other research. The 135 meter inland ship from the dissertation of Hekkenberg (2013) is implemented in the calculation model to compare it to the dissertation. Figure 2.7 shows the propulsion power versus the ship speed for different water depths.

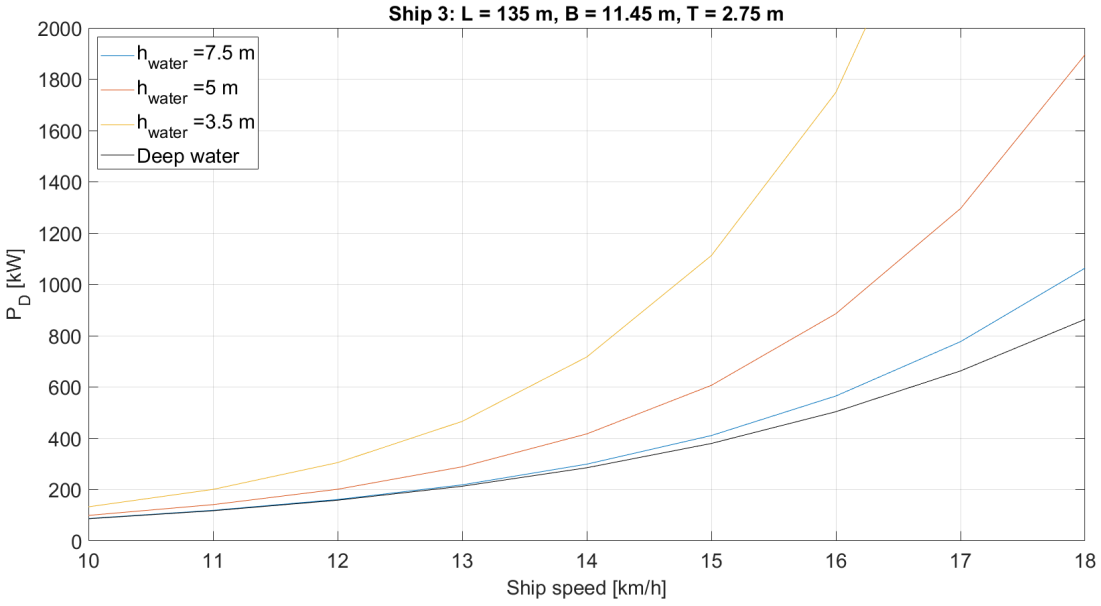

Figure 2.7: Propulsion power estimation of model for the 135 meter ship from Hekkenberg (2013)

Figure 2.7 is compared to figure 4-12 from Hekkenberg (2013). It shows that there is a difference between the propulsion powers. The figure from Hekkenberg shows validation of the powering calculations between the calculations from Hekkenberg and the DST. The data known about the ship from Hekkenberg is used, while other necessary data is kept the same as the model values of ship 3. Ship 3 is a 135-meter ship. The deep water resistance of the calculation model is slightly lower than the values obtained by Hekkenberg. The shallow water calculations show values for the propulsion power for the water depth of 7.5 meters and 3.5 meters different from the values of Hekkenberg. The calculation model of this thesis is lower compared to Hekkenberg. The 5-meter water depth values are slightly higher at higher ship speeds than the calculated powers from Hekkenberg. However, the model values are lower than the calculated powers form the DST. The deepwater resistance forms a basis for the calculation of the shallow water resistance in the calculation model. The deepwater propulsion powers are lower than Hekkenberg's values. Therefore, it is expected that the powers in shallow water are also slightly lower. The comparison shows that the order of power in which the model resides is good, but it also suggests that overall the model slightly underestimates the power.

2.3 PEM Fuel Cell

The power from the previous paragraph represents the power that the PEM FC has to supply.However, the PEM FC characteristics are different than the conventional diesel engine characteristics. To include the PEM FC behaviour a sub-model is developed.

2.3.1 Stack model

This research calculates the PEM FC stack performance according to the theories of Larminie, Dicks & McDonald (2003) and the model from Rabbani (2013). This basis gives a good representation of the PEM FC behaviour regarding the load it is carrying. To have a quick impression of the assumptions and the characteristics of the PEM FC in this model, table 2.7 is shown below.

Parameter	symbol	Value	Unit
Number of cells per stack	N_{cell}	96	–
Area of cell	A_{cell}	285.8	cm^2
Gibbs free energy of reaction	ΔG^0	-237.34	kJ/mol
Partial pressure oxygen	p_{O_2}	0.21	–
Partial pressure hydrogen	p_{H_2}	1.2	–
Operating temperature PEM FC	T_{FC}	333.15	K
Ambient temperature	T_{amb}	293.15	K
Exchange current density of cathode	$i_{0,c}$	$3 \cdot 10^{-6}$	A/cm^2
Exchange current density of anode	$i_{o,a}$	0.2	A/cm^2
Limiting current density	i_{lim}	1.6	A/cm^2
Current density loss	i_{loss}	0.002	A/cm^2
Transfer coefficient cathode	α_c	1	–
Transfer coefficient anode	α_a	1	–
Ionic resistance of cell	r_{ion}	0.2	Ωcm^2

Table 2.7: PEM FC characteristics

The characteristics and parameters in table 2.7 are explained in the upcoming explanations on the used formulas and methods. First, the ideal fuel cell potential is calculated based on

the Gibbs free energy of liquid water. This is given by equation 2.7.

$$E^0 = \frac{-\Delta G^0}{2F} \tag{2.7}$$

ΔG^0 is the Gibbs free energy, which is the potential energy available from the reaction that takes place in the cell. F is Faraday's constant and the 2 represents the number of electrons for a hydrogen and oxygen reaction. With the Gibbs free energy of water, which is -237.34 kJ/mol, a cell potential of 1.23 V is calculated. This potential would be the voltage of the cell at standard temperature and pressure. The following equation is used to account for the operating conditions:

$$E = E^0 + \frac{RT}{2F} \cdot ln\Big(\frac{a_{H_2} \cdot a_{O_2}^{1/2}}{a_{H_2O}}\Big) \tag{2.8}$$

In equation 2.10 the R is the universal gas constant and T the operational temperature of the fuel cell, which is 333 Kelvin (60 degrees Celsius). The a in equation 2.8 is the activity of the gases. Ideal gasses are assumed, which suggests that the activity of the gasses is equal to the partial pressure of the gas. The liquid water activity can be assumed 1 in these conditions. This adjust equation 2.8 to equation 2.9.

$$E = E^0 + \frac{RT}{2F} \cdot ln\Big(p_{H_2} \cdot p_{O_2}^{1/2}\Big) \tag{2.9}$$

The cell potential reduces due to operating temperature and the partial pressures of the fuel and the oxidant. This research assumes that the PEM fuel cell uses air instead of pure oxygen. Approximately 21% of the air is oxygen, so the partial pressure of oxygen in equation 2.9 is equal to 0.21. The partial pressure of the hydrogen is assumed 1.2. This assumption results in a slightly lower potential voltage of 1.22 V. Now the losses have to be calculated, which will lead to the stack power and efficiency. The losses present in the cell are the activation losses, ohmic losses and the mass concentration losses. The activation losses of the fuel cell are determined with equation 2.10. This loss is the voltage needed to overcome the energy threshold of reactions in the cell. In other words, a part of the cell potential is used to activate the fuel and the oxidant reactions in the cell. The subscript c and represent respectively cathode and anode.

$$V_{act} = V_{act,c} + V_{act,a} = \frac{RT}{\alpha_c F} ln\Big(\frac{i + i_{loss}}{i_{0,c}}\Big) + \frac{RT}{\alpha_a F} ln\Big(\frac{i + i_{loss}}{i_{0,a}}\Big) \tag{2.10}$$

The alphas are the transfer coefficient of the cathode and anode. These coefficients are assumed to be equal to 1. The i_{loss} term accounts for the losses due to the internal current generation and fuel crossover, and is assumed to be equal to 0.002 A/cm^2 (Rabbani, 2013). The exchange current densities, $i_{0,c}$ and $i_{0,a}$, are a measure of how well the anode/cathode proceeds with the electrochemical reaction. A high exchange current density means the surface of the anode/cathode is active. This characteristic results in low activation loss. It depends on the material used for the anode or cathode as well as the operating temperature. The exchange current density of the cathode and anode are assumed to be respectively $3 \cdot 10^{-6}$ and 0.2 A/cm^2 (Barbir, 2013). The exchange current density of the cathode is low compared to that of the anode. Therefore, the cathode determines the majority of the activation losses. The ohmic losses are determined with equation 2.11. The ohmic loss occurs because of three effects: a resistance of the ionic flow in the electrolyte, a resistance of the flow of electrons through the electrodes, and the contact resistance at the cell terminals (Rabbani, 2013). It depends on the conductivity of the electrodes and the conductivity of the membranes of the cells.

$$V_{ohmic} = i \cdot (r_{el} + r_{ion}) \tag{2.11}$$

The r_{ion} represent the ionic losses of the cell and r_{el} denotes the electronic resistance in the cell. However, the electronic loss is low compared to the ionic loss. Therefore the electronic loss is assumed to be zero. The ionic resistance is assumed to be 0.2 Ωcm^2 (Barbir, 2013). The mass concentration losses are determined with equation 2.12.

$$V_{conc} = V_{conc,c} + V_{conc,a} = \frac{RT}{n_e F} ln\left(1 - \frac{i}{i_{lim,c}}\right) + \frac{RT}{n_e F} ln\left(1 - \frac{i}{i_{lim,a}}\right) \tag{2.12}$$

The mass concentration losses occur because reactions of the fuel and the reactant (oxygen) happen faster than the fuel and the reactant molecules can reach the cell sites. This effect occurs at high current densities when the reactions in the cell happen quicker. This aspect makes the mass concentration losses dependent on the current and the limiting current densities of the cathode and anode, $i_{lim,c}$ and $i_{lim,a}$. These limiting current densities are assumed to be equal to 1.6 A/cm^2 (Barbir, 2013). With all the cell losses accounted for, the cell voltage and the losses are calculated and shown in the left graph in figure 2.9.

It is assumed that a stack consists of 96 cells. The FC system needs to condition the stacks to keep the cells from degenerating. These systems use power from the fuel cell stack. The following auxiliary systems are distinguished for the stack:

- The air compressor
- The fan/radiator
- The cooling pump

The fan/radiator power is assumed to be constant for the entire operating range of the fuel cell based on the paper by Tirnovan and Giurgea (2012). It is scaled down to comply with the number of cells present in the stack of this model. The fan/radiator system draws a low amount of power from the stack. The fan/radiator power is assumed to be around 0.080 kW, based on scaling between a stack with a larger amount of cells (Tirnovan & Giurgea, 2012) and the stack in this research. This research assumed a fan/radiator power of 0.300 kW for a stack that consists of 360 cells. The stack in this research is assumed to contain 96 cells, so $\frac{0.300}{360} \cdot 96 = 0.080$ kW. The power of the cooling pump is a function of the mass flow of the coolant. It is modelled with equation 2.13.

$$P_{pump} = \frac{P_{pump,max}}{\dot{m}_{coolant,max}} \dot{m}_{coolant} \tag{2.13}$$

The maximum power of the cooling pump is assumed to be 2.0 kW and occurs at the maximum current density of the fuel cell (Tirnovan & Giurgea, 2012). This research determines the maximum mass flow of the coolant at a slightly lower current density than the maximum current density. The model cannot calculate the mass concentration losses at the maximum current density because they would go towards infinity. The paper from Tirnovan & Giurgea (2012) presents the equations to calculate the mass flow of the coolant. This way the cooling pump power can be modelled as a function of the stack current.

The compressor is modelled based on a paper by Liso, Nielsen, Kær and Mortensen (2014). For this, the stoichiometry of oxygen, and the pressure drop need to be modelled. For each, a formula is expressed in excel based on data from Liso et al. (2014). This way has enabled to implement the parameters in Matlab as a function of the FC current. The power of the compressor is calculated with equation 2.14.

$$P_{compressor} = f_{comp} \cdot \dot{V}_{air} \cdot p_{drop}^2 \tag{2.14}$$

$\dot{V}_{air}$ is the airflow required for the fuel cell stack and p_{drop} is the pressure drop. Comparing the calculated compressor power to the powers determined by Liso et al. (2014) and Tirnovan

& Giurgea (2012) shows that the power from the model is too high. The model's compressor power with respect to the number of cells per stack is approximately 4 times higher than the power from Liso et al. (2014) and 2 times higher than the power from Tirnovan & Giurgea (2012). It is decided to introduce a factor to decrease the calculated compressor power based on this observation. The factor, f_{comp}, is set to 0.33 to decrease the calculated power. This factor results in a compressor power lower than that from Tirnovan & Giurgea (2012) and higher than that from Liso et al. (2014) based on the number of cells per stack. Also, it is assumed that the compressor needs a power of 0.1 kW at low loads. The inverters are also part of the system losses. The efficiency of the inverters is assumed to be 96% (Rabbani, 2013). Deducting the auxiliary systems' power from the stack power results in the net power. Figure 2.8 displays these results.

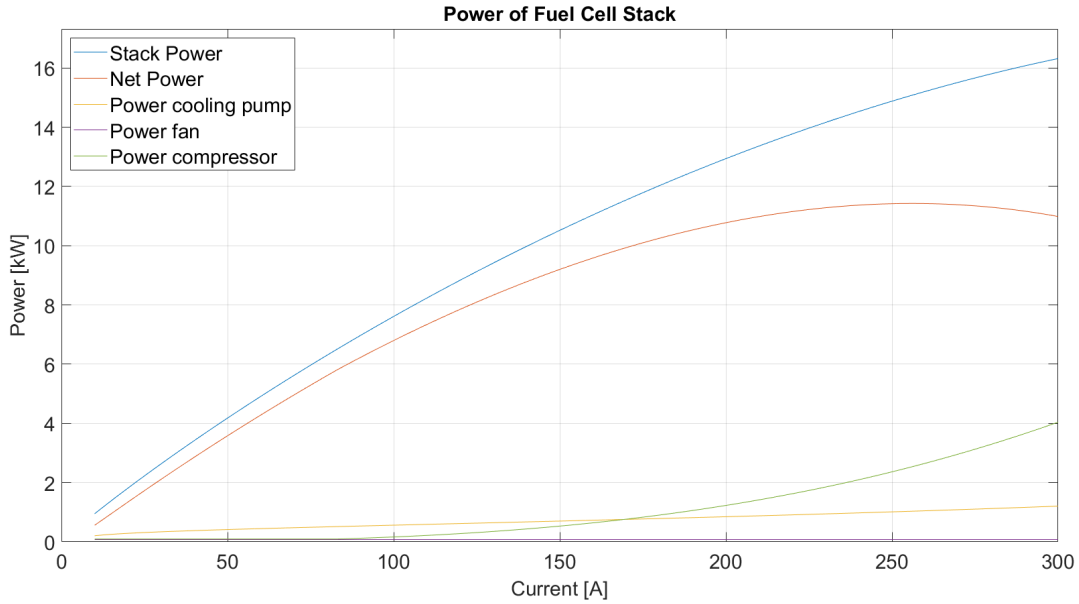

Figure 2.8: Power generated by the fuel cell stack

The maximum net power drawn from the stack is approximately 11.4 kW and occurs around a current of 256 Ampere. At higher loads, the net power starts to drop because the compressor power becomes too large. The model can determine the characteristics of the PEM fuel cell stack. Therefore, the model can move on towards the installed power calculations.

2.3.2 Number of stacks installed

The two situation sketched in paragraph 2.4 each show a situation in which the resistance is high: shallow water with low currents and HW depth with strong currents. For each ship, trip and situation the power requirement is determined. This leads to the determination whether the shallow water or HW depth will determine the minimum installed power on each ship type. The highest requirement determines the minimum installed power since it is chosen to have a power system installed that gives the skipper the opportunity to be able to sail the entire time of the year whatever the situation on the river might be. Dividing the minimum power requirement of the highest power demanding section of each trip with the electric motor efficiency of 95% and the maximum power of the stack gives the minimum number of stacks that should be installed for each ship type. For each ship and trip the number of installed stacks is varied by adding stacks (so installing more power). The corresponding load factors are calculated based on the power requirements during the trip and the installed power. Through the load factors

the withdrawn current from the PEM FC is calculated by multiplying the load factors with the maximum possible current of the stack. The maximum current of the stack is chosen to be equal to the current which corresponds to the maximum net power obtained from the stack. With this knowledge the system efficiency of the PEM FC stacks at that load is determined. The system efficiency is determined via equation 2.15.

$$\eta_{system} = \eta_{inverters} \cdot \eta_{cell} \cdot \left(1 - \frac{P_{aux}}{P_{stack}}\right) \tag{2.15}$$

Depending on the load of the stack, the power of the stack, the power required by the auxiliary systems and the cell efficiency changes. This results in the system efficiency of the stack and with it the mass flow of hydrogen fuel can be calculated. Equation 2.16 shows how to calculate the mass flow of the hydrogen fuel for each system efficiency and power.

$$\dot{m}_{H_2} = \frac{P}{\eta_{system} \cdot LHV_{H_2}} \tag{2.16}$$

The mass flow of hydrogen fuel, the speed on each section and the section length results in the consumed hydrogen for each trip. By assuming the ship sails 18 hours per day for 365 days minus 21 days of holiday the number of performed trips per year is easily calculated and leads to the total fuel consumption per year. Now every time the number of stacks is increased, the load on the fuel cell lowers and this system efficiency increases. This leads to lower fuel consumption, however it needs to be evaluated if the increase of number of installed FC stacks (increase in installed power) competes with lower annual fuel consumption in terms of cost. Other components needed for the entire power plant are included in the total cost to make a founded comparison in the evaluation between increasing the power installment, saving hydrogen fuel and lower the need of voluminous space for the hydrogen storage.

2.3.3 Verification

For the verification of the PEM FC model, it is necessary to evaluate if the calculation model of the fuel cell stack is implemented correctly. A few aspects of the fuel cell must be included in the model to be able to say that the behaviour of the fuel cell is correct.

- The activation losses should increase significantly for low currents and this increase subsides for higher currents.
- The ohmic losses of the fuel cell should dominate the decrease of the voltage for the mid range of the current.
- The mass concentration losses are almost negligible but become more significant for higher currents.
- The efficiency of the system should show and optimum at a low current and decrease as the current rises.

Figure 2.9 shows in the first plot the behaviour of the losses and the voltage of the cell and the second plot shows the comparison between the system efficiency and the cell efficiency.

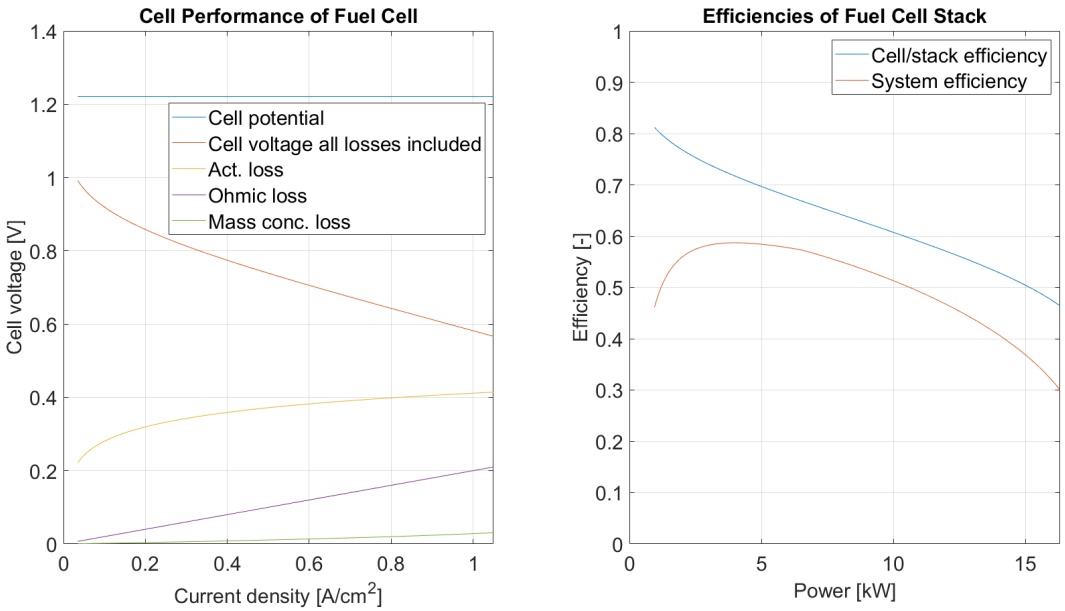

Figure 2.9: Fuel cell verification

The first plot in figure 2.9 shows the different behaviours of the losses of the cell, the only remark is that for the mid range of the current the activation losses still count for a large portion of the losses besides the ohmic losses. The last plot shows the difference in cell/stack efficiency and the system efficiency. To calculate the system efficiency the auxiliary systems have to be taken into account and this shows that the efficiency drops due to power demand of the auxiliary equipment. Seeing on which theory the model is based, the optimum of the system efficiency should lie at approximately 25% of the current range (Rabbani, 2013). This is reflected in the last plot. 25% Of the current, at which maximum net power is obtained, lies at 58 Ampere. The current at which maximum system efficiency is achieved lies at 47.6 Ampere and this is around 19% of the maximum current. Although the highest system efficiency occurs at a slightly lower current, it shows that the system efficiency is well represented in the model and that adequate calculations can be made with the fuel cell model. Due to the representation of the power development of the auxiliary systems with increasing loads, the maximum efficiency is obtained at a slightly lower current compared to the 25% of the maximum current. The information on this data is hard to find and often kept hidden by fuel cell manufacturers, which makes it difficult to determine the exact powers needed by the auxiliary systems especially in the low current region.

2.3.4 Validation

In case of modelling the PEM fuel cell, it is important that a realistic stack power and system efficiency is obtained. This means that the figures 2.8 and 2.9 should both represent a realistic behaviour of the stacks. The figures are compared with the data from the Nedstack FCS 13-XXL (2019). From the data of Nedstack FCS 13-XXL is found that it has a rated power of 13.6 kW at 230 Ampere and consists of 96 cells per stack (Nedstack, 2019). The stack power and the net power of the stack from the model is respectively 14.16 and 11.28 kW at 230 Ampere of current and the stack consists of 96 cells. This shows that the model has similar losses compared to the Nedstack FCS 13-XXL.

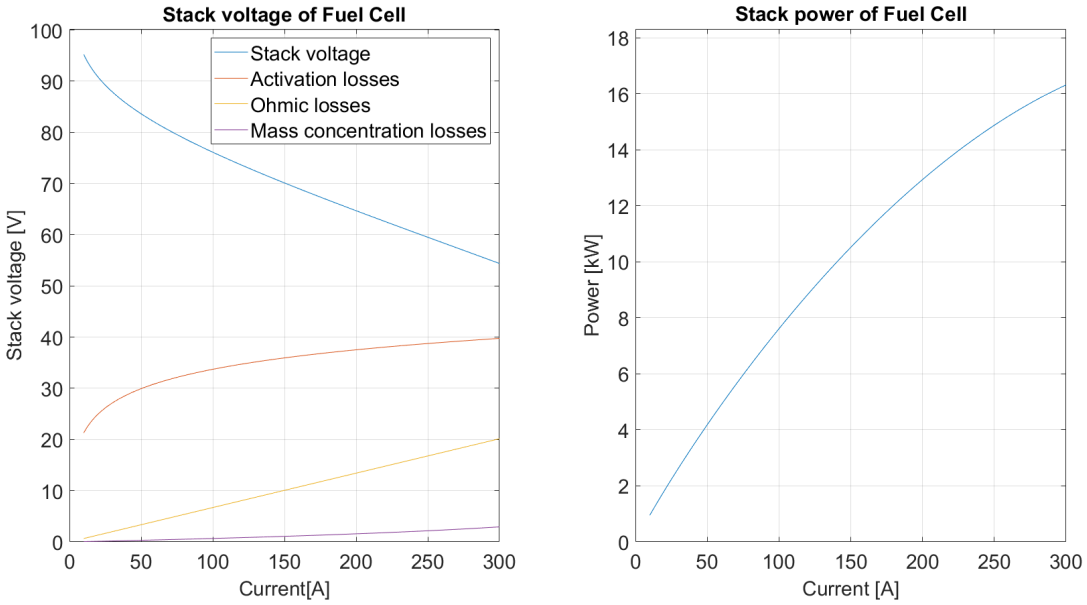

Figure 2.10: Stack voltage of fuel cell model

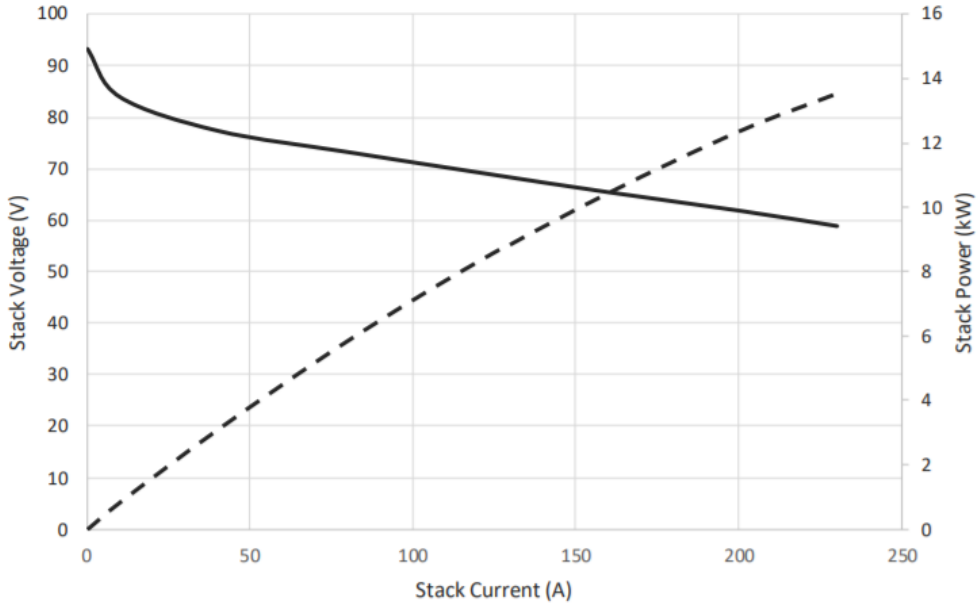

Current (A)	0	40	80	120	160	200	230
Stack Voltage (V)	93.2	77.4	73.2	69.3	65.5	61.9	58.9
Stack Power (kW)	0.0	3.1	5.9	8.3	10.5	12.4	13.6

Figure 2.11: Stack voltage and Power of Nedstack FCS 13-XXL (Nedstack, 2019)

Comparing the stack voltage of the model in figure 2.10 with the data from the Nedstack FCS 13-XXL from figure 2.11, it shows that the stack from the model delivers a slightly higher voltage at lower currents compared to the Nedstack, but the power output is very similar. This would indicate that the losses in the cells and the auxiliary powers are well modelled and that the stack from the calculation model is able to represent a real fuel cell stack.

2.4 Trip modelling

This paragraph describes the case descriptions and input values. These values are required to combine them with the other sub-models and determine variables such as the fuel consumption.

2.4.1 Model

Two approaches are used to model the trip for the inland ships. In the first approach, the ship speed and range are varied. This Thesis uses this approach to obtain knowledge of the PEM FC's influence on the inland ship's performance. This general approach makes it possible to establish the triangular relation mentioned earlier. The water depth is fixed to a value of 1.5 times the design draught of the inland ships. This research chose this water depth to enable the ships to have the same h_w/T relation in the Karpov resistance calculation. So in these calculations, the ships do not sail the same route concerning the water depth. The ship speeds range from 8 to 20 km/h. However, the water depth limits the speed at 70% of the critical speed in shallow water. Above 70% of the critical speed in shallow water, the power demand rises too drastically to consider. The range is set to values from 200 to 2000 km. This method sets the installed power to the maximum power demand required in the assumed water depth at the highest ship speed. This power includes the conventional diesel-generator power(s) that the PEM FC system replaces.

The second approach is to model two cases that resemble actual trips with ship speeds on different trip sections with varying water depths and a fixed trip range. This section elaborates more on the assumptions made for the second approach. The first trip is from Rotterdam to Duisburg and the second trip from Rotterdam to Basel. Both trips are modelled upstream and downstream. The upstream part and the downstream part of a trip form the total round trip. The first trip is divided into five sections and the second trip into 14 sections. For each section, a low current and a high current have been found. These currents correspond with LW depth and HW depth. Table 2.8 shows the characteristics.

Section	**Length section** [km]	**LW Current** [km/h]	**LW depth** [m]	**HW current** [km/h]	**HW depth** [m]
Nieuwe Maas	24	0	10	0	12
Noord	9	0	6	0	10
Beneden-Merwede	15	-1.5	6	-2	10
Waal	98	-4	5.16	-5	9.06
Millingen - Duisburg	87	-5	4.93	-7	8.83
Duisburg - Keulen	92	-5	4.7	-7	8.83
Keulen - Koblenz	102	-6	4.44	-8.75	8.79
Koblenz - St. Goar	29	-7	4.44	-10.5	7.61
St. Goar - Bingen	29	-8	4.35	-12.55	6.7
Bingen - Mannheim	103	-5	4.68	-7	7.03
Mannheim - Karlsruhe	65	-6	4.68	-8	7.03
Karlsruhe - Iffezheim	26	-6	4.74	-8	7.09
Iffezheim - Kembs	160	-4	5.95	-6	8.3
Kembs - Basel	4	-5	5.12	-7	7.47

Table 2.8: River section characteristics (Hekkenberg et al., 2017)

The first five sections of table 2.8 apply to trip 1, while all 14 together apply to trip 2. The order of sections top to bottom in table 2.8 represents upstream. The water depths in table 2.8 represent the values for ship 2 and 3 sailing trip 2. Appendix B show the other combinations. It is chosen to change the river depth for each ship and trip to a value at which

the lowest water depth of a section of the trip, the ship will have a clearance with the river bottom of at least 0.75 meters. The other water depths are scaled according to the "Pegel" of each section compared to the "Pegel" corresponding to the lowest water depth section on that trip (Binnenvaartkennis, 2020). This way, ships can sail with a full cargo hold and sail safely with just enough clearance in the lowest section with their desired speed. These water depths will correspond to the LW depth and low current situation. The HW depth and the current situation has been derived from the paper by Hekkenberg et al. (2017). This research will evaluate the HW depth situation to see the difference in power demand between high and low water depth. The scaling method for the LW depth situation is more like a snapshot of the river. Normally during a trip, the water depth changes continuously. This feature means that the water depth predictions can not be a 100% accurate representation of the river.

All ship speeds chosen are with respect to the ground. The ship speeds are chosen in a way that they resemble actual ship speeds seen from inland ships. These ship speeds might not be optimal ship speeds for the inland ships economically speaking. However, the trip will be sailed within a sailing time that resembles those found in the inland shipping sector. The ship speed chosen for trip 1 upstream is approximately 10 km/h with the first sections a slightly higher ship speed, due to low currents. For trip 2, an average ship speed of around 10 km/h is chosen, while sailing faster in the first sections and slower in sections 8 and 9. Section 9 is a special section of the Rhine for which an average ship speed of 6 km/h is more likely to be obtained for the HW depth case and 7 km/h in the LW depth case due to the water depth, sharp river bends and strong currents according to interviews with skippers. For trip 1 downstream, the chosen ship speeds are 17 km/h for the first two sections, 15.5 km/h for the next and 14 for the last two sections. The skipper is not likely to increase the power a lot due to slower currents. It is chosen for trip 2 downstream to have a ship speed of 17 km/h for the most part with last three sections the same ship speed as in trip 1 downstream in the LW depth situation. The HW depth situation allows larger velocities due to the stronger current. Therefore, most ship speeds in each section are set to 18 km/h. One should keep in mind that the ship speeds are speculative. The trip's due time could easily change, which would indicate that the ship could sail faster or slower. One can find the data in Appendix B that the model uses for the power prediction model. During trip 2, several locks have to be passed by the inland ships. 10 Locks are present between Karlsruhe and Basel, which means that the ships need to transverse 20 locks on the round trip. This research assumes that the ship needs 45 minutes to pass a lock based on Hekkenberg et al. (2017). This assumption indicates that the inland ships need 15 hours to transverse the locks. In this time, the inland ship does consume fuel. This research includes a factor to compensate for the fuel consumption when the ships pass the locks. The factor is 1.01, so the ships contain 1% of extra fuel to pass through the locks.

2.4.2 Verification

The power model verification partly verifies the trip model. The trip model applies the water depth and the water current on the power model, and this input results in power demand in each section.

However, there is one part to verify. The model calculates the power requirement in each section of the trip. The maximum power demand in either the LW or the HW situation determines for each ship and trip type the minimum installed power on the ships. The installed power leads to different power loads per section, which results in various FC system efficiencies. So as mentioned before, the increase of fuel cell stacks leads to lower load factors. In other words, the power increase results in higher system efficiencies and lower fuel consumption. This effect should be reflected by the inland ship's fuel consumption when the calculation model increases the number of stacks.

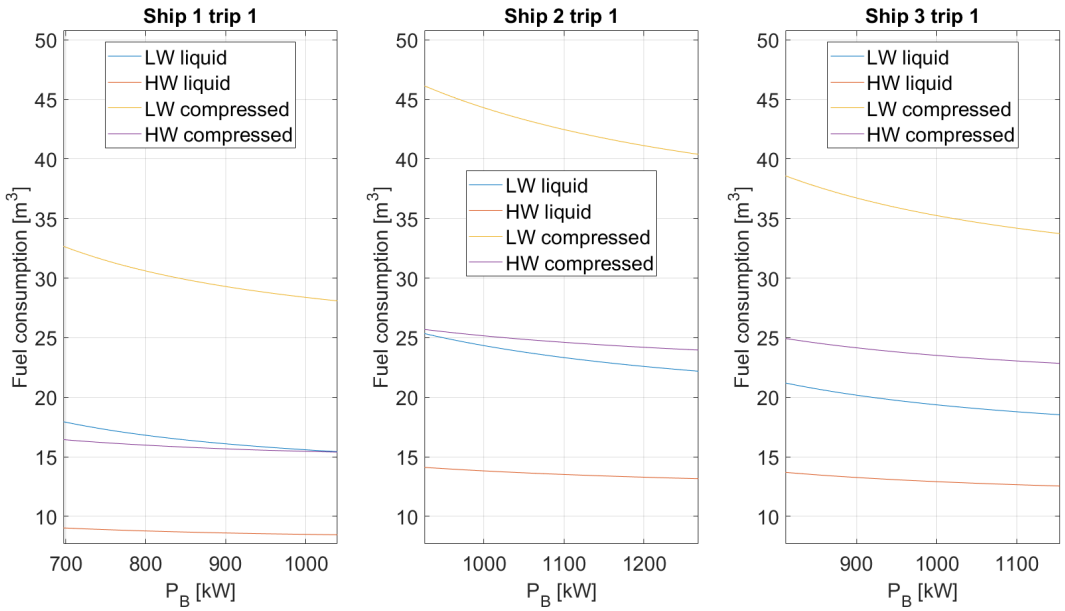

Figure 2.12: Fuel consumption for trip 1

Figures 2.12 and 2.13 show the fuel consumption versus the number of stacks installed for each ship in the HW and LW depth situation for compressed and liquid hydrogen storage. In other words, fuel consumption versus the power installed.

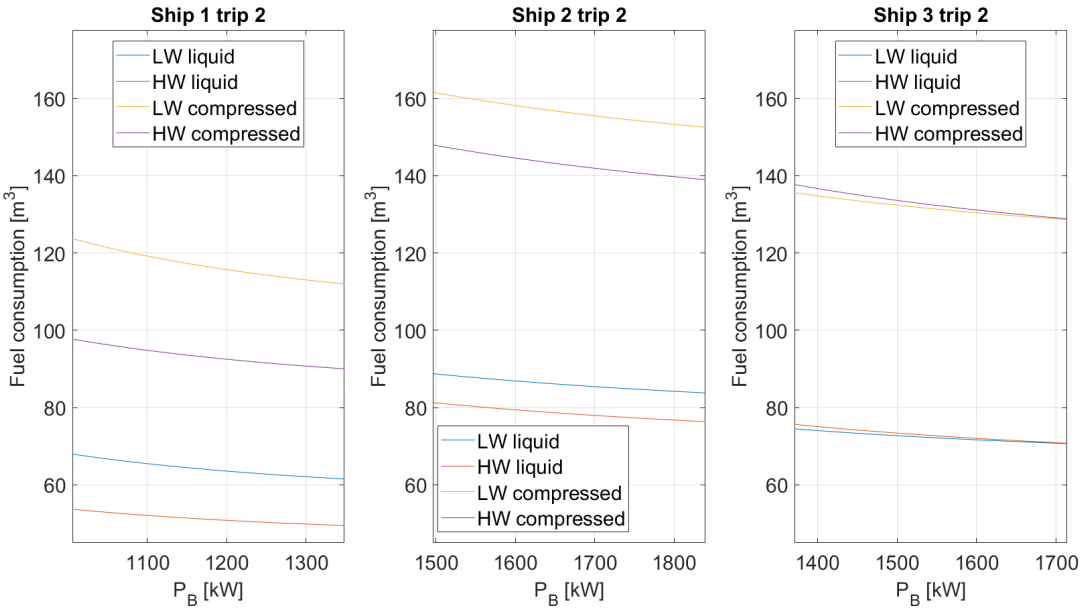

Figure 2.13: Fuel consumption for trip 2

The result mentioned earlier are reflected in figures 2.12 and 2.13, the fuel consumption per trip decreases with the increased power installed. However, for each trip, the ships have a smaller decrease in fuel consumption for the HW depth situation. In the HW situation, the power loads are already more beneficial than the LW loads. The lower power loads lead to less reduction in fuel consumption when the power is increased. The difference between compressed and liquid hydrogen in LW or HW is due to the difference in their storage densities. Liquid hydrogen has a density of 71 kg/m^3 and compressed hydrogen under 700 bar obtains a density

of 39 kg/m^3. In mass, the consumption of hydrogen is equal for the compressed and the liquid state. In volume, the compressed fuel volume is 1.82 times higher than the liquid volume. The difference in LW and HW fuel consumption is explained in the difference in power demand in the section. Overall, the power demand is higher in the LW condition compared to HW condition. Higher power results in higher required fuel flow for the engines and results in larger fuel consumption. The difference is larger between LW and HW for trip 1 compared to trip 2. The required powers in LW condition are much closer to those in HW condition for trip 2, hence the smaller difference in fuel consumption. This feature does not apply for ship 3 sailing trip 2. In ship 3's case, the overall power demand is slightly higher in the HW condition compared to the LW condition. This higher power has resulted in higher fuel consumption in the HW condition.

The power demand and fuel consumption heavily depend on ship speed and water depth. If one would choose higher velocities for the inland ship in the HW condition, it will lead to higher fuel consumption. The HW condition will then determine the minimal installed power. It will have higher power demands in this condition compared to the LW condition. Table 2.11 shows for the corresponding situations the fuel consumption in case of diesel fuel to compare these values to the values obtained in case of hydrogen fuel. Figures 2.12 and 2.13 with table 2.11 shows the difference in storage densities between the two fuels. The ships require much less volume for the trip completion in case of diesel fuel.

2.4.3 Validation

The validation of the trip model is also partly performed in the power model's validation for the same reasons as the trip model's verification.

One part to check is whether the total sailing time of the entire trip is realistic for an inland ship and the other part is to check if the calculation of the fuel consumption checks out with real inland ships. The total sailing times are given in table 2.9.

Trip in LW condition	**Sailing time**	**Unit**
Trip 1 up	23.6	Hours
Trip 1 down	14.2	Hours
Trip 1 total	37.8	Hours
Trip 2 up	89.7	Hours
Trip 2 down	50.1	Hours
Trip 2 total	139.8	Hours

Table 2.9: Predicted sailing time for each trip

The ship speeds are the same for each ship which means they have the same sailing time of each trip. The sailing time is quite speculative. Still, the chosen ship speeds should be realistic to result in viable values for fuel consumption. The length of the round trip 1 and 2 are 466 and 1686 km. The inland ships have an average ship speed for trip 1 and 2 of 10.3 and 9.9 km/h upstream. For sailing downstream, the ships have an average ship speed of 16.4 and 17.2 (LW and HW), and 16.8 and 17.8 (LW and HW) for trip 1 and 2. Trip 2's sailing time is excluding the extra time to pass the locks. This aspect means that a factor should be included for the average fuel consumption when passing through the locks for trip 2. From an interview with a skipper, knowledge has been obtained about sailing times for trip 2. It is a 135x11.45x3.6 meter ship that sails up and downstream from Rotterdam to Basel based on sailing 16 hours per day. The skipper performed several round trips and said that he needed six days to sail upstream and four days to sail downstream. These numbers result in 96 hours upstream, 64 hours downstream and total sailing time of 160 hours in lower water depths.

Between Mannheim and Basel are ten locks present. Therefore, 20 locks have to be passed for the entire trip as was mentioned earlier. The ships need approximately an additional 15 hours to transverse the locks. With this information, it seems the model does represent the trip well, see the comparison in table 2.10.

Sailing time	**Ship model LW**	**Ship skipper**	**Unit**
Upstream	97.2	96	Hours
Downstream	57.6	64	Hours
Total	154.8	160	Hours

Table 2.10: Sailing time trip 2, locks included

The ships from the model seem to sail faster downstream and slower upstream in the LW depth situation. This research has implemented diesel engine specifications to compare the calculated fuel consumption with values from inland ships. Specific fuel consumption of gas oil is assumed 210 g/kWh (Hekkenberg et al., 2017).

Ship	**Trip 1**		**Trip 2**		**Unit**
	LW	HW	LW	HW	
Ship 3 model	5.19	3.69	20.62	20.18	m^3
Inland ship skipper	6.5	7.5	22	28	m^3

Table 2.11: Comparison gasoil fuel consumption model vs. inland ships

In table 2.11 a comparison is displayed of the three ships from the calculation model and the inland ship mentioned earlier. The inland ship from the skipper is the 135-meter long ship, which this research uses in previous examples. The difference in fuel consumption is small between the ships from the model and the inland ship. Ship 3 model and inland ship skipper should have more similar values since they have the same dimensions and almost the same propulsion arrangement. In this comparison, the LW situation seems to give more appropriate values for simplified fuel consumption. On the other hand, the HW situation differs quite significantly. The skipper often uses more or less the same power throughout the entire trip, while in the model, the calculations for the fuel consumption are based on the minimal power demand per section. The fuel consumption is higher if the minimum required power installed in the inland ship is used to determine the fuel consumption for the entire trip. Also, the chosen speeds could be different from the ship speeds the skipper would choose. Also, in the model, a fuel buffer is included to increase fuel consumption. The river is not ideal in shape and bends, so this fuel buffer compensates for that slightly.

Chapter 3

Design Assumptions

This chapter elaborates on the design assumptions taken into consideration in this Thesis. This research needs to establish design assumptions to calculate several output variables, such as the total cost and the new cargo space capacity. These assumptions finalize the calculation model and enable the model to determine the necessary variables. The introduction of a LT-PEM FC system results in alterations in the propulsion system design and the cargo space capacity. As mentioned, an electric motor is introduced instead of the conventional diesel engine. The LT-PEM FC and the complex storage system has to be designed on the ship as well. This system is associated with regulations concerning the construction and the safety on the ship. This chapter discusses the design implications of the new system to create a concept design. This concept design is linked to the calculation model to make correct calculations. This research proposes three designs for the inland ships. Also, the bulk and container carrier design will be discussed for these designs. From these designs, one is chosen and incorporated in the calculation model. To be able to apply the calculation model, the design assumptions have to be determined. These assumptions come partly from the design proposal as well as some general assumptions. It is not discussed in the calculation model what happens with other propulsion and auxiliary system and how this is reflected in the total system lay-out so more elaboration on this in this chapter. This chapter also elaborates on the hydrogen storage size and the cost overview of the new system.

3.1 Costs

Although the costs are not directly a design implication, the new system does imply new cost components. These components need to be discussed and taken into account. This paragraph discusses a cost overview which enables this research to analyze the PEM FC system with hydrogen storage. The model applies this overview to different storage options and ship design. With the cost overview, a step towards the required freight rate of the ships is made. The inland ship's total cost includes building cost and operational costs. The overview of these cost components are given in tables 3.1 and 3.2.

Building costs System or part	Value	Unit	Note/source
Steering	$n_{prop} \cdot 50.000$	$Euro$	(Hekkenberg, 2013)
Propeller & shaft	$n_{prop} \cdot 60$	$Euro/kW$	(Hekkenberg, 2013)
Gearbox	40	$Euro/kW$	(Hekkenberg, 2013)
Diesel engine	220	$Euro/kW$	(Hekkenberg, 2013)
Navigation, wheelhouse, etc.	100.000	$Euro$	(Hekkenberg, 2013)
Other equipment	See Hekkenberg (2013)	$Euro$	Mooring, outfitting, raiseable column, bilge and hatch covers
Steel	See Hekkenberg (2013)	$Euro$	Includes hull, accommodation, piping and yard cost
Electric motor and controller	500	$Euro/kW$	(Abma, Verbeek, Kelderman, Hoogvelt, & Quispel, 2018)
Electrical system + Gen-set	500	$Euro/kW$	(Hekkenberg, 2013)
PEM FC	280	$Euro/kW$	(van Biert, Godjevac, Visser, & Aravind, 2016)
Storage liquid H_2	9.78	$Euro/kWh$	(Rivard, Trudeau, & Zaghib, 2019)
Storage comp. H_2 at 700 bar	15.98	$Euro/kWh$	(Paster et al., 2011)

Table 3.1: Building cost assumptions of ships

This research estimates the building cost of the inland ships to determine the depreciation and amortization cost. The depreciation charges consist of those of the hull, the machinery and other equipment. Amortization is included in the form of interest over the total investment. A few more assumptions are made in this Thesis to calculate the total cost of the cost components.

- The rest value of the machinery and hull is assumed to be 5% and 15% of its total value (Hekkenberg, 2013).
- The hull's depreciation period is assumed to be 30 years, based on Beelen (2011).
- The lifetime of the electric motor is 15 years (Barnes, 2003). Most machinery has the same lifetime as the electric motor.
- The lifetime of the PEM FC is set at 40.000 running hours (Smit, 2014).
- The lifetime of both hydrogen tanks types is assumed to be 15 years (Zhang, Lundblad, Campana, & Yan, 2016).

The costs of both hydrogen storage options show that compressed hydrogen tanks are more expensive than liquid hydrogen tanks. This difference occurs due to the expensive carbon fibre material needed to have a strong storage tank to hold the compressed hydrogen. This research has based the prices of the storage units on small tanks from the automotive industry. Large tanks for maritime purposes might reduce the cost per kWh. This uncertainty means that the hydrogen storage price could be less. The price of the PEM FC is assumed to be equal to 280 euro/kW (van Biert et al., 2016). This assumption is based on the automotive industry and depends on the production volume. The PEM FC price could be higher than 280 if the production volume of fuel cell vehicles is low. It could reach values up to 1000 euro/kW. This uncertainty means that the cost of the PEM FC system could be much higher. So a payback time of 20 years is assumed, with an interest rate of 5% on the investment. Furthermore, the owner should have at least 40% of the total investment as equity. The operational cost has to be included in the total cost as well. Table 3.2 displays these cost components.

Operational costs System or part	Value	Unit	Note
	9.54	$Euro/hour$	Apprentice sailor, CBRB (2020)
Crew cost	10.93	$Euro/hour$	Sailor, CBRB (2020)
	12.85	$Euro/hour$	Skipper, CBRB (2020)
O&M FC	41.65	$Euro/(kW * year)$	(Lipman, Edwards, & Kammen, 2004)
O&M DE	6.66	$Euro/MWh$	(Hekkenberg, 2013)
Liquid Hydrogen fuel	4.08	$Euro/kg$	(Collins, 2020)
Compressed Hydrogen fuel	4.00	$Euro/kg$	(Paster et al., 2011)
Diesel	350	$Euro/m^3$	
Insurance	1.5	% of total cost	(Hekkenberg, 2013)
Overhead	0	$Euro$	(Hekkenberg, 2013)
Maintenance ship fixed	5	$Euro/(m^3 * year)$	(Hekkenberg, 2013)
Maintenance ship variable	0.009	$Euro/(kWh * year)$	(Hekkenberg, 2013)

Table 3.2: Operational cost assumptions of ships

The model adds the operational costs to the cost components induced by the building cost to complete the total cost calculation. This research bases the operation and maintenance cost of the PEM FC on a medium-cost case of a 250 kW stationary FC unit (Lipman et al., 2004). This unit is somewhat smaller than the FC units in this research, so this cost component entails a bit of uncertainty. The overhead cost is assumed zero because it is much smaller than the other costs (Hekkenberg, 2013). The crew cost includes three different crew types, the apprentice sailor, a sailor and a skipper. It is assumed that the inland ships have to be able to sail 18 hours per day. This assumption and the regulations of the CBRB indicate the number of crew members that should have to be present on each inland ship. The number of crew members is:

- Ship 1: Two skippers, and one apprentice sailor.
- Ship 2: Two skippers, one sailor, and one apprentice sailor.
- Ship 3: Two skippers, one sailor, and one apprentice sailor.

This information shows the minimum amount of crew cost for each ship. All information above makes it possible to estimate the total cost of the inland ships. This research uses the information to determine a minimal required freight rate of the ships. The required freight rate will show the influence of the fuel cell installation and different hydrogen storages. The total cost for a conventional inland ship with a diesel engine is calculated to compare with the PEM FC configuration.

3.2 Hydrogen storage

With the base of the model ready, the calculations can move towards the cargo loss induced with the instalment of hydrogen storage with a PEM fuel cell onboard the inland ships. A few other steps have to be taken to get to the point of determining the loss of cargo space. First, the required fuel flow is determined during the trip. Afterwards, the minimum fuel capacity of a round trip is calculated and the loss of cargo space. The loss of cargo space determines to what extend the inland ships will miss out on revenue of fully-loaded trip. With this knowledge, the loss of cargo space can be determined as a function of the ship's range and the ship speed.

3.2.1 Fuel storage assumptions

With the ship speed, the range and the fuel flow, the calculation model can determine fuel consumption. The required hydrogen fuel is calculated by multiplying the mass flow of hydrogen of each section with the ship's sailing time on that section. These amounts of fuel are summed up and divided by the hydrogen density of each storage condition. This calculation results in the consumed hydrogen per trip or range. This amount of consumed fuel is not enough to count as the total amount needed to complete the trip. The skipper would not arrive at its destination with the slightest deviations in sailing during the trip. Therefore, it is assumed that the required fuel is 90% of the total fuel capacity present on the ship. Another issue regarding the fuel capacity is the ability to empty the tanks. According to Adams et. al (2018), 95% of the tank is available for usage, so the fuel capacity increases slightly.

3.2.2 Hydrogen storage tanks

It needs to be discussed how the hydrogen tanks would fit in a ship's space based on their cylindrical shape. Looking at the shape of a circle in a square, you would have a fraction of $\frac{Area\,of\,circle}{Area\,of\,square} = \frac{\pi r^2}{2r \cdot 2r} = \pi/4$ of volume available for storing the hydrogen, if assumed these cylinders need the square space. Also, the casing of the cylindrical tank takes up space outside the fuel volume itself. For the compressed hydrogen tanks, this is the material given the tanks' strength. For the liquid hydrogen tanks, it is the material for strength and insulation of the tank. These aspects reduce the fraction of volume of $\pi/4$ significantly. Another feature of the storage tanks is that the tanks have an elliptical shape as tank head instead of a flat head. The same idea as the circle in a square is assumed here. This feature reduces the volume fraction even further. The last part of the storage that needs to be considered is other necessary equipment, such as valves, pipes. This equipment will use space as well. These reasons have led to the idea to determine a volume fraction for the liquid and compressed hydrogen storage based on data on these storage units. Equation 3.1 shows the volume fraction calculation for the two storage options. The numbers in the liquid hydrogen fraction are based on an automotive tank from Aerogels et al. (2017) and the compressed hydrogen numbers on an automotive tank from Rivard et al. (2019).

$$\begin{aligned} f_{V,liquid} &= \frac{V_{fuel}}{V_{box}} = \frac{V_{fuel}}{L_{tank} \cdot D_{tank} \cdot D_{tank}} = \frac{100}{12.565 \cdot 4.522^2} = 0.39 \\ f_{V,comp} &= \frac{V_{fuel}}{V_{box}} = \frac{V_{fuel}}{L_{tank} \cdot D_{tank} \cdot D_{tank}} = \frac{29}{8.27 \cdot 2.79^2} = 0.45 \end{aligned} \tag{3.1}$$

The fuel volume V_{fuel} is the volume of hydrogen that can reside in the tank. The box volume V_{box} is calculated with the outer dimensions of the cylindrical tank. The volume fraction of the liquid storage units is approximately 0.39 $\frac{V_{fuel}}{V_{total}}$ and for the compressed hydrogen storage it is approximately 0.45 $\frac{V_{fuel}}{V_{total}}$. One should know that this research has based these numbers on automotive tank values. The compressed hydrogen storage cannot become much larger due to the strength restrictions of the tanks. Therefore, this number represents the tank size well. The liquid hydrogen could be stored in larger tanks, which is more beneficial in the required space. A large tank requires less insulation and strengthening material relative to the stored hydrogen than a small tank.

3.2.3 Other considerations

It might be possible to use some space of the original bunkers as hydrogen storage. The conventional bunker capacity of inland ship 1, 2 and 3 are assumed 40, 60 and 70 cubic meters. These bunkers probably cannot be used optimally in terms of space, because they are often divided in

starboard- and port-side tank close to the hull's side. The storage of hydrogen requires cylindrical tanks and other equipment, whereas gas oil can reside easily in the conventional bunkers. It is also not saved to store pressurised hydrogen close to the hull in case of collision. However, the equipment does not use all available space in the engine rooms, so it might be possible to play around with other tanks and equipment. It could create a space to store the hydrogen properly and replaces the old bunkers. So depending on design and regulation, certain spaces can and cannot be used for hydrogen storage. A few things have to be considered regarding the design of the hydrogen fuel storage:

- The storage tanks are cylindrical with elliptical tank heads, so they do not fit properly in every space.
- The conventional diesel engine and diesel generators are replaced with the electric motor, batteries and the fuel cell system.
- It depends on the type of storage if the hydrogen and on safety regulation if the hydrogen can be stored below deck.
- Instead of the bunkers, can we move other tanks or spaces to create a more optimal room for hydrogen fuel.
- Can the tanks be stationed near the crew residences, or should they be apart.
- The hydrogen tanks can also be in exchangeable 20 ft containers, which directly impact the cargo hold. However, this feature could prove problematic in terms of coupling the fuel lines to the ship. Fixed tanks are a more safe and reliable option.

3.3 Design assumptions

3.3.1 Cargo hold

The new system replaces the conventional configuration. This new system results in a difference in the cargo space and tonnage capacity of the ships. Therefore, the cargo hold dimensions need to be assumed amongst some other design-related aspects of the ships. Table 3.3 shows the conventional dimensions of the cargo hold of each inland ship.

Ship	1	2	3	Unit
Width hold	7.7	10.1	10.1	m
Length hold	56	80.5	105	m
Height hold	4.25	4.6	4.6	m
Volume hold	1833	3740	4878	m^3
Tonnage	1650	3200	3900	ton

Table 3.3: Cargo hold dimensions

The tonnage capacity and cargo hold volume of the conventional set-up are given in table 3.3. It is assumed that the diesel generators and diesel engine(s) are replaced with the electric motor(s), the batteries, the fuel cell system and the hydrogen fuel storage. This replacement leads to a difference in the tonnage capacity of the inland ships. Equation 3.2 shows the calculation of the new tonnage and cargo space capacity.

$$\begin{aligned} Tonnage_{new} &= Tonnage_{old} + \Delta_{weight} = Tonnage_{old} + Weight_{DE} - Weight_{FC} \\ Cargohold_{new} &= Hold_{old} + \Delta_{volume} = Hold_{old} + Volume_{DE} - Volume_{FC} \end{aligned} \tag{3.2}$$

The tonnage capacity from table 3.3 is transformed in the new tonnage capacity with the first equation from 3.2. The Δ_{weight} is equal to the weight of the conventional system minus the weight of the FC system. A similar calculation is performed with the cargo space capacity, only with the volumes of the different components. The changes in the cargo hold depend on the design assumptions made. The reduction in the cargo hold volume and tonnage capacity will result in loss of revenue. This loss even occurs in lower water depths when the skipper is not able to fully load the ship. Container ship owners construct the corners of the cargo hold on the first layer with dummies of 20 ft. containers to increase container carrying capacity. This research assumes that the ship can use two of these boxes fuel or equipment storage (depending on the design all four could be used). This assumption makes the impact of hydrogen fuel storage slightly less significant. These spaces cannot be assumed as a full volume of a 20 ft container, since they fill up the hold's corners, where the ship starts to bends inwards due to the hull's shape. So it is assumed that 2/3 of these spaces is useful for storage if allowed due to regulation.

3.3.2 System components

The diesel generators are replaced with a smaller PEM FC or multiple FC systems to supply electricity to the ship's net to move towards an all-green design. The bow thruster(s) need to be replaced with ones running on an electric motor. The electricity fed to the bow thruster(s) will also come from a PEM FC. Also, a battery pack is necessary to deal with the fluctuations of power demand while sailing. If one does not install a battery pack on board of the ship, the FC system will deteriorate faster than it is supposed to. This deterioration will reduce the total lifecycle of the PEM FC system dramatically. The PEM FC's size is scaled according to the mass and volume of a 500 kW PemGen unit from the company Nedstack. From an interview with the Application Manager Maritime, it has become know that all auxiliary equipment is included in the containerised design of the 500 kW PemGen unit. This assumption will result in the PEM FC's mass and volume of the ships in this research. Table 3.4 shows an overview of all design assumptions and dimensions of the equipment that this calculation model incorporates.

Parameter	Value	Unit
Volume of 20 ft. container	33.2	m^3
Volume fraction liquid hydrogen storage	0.39	$V_{fuel}/V_{storage}$
Mass fraction liquid hydrogen storage	0.075	$m_{fuel}/m_{storage}$
Volume fraction compressed hydrogen storage	0.45	$V_{fuel}/V_{storage}$
Mass fraction compressed hydrogen storage	0.057	$m_{fuel}/m_{storage}$
Power density of lithium ion battery	220	kW/m^3
Specific power of lithium ion battery	110	kW/ton
Energy density of lithium ion battery	270	kWh/m^3
Weight of outfitting equipment	0.001	ton/kW
Mass of PEM FC + auxiliary equipment	21.9	kg/kW
Volume of PEM FC + auxiliary equipment	0.054	m^3/kW
Mass of diesel engine	5	kg/kW
Volume of diesel engine	0.01	m^3/kW
Mass of diesel generator	9	kg/kW
Volume of diesel generator	0.015	m^3/kW
Mass of electric motor	$2.4 \cdot P_B + 2.92$	ton
Volume of electric motor	4.25	m^3

Table 3.4: Design assumptions and equipment dimensions

The battery size is assumed to be equal to 10% of the minimum required power of the inland ships. The calculation model determines the battery pack's volume and weight with the battery

specifications from table 3.4 and the power assumption. The battery's power divided by the power density results in the volume. The battery power divided by the specific power results in the weight. The table shows that the PEM FC system is significant in volume and weight compared to the diesel engine. The FC system is based on the containerised design of the 500 kW PemGen from Nedstack. The containerisation results in a larger volume and weight relation concerning the power. This assumption gives some uncertainty to the installation size of the PEM FC system. Other companies might make systems more rivalling with the weight and volume specifications of diesel engines.

3.3.3 Regulation

The regulation for storing different hydrogen types as fuel is not yet determined. Therefore, this research has made assumptions about what is possible in designing the ship with hydrogen fuel. The liquid hydrogen storage cannot be stored below deck as a cargo (Tronstad et al., 2017). For the compressed hydrogen as cargo, a classification society needs to evaluate the case whether it is safe enough to store it below deck. The regulation on the liquid hydrogen as a fuel should be just as strict as the regulation for LNG fuel for ships (Tronstad et al., 2017). Not a lot of inland ships run on LNG at the moment besides some tankers. However, one ship could clarify the storage possibilities of hydrogen fuel. The Eiger-Nordwald is an inland ship refitted with dual-fuel engines running on LNG most of the time. This ship is outfitted with a 60 cubic meter LNG tank placed below deck in front of the engine room bulkhead in a special tank room (Danser, n.d.). The tank room replaces 6 TEU of capacity. This tank room is open on the top, and the side and is mechanically ventilated. The source of this information showed that Lloyd's Register approved the detailed design of this refit. This Thesis can use this example to determine the liquid hydrogen tank(s)'s location on the ships. In the Eiger-Nordwald the LNG tank is placed below deck in the cargo hold. Keeping the regulation as strict as LNG would mean that the hydrogen tank can be placed below deck in the cargo hold as a fuel. Tronstad, Åstrand, Haugom and Langfeldt (2017) becomes clear that one cannot store liquid hydrogen as cargo below deck. This research assumes that the LNG fuel comparison rule and the other considerations result in the assumption that liquid hydrogen can be stored in the cargo hold on the other side of the engine room bulkheads. The compressed hydrogen can also be stored in the engine rooms. These assumptions mean the compressed hydrogen can be stored in the engine room, on deck and in the cargo hold in these design proposals. The liquid hydrogen can be located on deck and in the cargo hold in the design proposals.

3.4 Bulk carrying inland ships

Bulk carriers are characterised by their volume and tonnage carrying capacity. They are a bit fuller in shape compared to inland container ships. The placement of heavy components is crucial for these ships. When the equipment is placed beneficially, the ships can have a more "smooth draught" and carry more cargo in extreme LW conditions. This research means with "smooth draught" that the ship has zero or a small trim forward. This trim allows it to carry more cargo and not have problems with the aftship being too deep in the shallow water conditions. When the ship needs additional space for the hydrogen storage, the cargo hold bulkhead could be moved to obtain room. This aspect reduces the cargo hold volume. Also, a part of the cargo hold could be used as storage. For example, the cargo hold's corner(s) could be enclosed and outfitted with hydrogen storage tanks.

3.5 Container carrying inland ship

Container inland ships are built to carry as many containers as possible. They are built a bit more slender in the fore- and aftship to have less fuel consumption than bulk carrying inland ships. Due to these more slender shapes, dummy containers are placed in the cargo hold to increase container capacity. Some larger container inland ships even have 40 ft. instead of 20 ft. dummy containers in corners of the cargo hold, depending on the slenderness of the hull's design.

3.6 Option 1: PEM FC and fuel in the aftship

3.6.1 Design

Carrying out the first option would mean that the entire fuel cell system and the storage is placed in the engine room in the aftship. When there is a lack of space in the engine room, it is taken from the cargo hold. This research assumes that the liquid hydrogen storage can reside in the cargo hold or above deck. In case of compressed hydrogen, a design with storage below deck is usually not allowed. However, the rules are open on a case by case basis (Tronstad et al., 2017). For compressed hydrogen, the aft engine room is used for storage if space is available. Otherwise, the calculation model subtracts space from the cargo hold. The liquid hydrogen is primarily stored in the cargo hold, but it could be stored on the deck behind the wheelhouse. When this would be the case, the design should consider the ship's height because of low bridges.

3.6.2 Pros & Cons

Every design has its advantages and disadvantages, which this paragraph will discuss. This discussion will shed a light on which design proposal performs better in terms of cost, redundancy and safety. Pros:

- The distance between the components in the whole system is short. Everything is located in the aftship, which means no long pipes, large pumps or cables. This aspect would save money.
- In terms of refuelling, all tanks are located in the aftship. This feature could prove beneficial in saving time compared to when tanks in different sections on the ship have to be refuelled after one another.

Cons:

- All the mass of the new system is located in the aftship. This aspect results in a larger trim in the aftship in empty sailing condition because the new system is heavier than the conventional system. This trim means the ship reduces its cargo capacity in more extreme LW conditions.
- The hydrogen fuel storage could propose extra safety measures because the distance between the storage, the wheelhouse and accommodation are very short.
- The ship's height could be an issue when a storage tank is placed on top of the deck behind the wheelhouse. For some ships, it could impose problems regarding their operational area.

3.7 Option 2: PEM FC and fuel in the foreship

3.7.1 Design

Another approach is to outfit the engine room in the foreship with the entire PEM FC system and the hydrogen storage. Again the compressed hydrogen unit could partially be placed in the engine room if space allows it and the remaining volume required is subtracted from the cargo hold. Now the front bulkhead is moved a certain length to the aft of the ship or spaces are enclosed to serve has storage (or engine) spaces. Usually, on top of the fore engine room, an accommodation for one or multiple crew members. This accommodation could be taken from the foreship and added to the aftship since space becomes available in this area. There is often already some space unused in the aft engine room in the conventional design of inland ships. With the diesel generator and diesel bunkers gone, additional space is created. Space could be created aft of the wheelhouse and below the front area of the aft-accommodation. This enlarged aft-accommodation could fit all crew members. This way a lot of deck space becomes available on the foreship section, which could be used to store liquid and compressed hydrogen. This way, the storage units do not directly impact the cargo hold. These storage units' height should be considered in the ship's design when installed on the deck. The shipowner might not want to exceed a certain height, so he/she can safely sail under low bridges. This suggestion depends on the sailing profile of the ship. For a container carrying inland ship, height is (often) not an issue.

3.7.2 Pros & Cons

Pros:

- The fuel storage is a significant distance away from the accommodation and the crew, which can prove beneficial in terms of safety measures.
- The distance between the components in the whole system is short. Everything is located in the foreship except for the electric motor(s), which means no long pipes or large pumps.
- Almost all mass of the new system is located in the front, except for the electric motor(s). This feature could shift the longitudinal centre of gravity more to the foreship in the empty condition. If this trims the ship more forward, the ship can obtain a more "smooth draught" in extreme LW conditions and carry more cargo.
- All hydrogen fuel is located in the foreship section. This aspect could have a positive effect on refuelling time.

Cons:

- A long and thick electricity cable has to be laid to feed the electric motor(s). This long cable induces a voltage loss when high currents occur. Other cables are present to deliver electricity to all equipment on board of the ship, so it might not be an issue to have another long cable.
- It might impose problems for the shipowner depending on the operational area if the hydrogen fuel storage becomes too high on deck. If the owner wants to operate in areas with low bridges, he/she might not be able to transverse under the bridge if the hydrogen storage tanks are too high.

3.8 Option 3: Distributed design

3.8.1 Design

A distributed design gives a bit more freedom in outfitting both engine rooms. The PEM FC could be split into two or several smaller systems with at least 1 in each engine room. This way, the hydrogen storage tanks have to be distributed among the aft- and foreship, to have a short distance between the fuel tanks and the fuel cells. The location of the battery packs is not dependent on the fuel supply or the fuel cell itself. This aspect could prove beneficial in terms of how the ship is trimmed in empty condition, which will have an advantage in loading the ship when it sails in extreme LW conditions.

Another option is to install the PEM FC in the aftship engine room, and the hydrogen storage completely integrated the foreship. This aspect requires extra attention to fuel pump system to have sufficient flow to the FC system since the distance between the fuel tanks and FC system is significant.

3.8.2 Pros & Cons

Pros:

- It could be beneficial in terms of space if the PEM FC and the hydrogen storage are divided into smaller FC's and storage units. As a consequency, the unused spaces in the engine rooms and on deck(s) are used for hydrogen storage first. This feature could reduce the hydrogen storage's impact on the cargo hold volume.
- It gives more redundancy to the entire system to have multiple smaller FC units. Other FC unit(s) can still supply electricity when one unit is out of service, due to maintenance or repairs. In the other two design options, the FC system could also be divided into smaller systems.

Cons:

- If the hydrogen storage is separated from the PEM FC system, the FC requires a pump to obtain a sufficient fuel mass flow. This aspect would make the system more complicated and more costly.
- As mentioned before, using deck spaces for hydrogen storage could impose problems with the total height of the ship.
- Having storage in the aft- and in the foreship, could lead to a longer refuelling time. This time loss does depend on whether the refuelling station, ship or truck(s) can refuel one or multiple tanks at a time.
- With a distributed electricity system, more cables have to be laid to supply the ship's net. More cables will cost more money and voltage losses.
- In case of liquid hydrogen storage units there exists a boil-off rate. The ship could sail on the storage's boil-off if the system is designed correctly. However, if multiple units are installed on the ship, it could impose issues. This feature could mean when the storage is distributed over the entire ship multiple FC system might need to be running due to the constant boil-off. However, this does also depend on the insulation of the tanks. The insulation impacts how long the tanks can remain unused before the pressure becomes too high due to liquid hydrogen tank heating up.

3.9 Design Choice

3.9.1 Choice & reason

The calculation model incorporates one design from the three design proposals. The design choice influences the design assumptions and the impact of the PEM FC system with hydrogen storage. Based on the advantages and disadvantages proposed in all three option, it is decided that option 2 could prove more beneficial compared to the other two options. Option 2 seems more simplistic because all components of the system are near each other. The electricity cables to the back of the ship do not pose a lot of problems, because in conventional designs a lot of these cables are also present. Option 2 shows more freedom in the storage tanks' location and FC unit(s) when the accommodation is moved to the aftship. The residences are a long distance away from the storage tanks. This feature could provide more safety. The height limitation does not have to be an issue. It can also be a design choice between losing cargo space or higher storage tanks. The container carrying inland ship does not have a problem with the height limitation, because the containers themselves rise well over the hatch coaming. The improved draught in low load conditions can prove beneficial for the revenue in more extreme LW conditions. These reasons make design option 2 also more attractive compared to the other two options.

3.9.2 General arrangement adjustment

A general arrangement plan of an inland ship is used to display what the design should roughly resemble and have a better idea on how design option 2 could look. Figure 3.1 shows the original general arrangement (GA) plans of an inland ship that resembles ship 3.

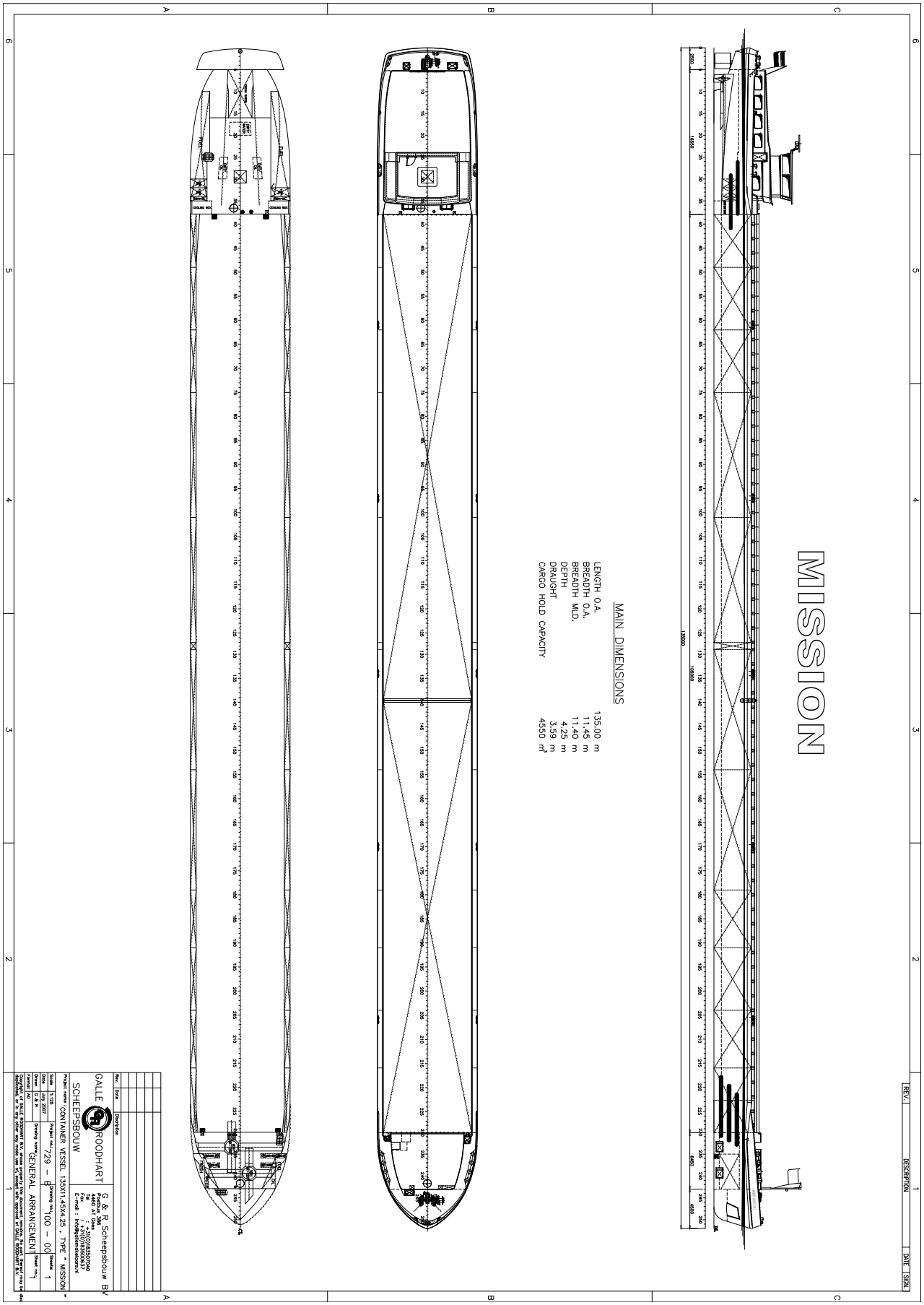

Figure 3.1: GA of inland ship type Mission (G&R, 2007)

If design option 2 is applied to the GA plan in figure 3.1, an adjustment is made in the foreship. Hydrogen tanks replace the residence in the foreship and adjustments are made in the cargo hold. Figures 3.2 and 3.3 show a sketch of the adjustments that are proposed by the design.

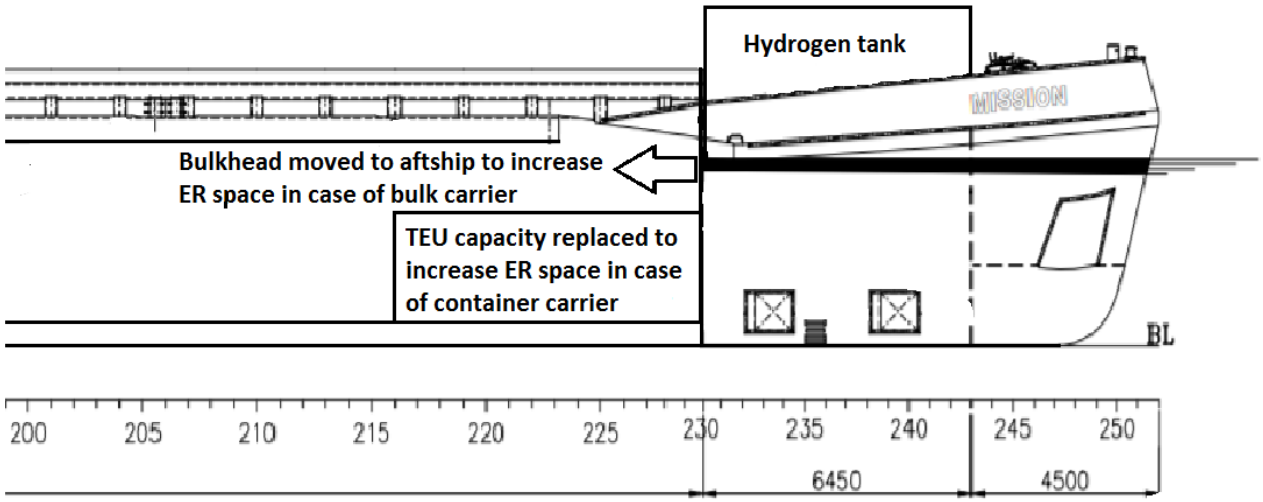

Figure 3.2: Adjusted foreship based on the proposed design option 2, side view

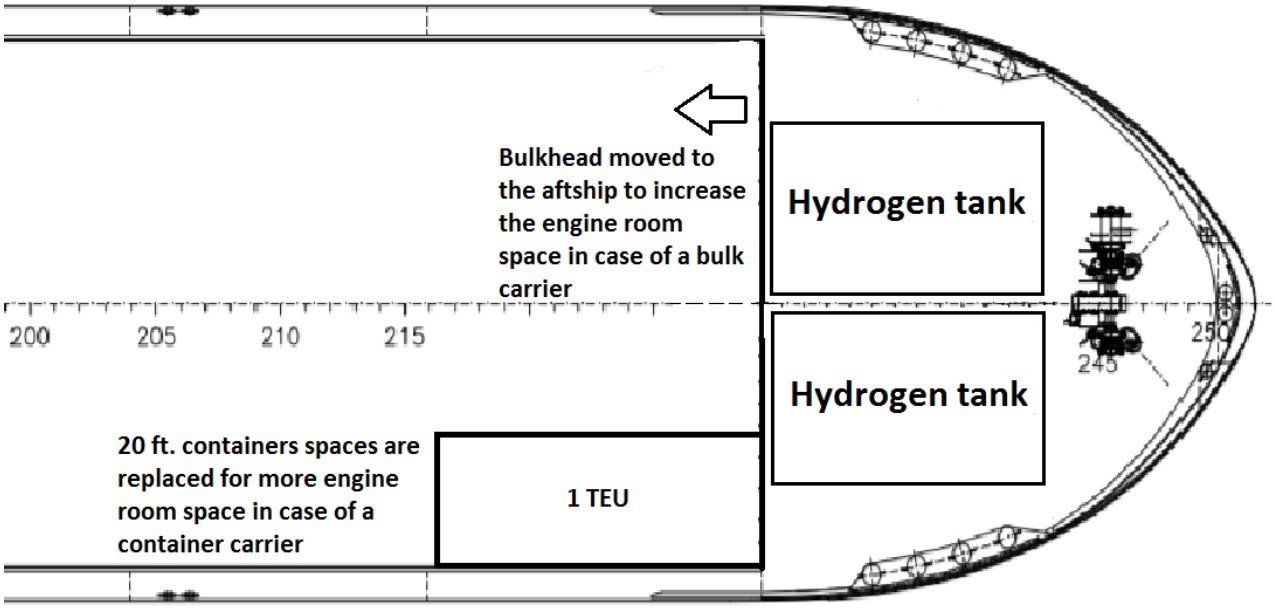

Figure 3.3: Adjusted foreship based on the proposed design option 2, top view

As figures 3.2 and 3.3 display, the tanks on deck are used first and afterwards, the calculation model takes space from the cargo hold for the hydrogen storage. The bulkhead of the foreship engine room (ER) is moved to the aftship to create space. This research installs two larger tank spaces on deck. They replace the original accommodation in the foreship. The figures only display the room used for the tanks, not the actual volume. The cylindrical tanks and the support equipment are placed inside this space. The length between the bulkhead and the front of the accommodation is approximately 6.45 meters for the 135-meter inland ship. It is used as a benchmark for the other two ships. The tank length of the other ships is approximated

by the ratio between the tank length and the ship's overall length of the 135-meter ship. The width and the height of the space on deck are trickier to assume. The hydrogen tanks on deck cannot have the same width as the cargo hold due to the ship's shape. The possible width of the two tanks together is approximately 60% of the ship width as it is sketched in figure 3.3. This research uses this measurement for the tanks' width for the two smaller inland ships. So, a singular tank has a width of 30% of the ship's width. Therefore, the tank widths are 2.85, 3.435 and 3.435 meters for ships 1, 2 and 3. The liquid hydrogen tanks can be as large as the dimensions assumed here, while the compressed tanks cannot become that large due to the strength needed for the 700 bar pressure. Aside from this, this research presumes that the tank height is the same as the width. The accommodation in the foreship is recessed in the main deck. Usually, the residence is about 2.5 meters high, so comparing this to the height assumption the tanks will be higher than the accommodation, especially for ship 2 and 3. Table 3.5 shows an overview of the approximated tank dimensions and volumes of fuel the tanks can hold.

Ship [−]	Tank length [m]	Tank width [m]	Tank height [m]	Volume tank space [m^3]	Volume liquid H_2 [m^3]	Volume comp. H_2 [m^3]
1	4.06	2.85	2.85	33.0	13.2	14.8
2	5.26	3.435	3.435	62.0	24.8	27.9
3	6.45	3.435	3.435	76.1	30.4	34.2

Table 3.5: Approximated hydrogen tank dimensions

The table shows the amount of fuel that can reside in the tanks. Less hydrogen can be present in the liquid storage compared to the compressed hydrogen. This difference is a result of the storage configuration assumed in this research. The volume needed to store a certain amount of hydrogen is assumed larger for liquid hydrogen than compressed hydrogen. The results of design option 2 results in less impact on the cargo hold volume. The volumes of hydrogen, approximated in table 3.5, are incorporated in the calculation model. First, these tanks are filled with hydrogen fuel. Afterwards, the calculation model subtracts the residual volume needed by the new system from the cargo hold.

Aside from the hydrogen storage, other components have to be installed on the ships as well. The EM(s) have to be installed in the aftship and do not contribute to the space requirements in the foreship, because the EM(s) drive the propellers. That leaves the PEM FC system and the batteries. The batteries are small compared to the FC system and do not pose a problem fitting them in the engine room. The PEM FC is quite voluminous and heavy compared to a diesel engine of similar power. The PEM FC size includes all auxiliary systems for cooling, air and hydrogen treatment, and control of these components aside from the fuel cell stacks. Only the power electronics after the fuel cell and an external cooling system are not included.

Chapter 4

Results of PEM FC Relations

In this chapter, the model of Chapter 2 and the design assumptions from chapter 3 are used to calculate the results for the PEM FC relations. The calculation model uses a speed range and a ship's range on a given water depth. This chosen speed range is from 8 to 20 km/h, and the ship's range from 200 to 2000 kilometre. The speed is limited, because of the water depth of 1.5 times the ship draught. The ship speed may not exceed 70% of the critical speed in shallow water, because otherwise, the resistance rises strongly resulting in too high power demands. The installed power affects the system efficiency of the PEM FC system. Low power loads result in high efficiency and high loads in lower efficiency. However, to obtain low loads at higher ship speeds a significant amount of power needs to be installed. The trade-off between installing more power, which increases the total cost, and lowers specific fuel consumption, which decreases fuel cost, needs to be investigated. The goal is to develop relations between the ship speed, the ship range and the cargo capacity. However, this chapter will discuss some intermediate results first to get to the cargo capacity. Afterwards, this chapter can evaluate the required freight rate of inland ships. The required power and installed power is determined, and together with the range and the ship speed, the fuel consumption is determined. Afterwards, the storage size is determined. The storage size and design assumptions result in cargo space losses. The mass difference between the conventional system and the new system results in a tonnage capacity difference. The cost is determined via the size of the components and the overview given in tables 3.1 and 3.2. The total cost with the cargo capacity determines the RFR. Figure 4.1 shows the process of the calculations. In figure 4.1, the blocks after the calculation model block are the results that this chapter discusses.

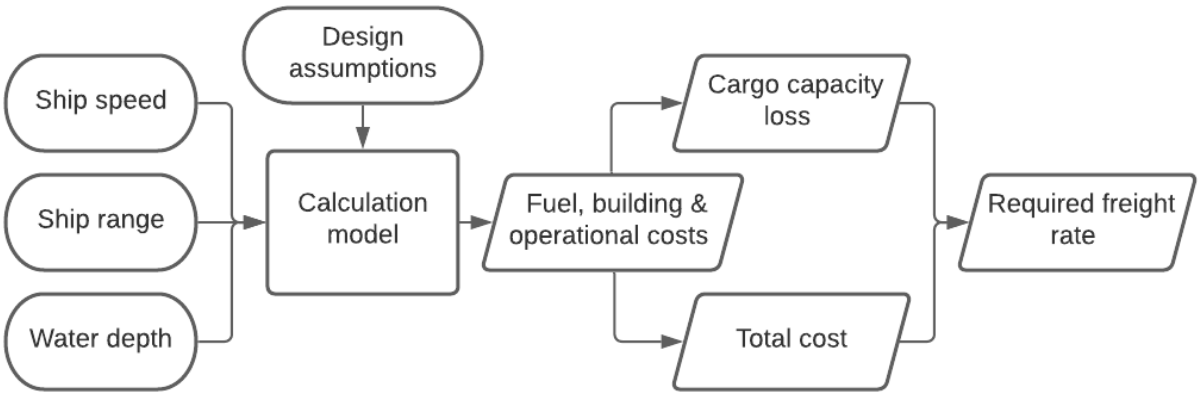

Figure 4.1: Process of general calculations

4.1 Cargo space capacity

As the chapter describes above, the first step is to determine the power demand for different ship speeds and determine the installed power. The water depth is assumed to be 1.5 times the design draught of the inland ships. This relation is chosen to enable the ships to have the same h_w/T relation in the resistance calculation of Karpov. This relations also means the ships do not sail the same route concerning the water depth. The water depths for ships 1, 2 and 3 are respectively 4.5, 5.4 and 5.4 meters. The water depth and speed lead to different power loads and therefore, to different propulsion efficiencies. With the propulsion efficiency, the calculation model determines the propulsion power. The installed power is assumed to be equal to the power required when the ship sails in water depths of 1.5 times the ship draught and at the highest possible ship speed. This assumption results in installed powers of 1314, 2559 and 2274 kW for ship 1, 2 and 3. With the installed power, the different loads on the PEM FC and the different system efficiencies are calculated for each ship speed.

4.1.1 Storage size fuel

This calculation quickly results in fuel consumption for different ship speeds and different ranges. Dividing the fuel consumption with the volume fractions gives us a quick impression on how much space each fuel storage needs. The trends of the variables are the same between the different ships. Therefore, the following figures show data from ship 2. Figure 4.2 shows the storage volume needed for ship 2 as a function of the range. Figure 4.3 shows the storage volume that ship 2 needs as a function of the ship speed.

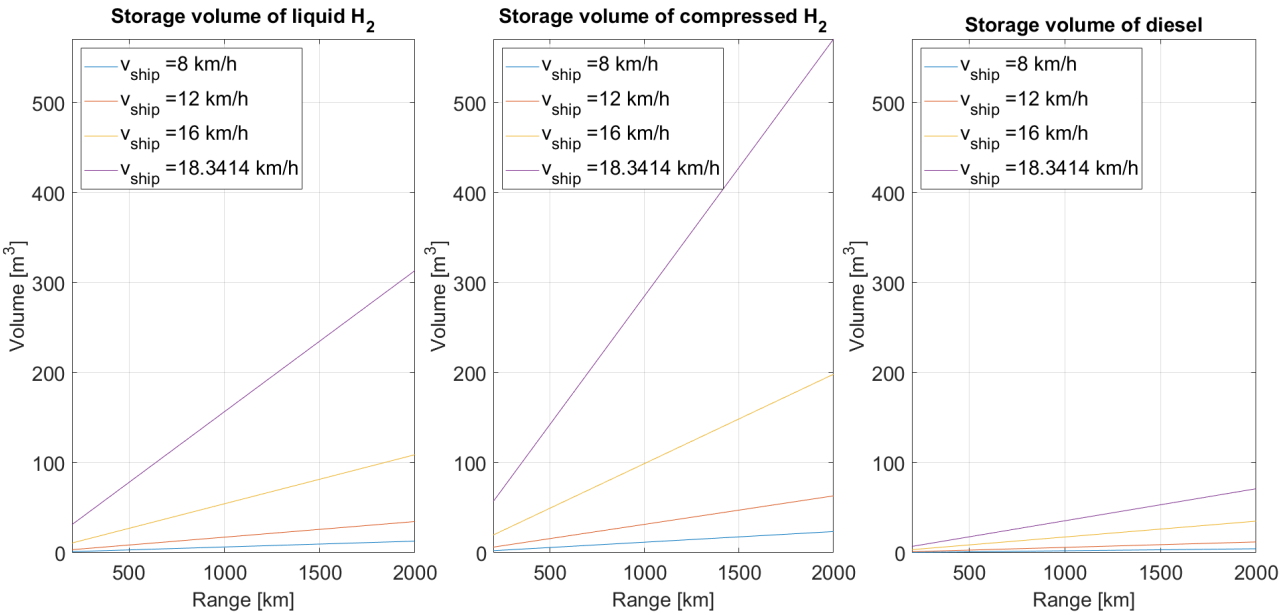

Figure 4.2: Ship 2: Fuel storage volume versus Range

Figure 4.2 shows how the fuel storage size changes for the range given certain ship speeds. The figure shows a linear dependency between the range and the fuel storage size. Although the calculation sets the ship speed up to 20 km/h, the calculation model cuts it off due to the critical speed criteria. Above 70% of the critical speed, the power demand rises drastically in shallow water. The rise of the fuel storage size becomes larger for higher speeds. This effect shows the non-linear relation with ship speed, but more on that in figure 4.3. The figure shows that the compressed storage is larger than the liquid hydrogen. Both hydrogen storage options

are also more significant in size than diesel storage. This event is expected when the storage densities than to each other. Although ship 2 is smaller than ship 3, the fuel storage is more significant. Due to the significantly better propulsive performance of ship 3, it needs less power to sail the same speeds as ship 2. This characteristic of ship 3 results in less fuel consumption.

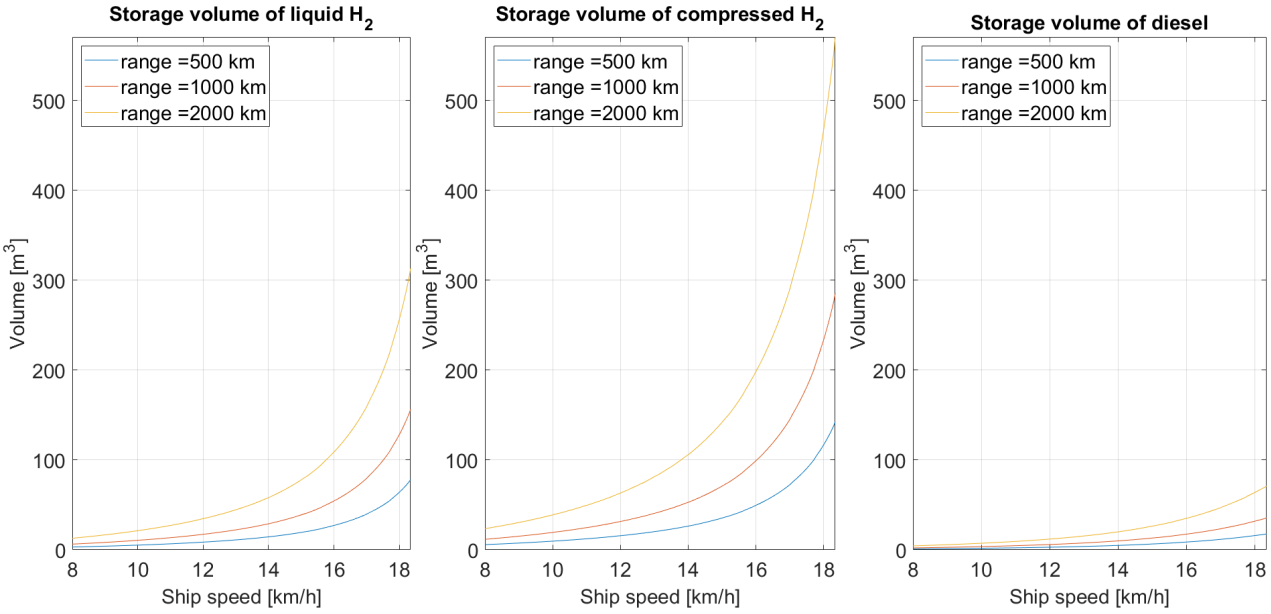

Figure 4.3: Ship 2: Fuel storage volume versus ship speed

Figure 4.3 shows a non-linear between the ship speed and the fuel storage size. At higher ship speeds the fuel storage size rises more strongly than at lower ship speeds. The power is dependent by the speed approximately to the power third, and the shallow water correction comes on top of this third power. The decrease of the system efficiency strengthens this dependency on the speed at higher loads of the PEM FC system. The figure shows how hydrogen fuel requires much more space in comparison to diesel. The compressed hydrogen option needs more space compared to the other two fuel options. The lines in the diesel sub-figure show that the ships require less space for the diesel fuel. Comparing the values to the conventional bunker sizes suggest that the inland ships can sail quite some distance even at higher speeds. Comparing this to the hydrogen fuel shows that an obscene amount of space is required to comply with such range. It will probably be better to increase the bunker frequency. If the assumptions from paragraph 3.9 are applied on the ships, the calculation model can determine the cargo space losses.

4.1.2 Bulk carrier capacity losses

Now that all design assumptions are incorporated in the model, the cargo space alterations are determined. The components' mass and volume of the new system are subtracted from the conventional components to determine the difference. This difference is the reduction in tonnage and cargo space capacity of the ships. Figure 4.4 shows the tonnage capacity of ship 2 as a function of the speed for both storage options.

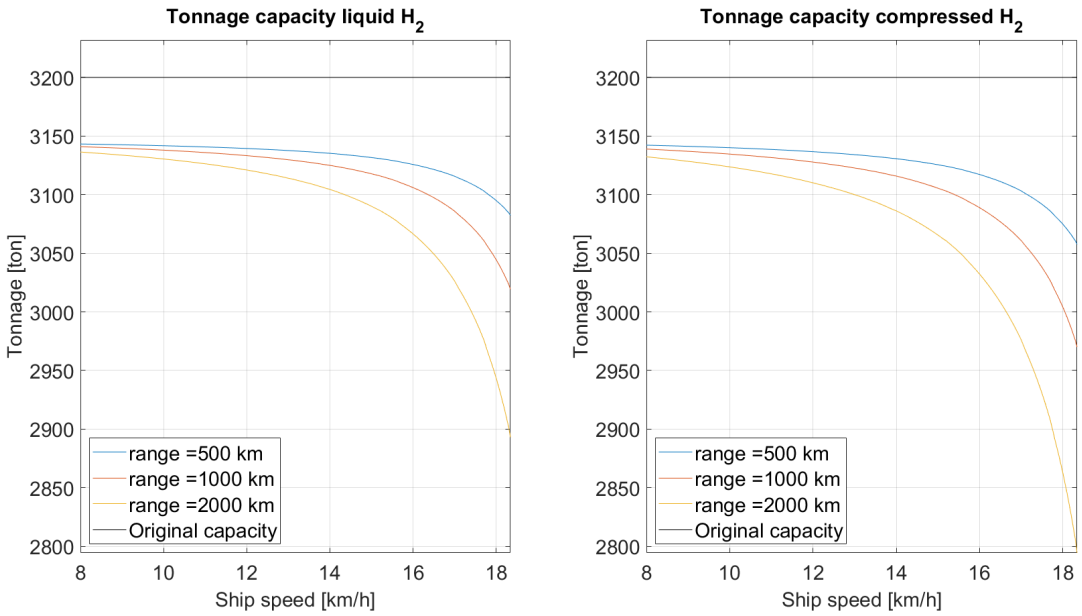

Figure 4.4: Ship 2: Tonnage capacity versus ship speed

In terms of mass, the new system is always heavier compared to the conventional set-up. The original tonnage capacity of ship 2 is 3200. The figure shows a lower tonnage capacity even at the lowest ship speed and range. The maximum new tonnage capability for the inland ships is always lower than the conventional capacity, meaning the ship initially weighs more even at the lowest ships speed and range. All ships lose tonnage capacity when the speed and the range increases. This aspect is expected because increasing the speed and range lead to an increase in the required hydrogen storage space. This decrease will affect the revenue potential of the ships. The compressed storage option is always heavier than the liquid hydrogen storage option, due to the more significant weight of the compressed hydrogen storage units. At certain speeds and range combinations, the decrease in tonnage capacity becomes more significant. When the speed increases further, the power demand becomes closer to the installed power. This speed increase results in higher power loads on the PEM FC and higher power demands. These increases lower system efficiency and raise fuel consumption. If the fuel consumption rises, the fuel storage becomes larger. The higher fuel consumption increases the weight, which lowers the tonnage capacity.

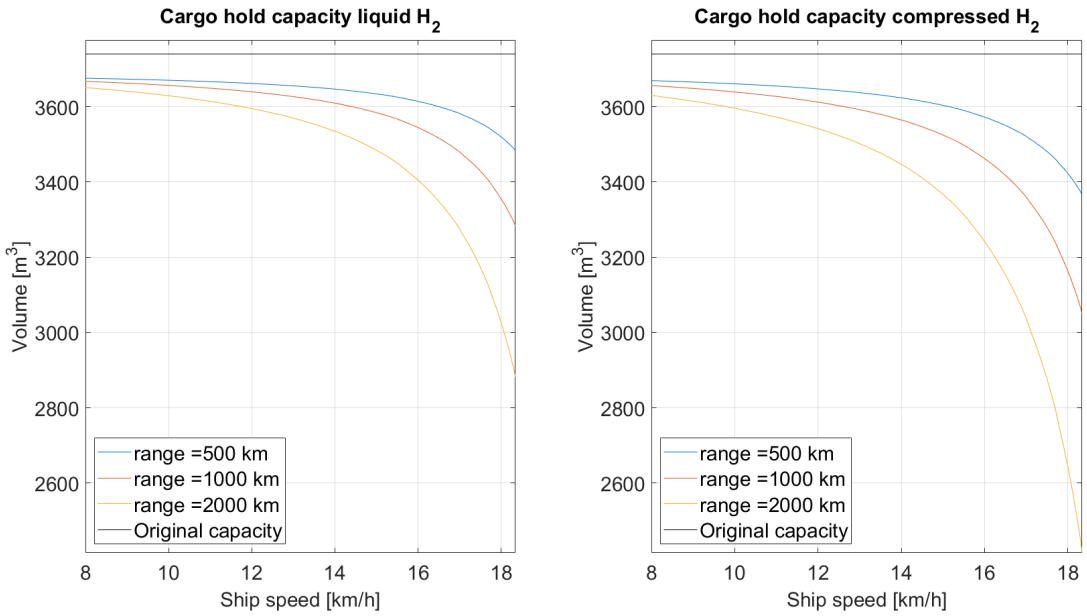

Figure 4.5: Ship 2: Cargo space capacity versus ship speed

The cargo space in figure 4.5 shows the same characteristic as the tonnage capacity. The hydrogen fuel storage requires more volume for longer ranges and higher speeds. These volumes are subtracted from the cargo hold volume. The space requirement for compressed hydrogen storage is more voluminous compared to liquid hydrogen. The same effect occurs to the cargo hold volume when the speed increases. In tonnage capacity, the ships can lose from 2% up to more than 12% of their conventional tonnage capacity. Comparing this to the volumetric losses shows much more loss in terms of space. The cargo space is reduced by at least 2%. This reduction can move up to 35% for ship 1, 32% for ship 2, and 20% for ship 3. Ship 3 can perform better in terms of the propulsive efficiency, which leads to less fuel storage requirements overall. At highest range and ship speed ship 1 loses in terms of tonnage and cargo space: 11.9 and 35.0 percent respectively, ship 2: 11.6 and 32.4 percent, and ship 3: 8.0 and 20.4 percent. These losses are in case of the compressive hydrogen storage option. The liquid hydrogen variant saves up to 2.9 for ship 1, 2.8 for ship 2, and 1.9 percent for ship 3 for the tonnage capacity compared to the compressed storage. In terms of cargo space-saving 12.8 for ship 1, 11.8 for ship 2 and 7.6 percent for ship 3. Due to the higher storage density of the liquid hydrogen, the loss in tonnage and cargo space capacity is less. The loss in tonnage and cargo space capacity is also dependent on the range. Figures 4.6 and 4.7 show the tonnage and cargo space capacity as a function of the range of the ships.

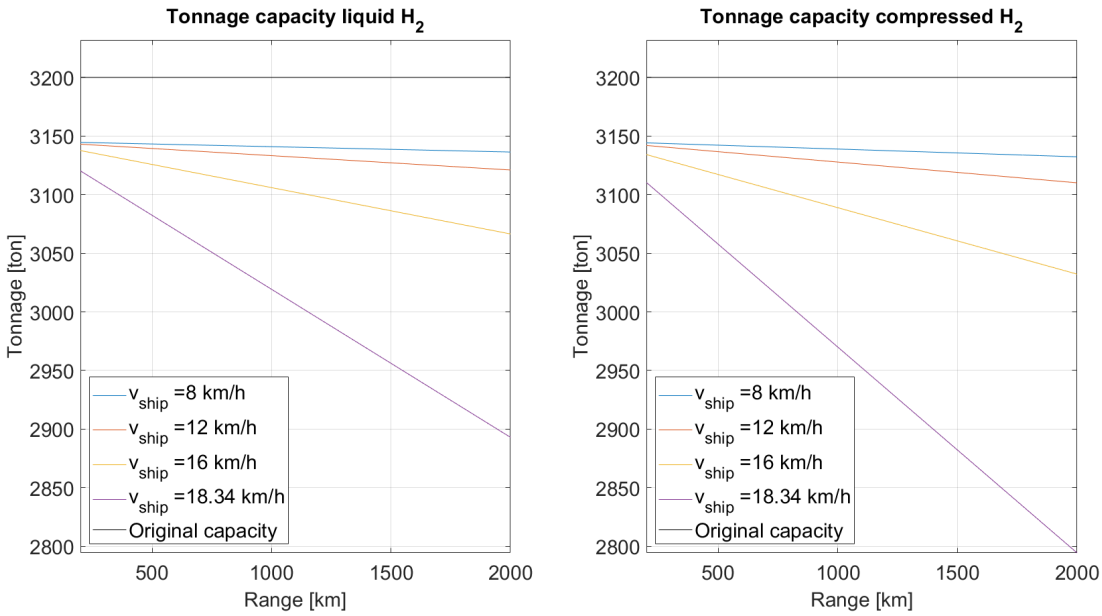

Figure 4.6: Ship 2: Tonnage capacity versus range

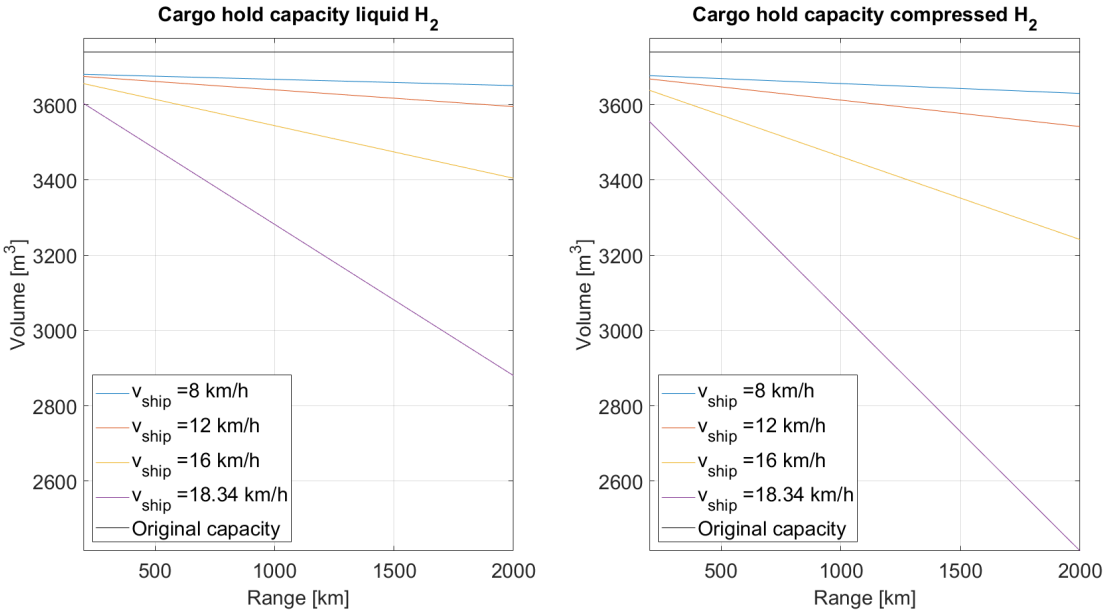

Figure 4.7: Ship 2: Cargo space capacity versus range

The cargo capacity loss is linear dependent on the ship's range because fuel consumption is linear to this range. The ships do not lose a lot of cargo capacity at very low ship speeds even for very high ranges. The decrease in capacity becomes larger at higher ship speeds due to the higher power demands. The PEM FC's low system efficiencies amplify this decrease. All figures show that the new system, keeping in mind the design assumptions made, requires more volume than the conventional set-up and the mass on board of the ship increases compared to the original set-up.

4.1.3 Container carrier capacity losses

The decrease in cargo space capacity affects the container capacity of the ships. The only difference in the cargo hold reduction and the container capacity reduction is that ship 2 and 3 have 20 ft. dummy containers placed in the cargo hold. 2/3 Of two dummies' volume in the foreship are assumed to be usable. The model subtracts these volumes from the volume required by the new system. Figure 4.8 shows the container capacities of ship 2 as a function of the ship speed.

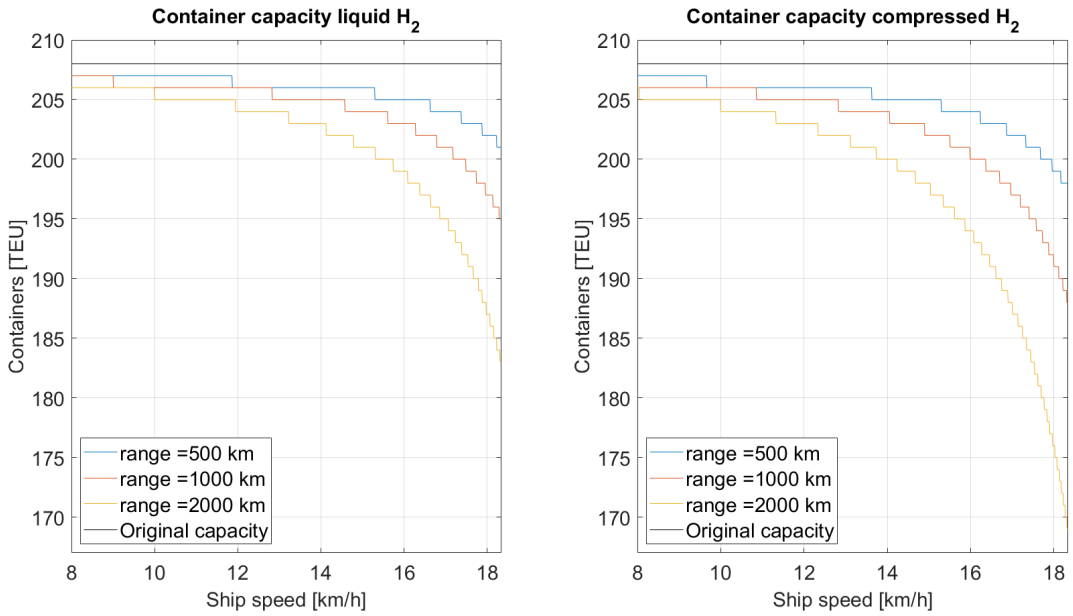

Figure 4.8: Ship 2: Container capacity versus ship speed

The container capacity of ship 2 shows a similar characteristic to the cargo volume figure. The difference between the cargo hold volume and the container capacity is that the volume is replaced with 20 ft dummy containers as it was explained earlier. When the new system's volume fills one 20 ft container, another dummy is installed. It decreases the container capacity step by step when the speed or the range increases of the inland ships. It stands out that the decrease in container capacity becomes larger at higher speeds or ranges. This fast decrease in capacity is also visible in figures 4.4, 4.6, 4.5, and 4.7 about the tonnage and cargo space capacity.

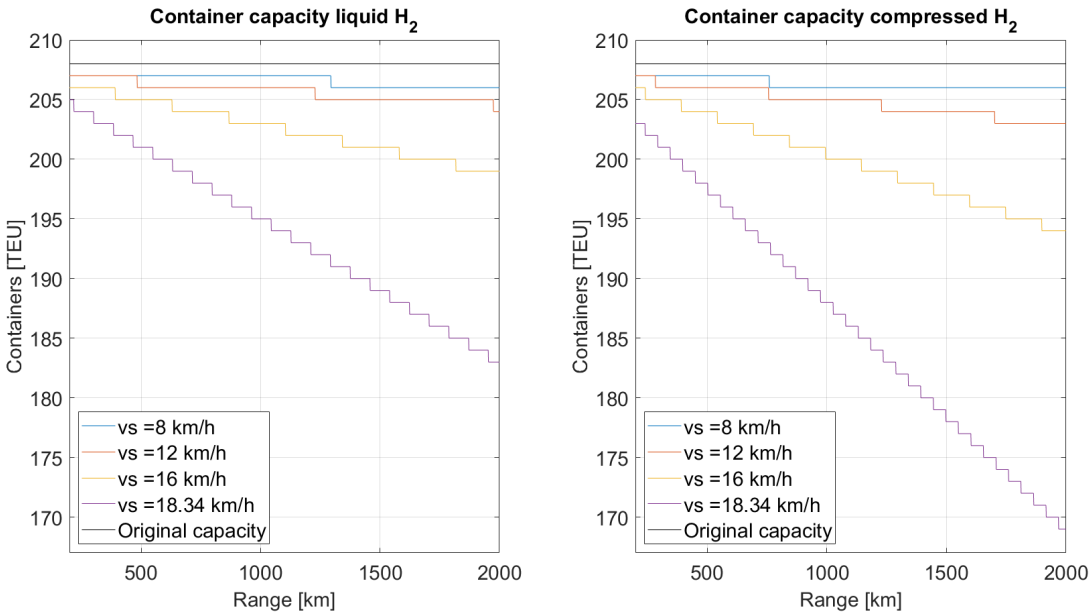

Figure 4.9: Ship 2: Container capacity versus range

As is also displayed in figure 4.9, initially ship 2 already loses space. This feature happens due to the electric engine, battery pack, PEM FC, and fuel storage volumes at the lowest range and lowest speed. Ship 1 already loses 2 container spaces for both the liquid and the compressed storage option, see figure D.1 and D.2. Ship 1 and 2 lose one container space initially for both storage options. Ship 3 does not lose any capacity for both liquid and compressed hydrogen storage. The ship has enough space for the new system at low ship speeds and ranges not to lose container capacity. These losses can go up to 18 and 30 for the liquid and compressed storage options respectively when the owner of ship 3 sails the longest range as fast as possible. Ship 1 and 2 can lose even more container capacity relative to their original container capacities. The shipowner should make careful consideration in what he or she wants to achieve. Therefore, this research should look at the cost and the required freight rate to say more about the cargo space losses. The linear dependence on the range and non-linear dependence on the ship speed are visible in figures 1 and 2 about the container capacity. Only the stepwise reduction in the container capacity makes the lines different from the cargo space capacity reduction.

4.2 Total Costs

The model determines the total cost because it is the final component needed for the RFR. To calculate the total cost, the cost overview in tables 3.1 and 3.2 are used. This table shows the building and operational cost components. The depreciation cost is determined of the parts of the building cost. The calculation model determines the interest based on the total investment. These costs are added to the operational cost. All cost components are scaled to different ship speeds and sailing times. This calculation results in the total cost being dependent on the ship speed and the range. First, this paragraph discusses some cost components. A few components depend on the installed power of the ship. The installed power is assumed constant, which makes the investment cost of these components fixed. The fixed cost components are given in table 4.1.

Part/system	Ship 1	Ship 2	Ship 3
The PEM FC system	352.000	691.000	605.000
The electric motor	588.000	1.180.000	1.020.000
The batteries	21.700	43.400	37.500
The gearbox	47.700	94.300	81.600
The propeller	70.600	141.000	245.000
The steering equipment	50.000	50.000	100.000
The hull (steel + yard)	2.500.000	3.800.000	4.890.000
Other machinery	295.000	392.000	410.000
Investment without hydrogen storage	3.920.000	6.390.000	7.390.000
Investment of ship with diesel	3.260.000	5.050.000	6.240.000

Table 4.1: Investment cost of building components

Table 4.1 shows that the ships' total investment without the fuel storage is already significantly higher than conventional inland ships. The electric engine is expensive while the PEM FC system also costs more than a conventional diesel engine. The FC's price is already an optimistic price of 280 euro per kW (van Biert et al., 2016). Only the storage cost of the hydrogen fuel is not a fixed cost among the building cost. It is dependent on the range of the ship as well as the ship speed. The liquid hydrogen storage cost ranges from 27.700 to 3.760.000 euro for ship 1, 42.300 to 7.080.000 euro for ship 2 and 36.800 to 5.950.000 euro for ship 2. The storage cost can become a large portion of the total cost when the shipowner would decide to sail fast and have a long-range. The depreciation cost is calculated according to the rest value and lifecycle period of each component. All component's cost added together result in the total depreciation cost. The operational costs are added to this depreciation cost, which results in the total cost. An overview is made to show the cost components relative to the total cost. Figure 4.10 displays this overview of ship 2. Appendix D displays the overviews

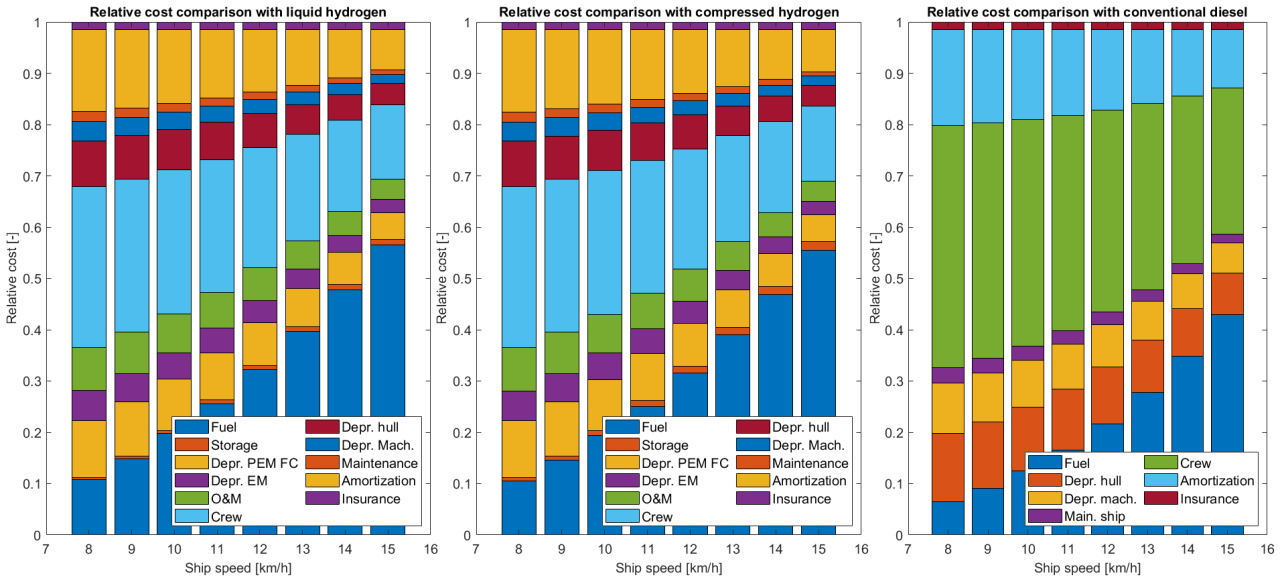

Figure 4.10: Ship 2: Relative cost of cost components

of ship 1 and 3, which show the same trends as ship 2. The cost overview is given for a ship speed from 8 to 15 km/h with a range of 500 km. Figure 4.10 shows that hydrogen fuel cost is a significant portion of the total cost, especially at higher ship speeds. The fraction of the hydrogen fuel cost is higher compared to the part of the diesel fuel cost. The total investment

cost of the PEM FC configuration is already higher compared to the conventional diesel ship. The hydrogen fuel cost would be higher than the diesel fuel cost when the relative hydrogen cost is equal to the relative diesel fuel cost. However, the relative cost of hydrogen fuel is even higher, meaning the cost is much larger. The price of hydrogen fuel at the moment is very high compared to the diesel price. The figure shows that the relative storage cost of the compressed hydrogen is more significant than liquid hydrogen. This feature occurs since the compressed hydrogen storage is more expensive than the liquid hydrogen storage, while the ship also needs a smaller storage unit to store liquid hydrogen. The crew cost between the diesel and hydrogen fuel systems is the same in the figure. However, the relative cost is higher for the conventional diesel ship. This aspect also means that the total cost on these speeds and this range is higher for the hydrogen fuel ship than the diesel fuel ship. These overviews provide enough insight into the total cost development of the ships to discuss the total cost. Figure 4.11 displays the total cost of ship 2 versus the range.

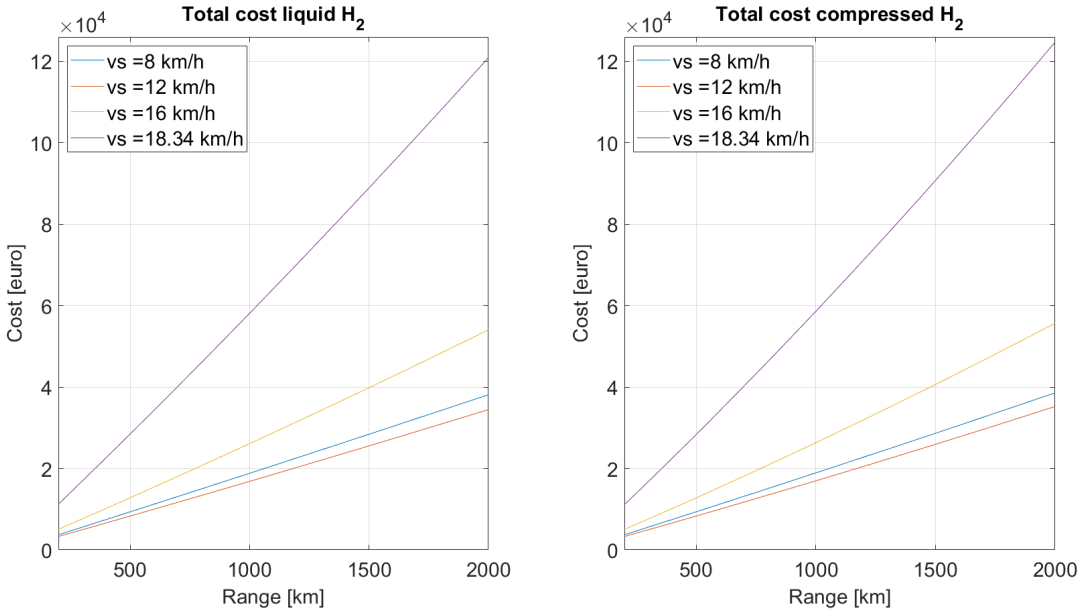

Figure 4.11: Ship 2: Total cost versus range

The figure shows that the cost is linear at a given speed, but as it increases the cost linearity becomes steeper. At a given range, the cost increase is not linear when speed increases. This characteristic occurs because the resistance and the power do not scale linearly speed. Also, the power demand comes closer to 100% power demand of the PEM FC system. At these work point of the FC, the system efficiency becomes lower. This effect increases fuel consumption and results in larger fuel and storage costs. This increase amplifies the cost increase. Among all ships, ship 2 has the highest cost overall. Due to the favourable propulsive performance of ship 3 (two K_a-propellers), it can cope with a lower installed power compared to ship 2. This aspect results in lower costs for the electric engine, PEM FC, fuel, fuel storage and battery pack. Despite ship 3 being larger in dimensions, and therefore having more cost in the hull and the propulsion arrangement, the engine part of ship 2 raises the total cost higher than that of ship 3. Ship 1, having a similar propulsive arrangement as ship 2, has a lower cost because it is a smaller ship requiring lower required installed power.

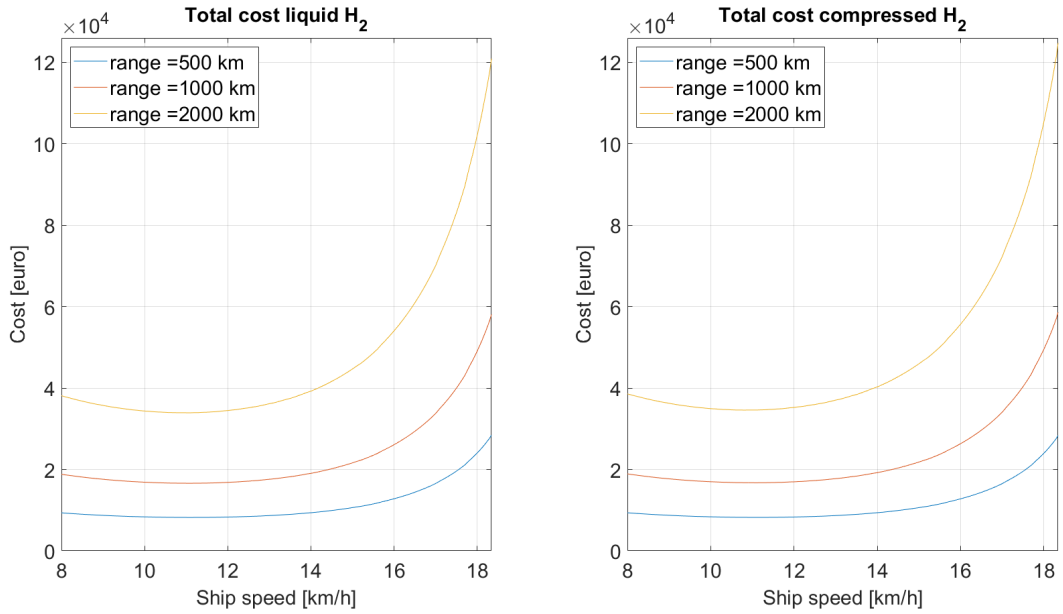

Figure 4.12: Ship 2: Total cost versus ship speed

The figure shows a minimum of the total cost for certain ship speeds, at the higher ranges this is visible. Increasing the ship speed seems to lower the total cost slightly. When the speed increases, the time it takes to complete the defined range decreases, which means that over cost over that period also decreases. So the total cost decreases as the speed increases at particular ranges. However, the total cost increases when the speed becomes greater than a specific value. This event happens because the fuel and storage costs are rising faster than other cost components are decreasing. This aspect creates the minimum in the total cost figure at certain speeds for the defined ranges. The minimal RFR in Euro per ton per kilometre will show the most beneficial choice for the shipowner, whether he or she installs more storage to comply with longer ranges or sails on a specific ship speed to obtain the lowest RFR.

4.3 RFR

The calculation model divides the total cost by tonnage capacity and range that comply with that cost to investigate the ships' minimal RFR. This research added a profit margin of 5% to the calculation. Combining the total cost and tonnage capacity with the range result in figure 4.13 about the RFR versus this range, and 4.14 about the RFR versus the ship speed. Both figures display the RFR of ship 2.

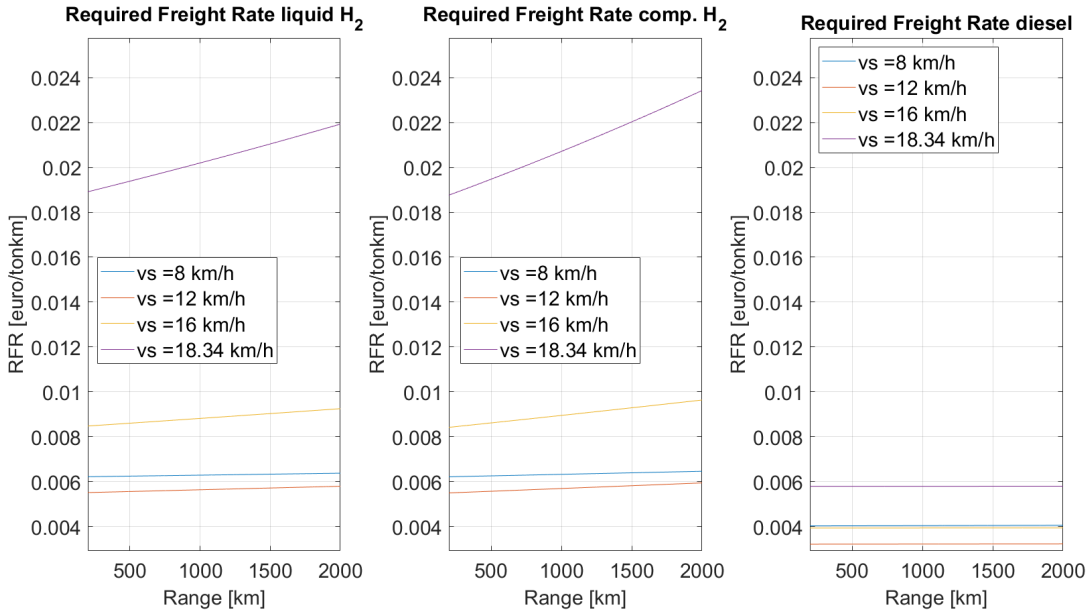

Figure 4.13: Ship 2: RFR per ton per kilometer versus range

At low ship speeds, the range does not increase the RFR as significant as it does at higher ship speeds. The compressed hydrogen option results in a higher RFR among all ships and is directly related to the total cost. The investment cost of the compressed hydrogen is higher than the liquid hydrogen. Therefore, it results in higher RFRs. Between the ships, the RFR becomes lower for the larger ships. The cost can be carried by a greater amount of cargo over the same range, while the total cost does not increase to intensely for the larger ship. Two effects are noticed when one looks into the combination of the range and ship speed. The dependency of the RFR on the range becomes larger while the initial value of RFR also becomes larger for higher ship speeds. The initial rise in RFR at higher speeds is due to the increased fuel consumption at these power demands. This increase results in a more significant fuel cost and hydrogen storage cost, which raises the total cost significantly. The larger fuel consumption is also what makes the dependency on the range more significant. The ship operates at a lower system efficiency on these speeds, so the fuel consumption and storage size increase more intense than at lower ship speeds. With the tonnage capacity becoming lower at these speeds, the RFR's dependency on range becomes steeper at higher ship speeds. The third sub-figure in figure 4.13 shows the RFR of ship 2 if it would have a diesel engine. The conventional ship always has a lower RFR than the hydrogen ships comparing between ship speeds. The hydrogen ships' cost is higher due to the higher depreciation cost, investment cost, and fuel cost. The range dependency of conventional diesel ships is small because the cost components do not increase significantly with range. The figure shows that the optimal speed is not the design speed of the ship. A ship speed of 10 km/h seems to give the lowest RFR for the hydrogen ships and around 12 km/h for the conventional ships. The following figure shows the RFR of ship 2 versus the speed.

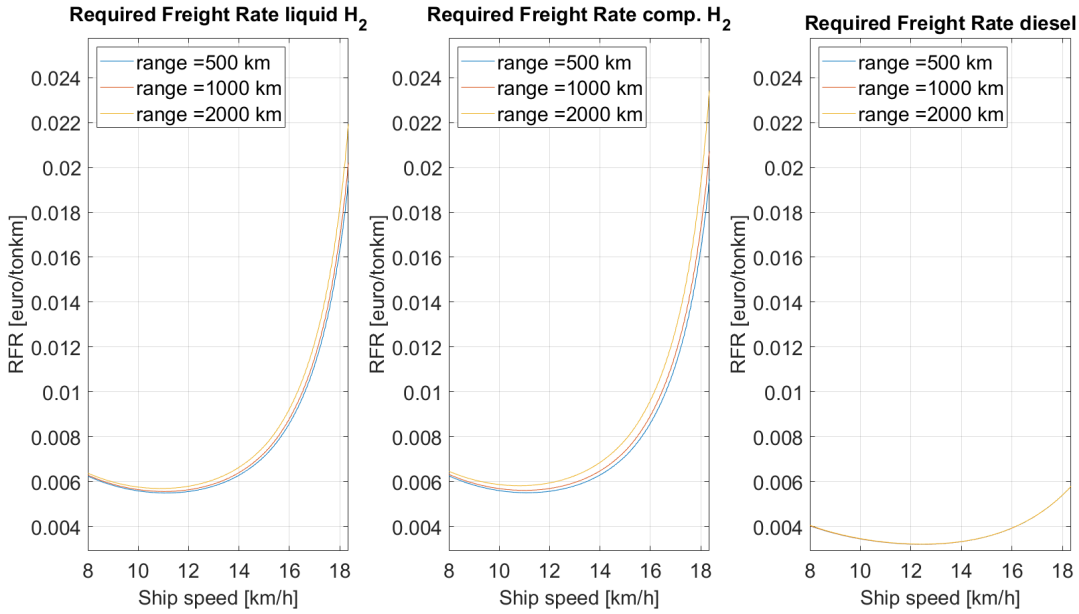

Figure 4.14: Ship 2: RFR per ton per kilometer versus ship speed

The RFR for the liquid storage is slightly lower than the compressed storage option. This aspect makes the liquid storage a better alternative from an economic perspective. The liquid hydrogen option would give the shipowner a more competitive position on the market than the compressed hydrogen option. The figures also show that increasing the speed results in higher RFRs. The storage, fuel cost, and decrease in tonnage capacity become more significant at these ship speeds. The RFR for the compressed storage option rises faster compared to the liquid storage option. This feature is expected of the compressed hydrogen, because of the higher storage cost and lower storage density. The optimal speed found for ship 1, 2, and 3 are 9.5, 9.7, and 10.2 km/h for both storage options for ranges up till approximately 1000 kilometre. The optimal speed slightly drops to 9.2, 9.5 and 10.0 km/h for the liquid storage option and 9.2, 9.3 and 9.9 km/h for the compressed storage option at a higher range. The ships can reduce the fuel and storage cost in decreasing the speed at these high ranges. The slightly reduced speed will decrease fuel consumption compensating for the higher cost of the hydrogen storage system. The difference between the optimal ship speed for the liquid and compressed storage at higher ranges occurs because of the higher cost and the lower density of the compressed hydrogen storage. Although these low speeds result in the lowest possible RFR, these speeds will make it difficult for the inland ships to deliver cargo upstream due to the strong current. It will be inevitable for the inland ships to sail faster due to the delivery time of the freight they are carrying. The conventional ship with diesel fuel has a lower RFR and a higher optimal speed. The optimal speeds for ships 1, 2, and 3 are 11.2, 11.5, and 12.1 km/h. Due to a lower fuel cost, it is more beneficial to sail faster. Diesel fuel is much less costly compared to hydrogen fuel. The assumed values for the diesel, liquid hydrogen, and compressed hydrogen fuel are 0.417, 4.080, and 4.004 Euro per kilogram. Both hydrogen fuels are almost ten times as expensive as diesel fuel. However, the energy content of hydrogen is about three times more than diesel. It will be interesting to see how the RFR, and optimal ship speed relate to the hydrogen fuel cost.

The figures of the other two ships are given in Appendix D as well as the other figures on the RFR. Figures D.11, D.12 and D.13 show the relation between the cargo space capacity and the ship's range, and figures D.14, D.15 and D.16 show the relation between the cargo space capacity and the ship speed. These figures show that the RFR is more dependent on the cargo space capacity than on the tonnage. This happens because the hydrogen fuel and storage unit

increases more in terms of volume than in mass, resulting in a faster decrease in the cargo space capacity. This is reflected in the faster increase of the RFR based on the cargo space capacity and RFR based on the container capacity. In appendix D the figures D.17, D.18, D.19, D.20, D.21 and D.22 show the relation between the RFR, container capacity, the range and the ship speed. The jumps in the container capacity are slightly visible in these figures.

4.4 Sensitivity of RFR

As said earlier, the RFR shows a significant dependency on the fuel cost. The price of hydrogen fuel is not fixed in the upcoming years. The price assumed in this research is a bit optimistic. So that bears the question of what would happen if the price of hydrogen fuel is higher or lower. Also, other variables could be a significant influence on the RFR. In this paragraph, the RFR is evaluated on its sensitivity for several variables.

4.4.1 Price of hydrogen fuel

This research varies the price to values of 1, 5, and 10 Euro per kg to check the sensitivity of the RFR on the hydrogen fuel price. Figures 4.15, 4.16 and 4.17 show the RFR of ship 2 as a function of the ship speed for respectively a hydrogen fuel price of 1, 5 and 10 euro/kg.

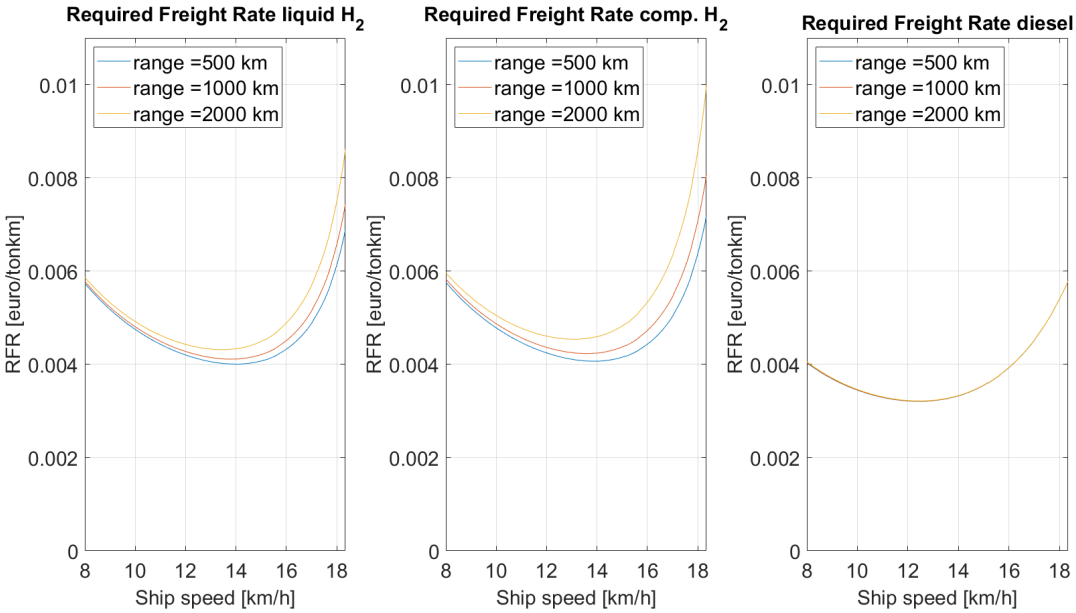

Figure 4.15: Ship 2: RFR with price H_2 of 1 euro/kg

The sub-figure of the RFR with diesel is a reference to compare to the hydrogen figures. Figure 4.15 shows the RFR curves when the hydrogen fuel price would become 1 Euro/kg. The decrease in fuel cost results in a significant reduction in the RFR. Also, the optimal speed shifts towards higher ship speeds. At a lower fuel price, the dependency on range seems to become more significant. This feature occurs because the fuel storage cost depends on the range and units' cost. Earlier in paragraph 4.2, the storage price can become a very significant part of the total investment. This characteristic is also visible in the figure. So the RFR versus the range becomes less dependent on the fuel cost, but more dependent on the other cost elements such as the depreciation cost of the hydrogen storage system. At higher ranges, the optimal ship speed becomes lower compared to shorter ones. This aspect suggests higher ranges increase storage cost significantly, and sailing slower reduces these costs. Low hydrogen fuel prices result

in RFR values closer to the ones found for the conventional diesel ship. Table 4.2 shows the ships' RFR at the most optimal ship speed and range.

Fuel option –	Range km	Ship speed km/h	RFR $10^{-3} euro/tonkm$
Liquid hydrogen	200	12.8	3.829
Compressed hydrogen	200	12.7	3.856
Diesel	200	11.4	3.319

Table 4.2: Ship 2: RFR at optimal conditions with price H_2 of 1 euro/kg

Table 4.2 shows that the ship with hydrogen as its fuel would "only" be approximately 15 to 16% more expensive than the conventional ships. This hydrogen fuel price shows a prospect of the competitiveness between conventional ships and PEM FC ships.

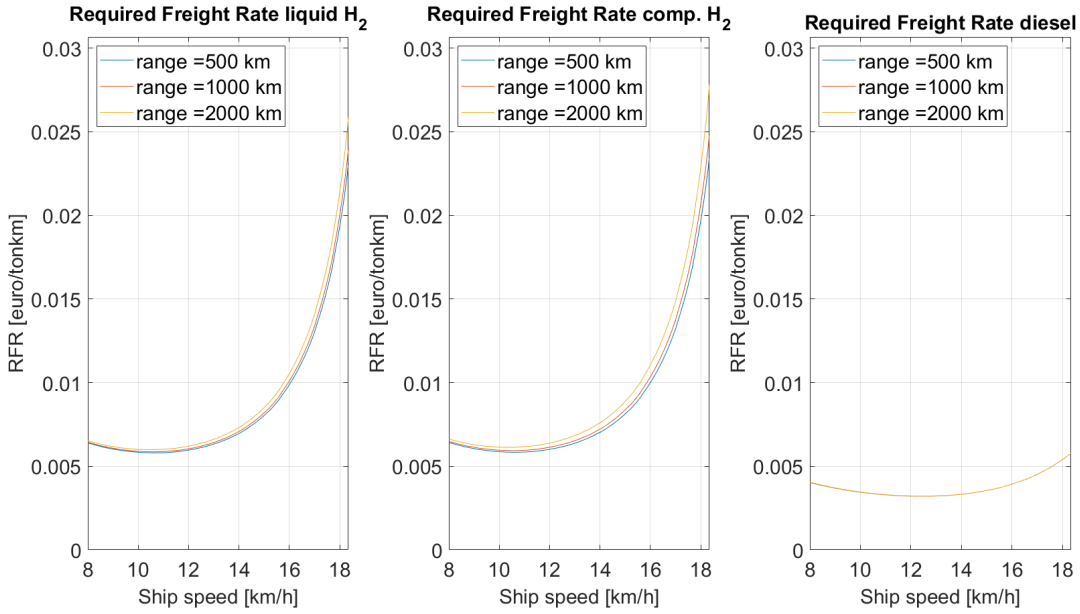

Figure 4.16: Ship 2: RFR with price H_2 of 5 euro/kg

Figure 4.16 shows very similar characteristics as was shown before in figure 4.14. The price of fuel is this figure is about 1 euro more expensive. The optimal speed at this fuel price is about 3 km/h slower than at 1 euro/kg of hydrogen fuel. The RFR becomes much higher at this fuel price, which table 4.3 shows.

Fuel option –	Range km	Ship speed km/h	RFR $10^{-3} euro/tonkm$
Liquid hydrogen	200	9.7	5.535
Compressed hydrogen	200	9.7	5.550
Diesel	200	11.4	3.319

Table 4.3: Ship 2: RFR at optimal condition with price H_2 of 5 euro/kg

The price of hydrogen fuel is five times costlier while the RFR has become approximately 1.44 times higher than the lower fuel price. At fuel prices around 5 euro/kg, the PEM FC ships are around 67% more expensive than the conventional ships, which is quite a lot of RFR that the PEM FC ships would have to acquire from the shipping companies.

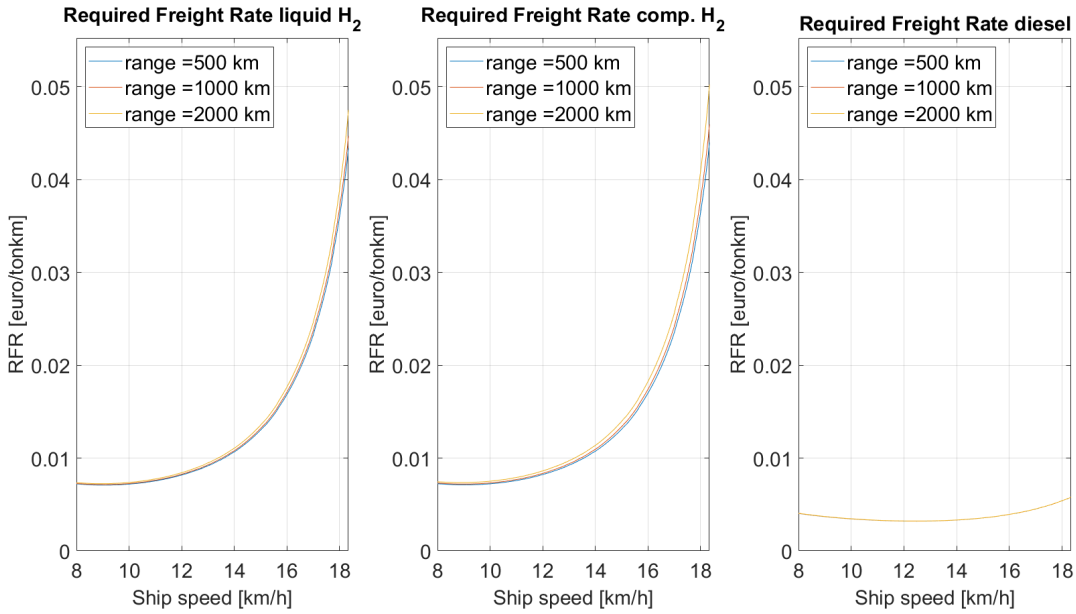

Figure 4.17: Ship 2: RFR with price H_2 of 10 euro/kg

At a hydrogen price of 10 euro/kg, the PEM FC ships become very expensive, and the optimal speeds drop to very low ship speeds. The high hydrogen fuel price and fuel consumption result in very high fuel costs. This aspect overshadows the influence of the other cost elements. The dependence of the RFR on the range increases slightly when the price of hydrogen fuel increases. However, this effect does not show in the graph. The increase in RFR for higher speeds becomes large enough to make the effect of range seem negligible. Table 4.4 shows the optimal conditions when the price of hydrogen fuel would be 10 euro/kg.

Fuel option –	Range km	Ship speed km/h	RFR $10^{-3} euro/tonkm$
Liquid hydrogen	200	8.3	6.725
Compressed hydrogen	200	8.3	6.736
Diesel	200	11.4	3.319

Table 4.4: Ship 2: RFR at optimal condition with price H_2 of 10 euro/kg

With the fuel price of hydrogen increased, the RFR of the PEM FC ship becomes twice as high as the conventional ship. This price increase reduces the ship's optimal speed even further down to 8.3 km/h. The figures and tables show that the RFR is very dependent on the hydrogen fuel price. At higher ships speed this dependency becomes significant, which the graphs show where higher fuel prices result in lower optimal ship speed. For high fuel prices, the ship can improve the RFR with sailing slower, reducing fuel consumption. The market position of PEM FC ships compared to other inland ships depends heavily on the fuel price.

4.4.2 Price of PEM FC

In the cost overview, this research assumes a price of 280 euro per kW of power. This price is optimistic. Therefore, it suggests checking what happens to the RFR if this price becomes higher or lower. This section evaluates the RFR's behaviour when the PEM FC's price becomes 500 euro/kW. This increase is almost twice the assumed price. Figure 4.18 shows the comparison between the two prices for ship 2.

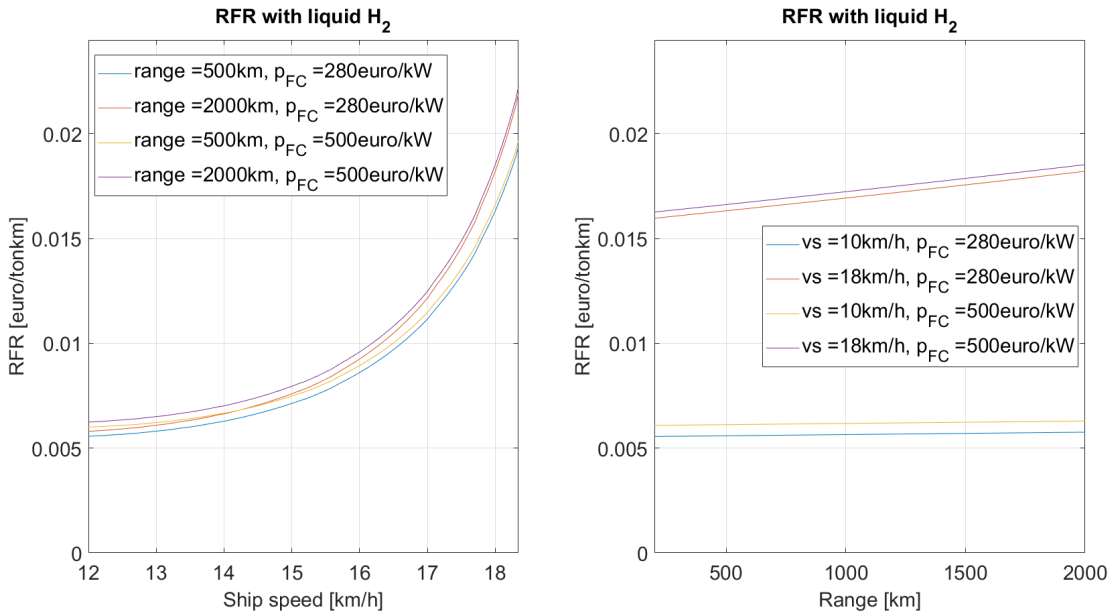

Figure 4.18: Ship 2: RFR for different PEM FC prices

Figure 4.18 shows that the influence of the PEM FC price on the RFR is small. The RFR increases slightly when the price of the PEM FC increases, because of two events. The price increases the total cost on the PEM FC system, which raises depreciation costs. The increase of the PEM FC's cost increases the investment cost, raising the interest cost. This increase is slightly more effective on the RFR for lower ship speeds and ship ranges. The installed power, which determines the magnitude of this cost, is fixed. Other cost elements such as the fuel cost, become much higher than the induced cost by PEM FC system at high speeds. Overall, the effect of the PEM FC price is small. At a ship speed of 10 km/h, the increase in RFR is approximately 9.1% in RFR. At a ship speed of 18 km/h, this rise is only 1.7%.

4.4.3 Price of hydrogen storage units

A look is taken into the investment since the interest cost is also a large part of the total ships' cost. The price of the hydrogen storage units is a significant contributor to the total investment when the speed and the range increases. The current assumed prices are 9.95 and 15.98 euro/kWh of respectively liquid and compressed hydrogen stored. This research evaluates the effect of a reduction in storage price. The price for the liquid hydrogen storage is set to 5 and 10 euro/kWh.

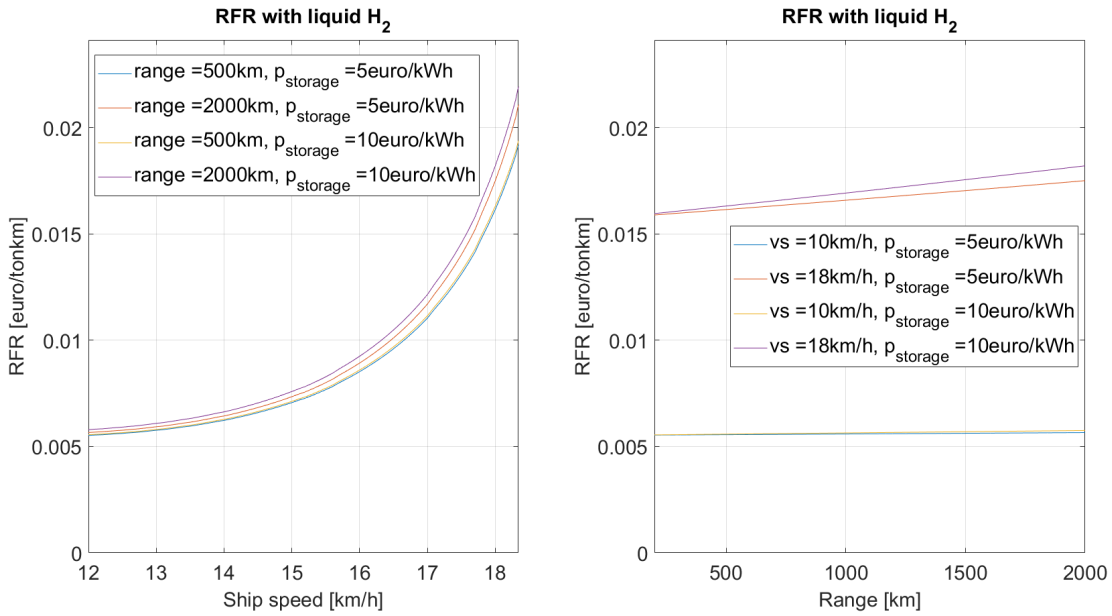

Figure 4.19: Ship 2: RFR for different storage prices

Figure 4.19 shows that the RFR decreases due to the reduction in storage price. However, the decrease in RFR is small. The effect of the price of the storage on the RFR is small and reduces the impact of the range on the RFR, especially at low ship speeds. Although the storage cost can be a large portion of the total investment, it does not change the RFR much. At low ship speeds, the price difference results in a small increase compared to higher ship speeds. At high speeds, the difference in RFR becomes more significant for long ranges.

4.5 Conclusions

This paragraph sketched the general relations of the influence of a PEM FC system running on hydrogen for inland ships. This research varied the ship speed and range to see how inland ships would perform in the RFR. Evaluating the results lead to the following conclusions:

- The required storage for hydrogen fuel is much larger compared to diesel fuel.
- The PEM FC system has more influence on the volumetric capacity than the tonnage capacity of inland ships.
- The hydrogen fuel is a large cost component, which rises strongly with an increasing ship speed or range. The hydrogen fuel price has a strong impact on the optimal ship speed. Therefore, it has a significant effect on the ship's competitive position on the market.
- The range influence on the RFR is low at low ship speeds. This influence becomes larger at higher ship speeds. The PEM FC's system efficiency drops, and the power demand is high, which results in large fuel consumption. At these operating points, the fuel cost and storage cost react more significantly to the range.
- The ship speeds has a significant influence on the RFR of the inland ships. They obtain an optimal RFR at low ship speeds around 10 km/h.
- The liquid hydrogen storage option outperforms the compressed hydrogen storage option in terms of costs. Therefore, the liquid hydrogen fuel results in lower RFRs than compressed hydrogen fuel. The shipowner would have a better competitive position in the market with a liquid hydrogen option.

The conclusions drawn are straightforward in giving an overview of the characteristics of the new system. The only issue would the optimal ship speed. The low ship speed can not guarantee that the inland ships can sail to every port along the rivers. Strong currents will prevent the inland ships from reaching its destination at these low ship speeds. Therefore, the current forces the shipowner to sail faster in particular sections of the river and consume more fuel. This aspect can give the incentive to look into shorter ship ranges to save cost and decrease the RFR of the inland ships as shown in figures D.6, 4.13, and D.8. Therefore, it is chosen for the cases in the next paragraph to chose a sensible ship speed concerning the current for sailing upstream in being on time with the cargo. This fast sailing is slightly compensated for sailing downstream because the current reduces the ship speed downstream.

Chapter 5

Results of Cases

Chapter 4 sketched the relations of the PEM FC system running on hydrogen. The knowledge obtained from this chapter helps to understand the results and optimisation of the cases. This chapter evaluates the two trips that paragraph 2.4 describes. Additional information about the trips is given in appendix B. The trips are a combination of different points of the ship speed and range relation. These trips will give a bit more insight into how the PEM FC system influences the inland ships' performance during its operation. The sections during the trips all have their slightly different conditions. These different conditions change power demand. This chapter evaluates whether increasing the installed power could improve the RFR of the inland ship. Adding one stack of fuel cells increases the power of the initial installed PEM FC. This way, the installed power increases with approximately 10 kW per added stack. A few steps have to be taken to get to that point of this installed power evaluation, such as calculating fuel consumption, storage size, total cost, and the cargo carrying capacity. Figure 5.1 displays the approach to determining the case results.

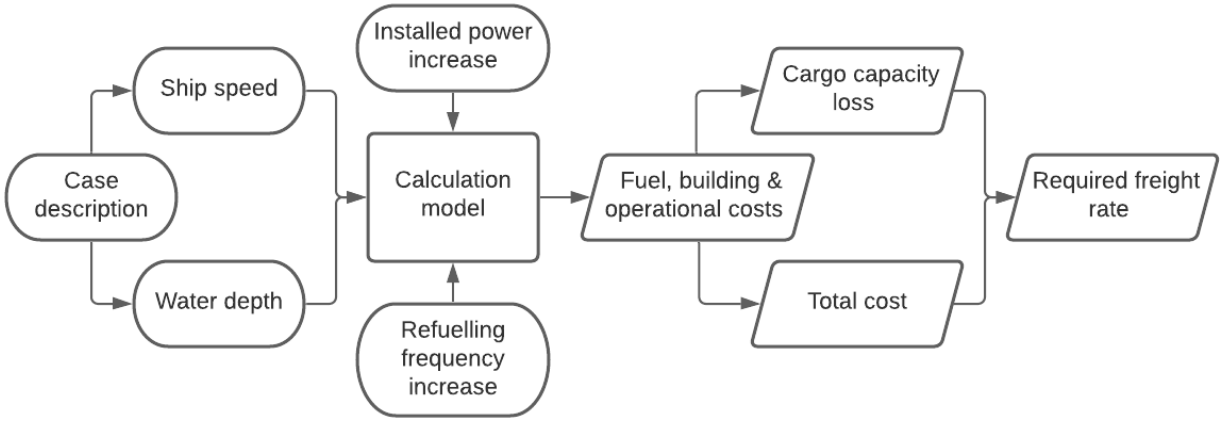

Figure 5.1: Process of case calculations

Figure 5.1 shows that the case description determines the input for the calculation model. The output variables are the same ones from chapter 4. This chapter elaborates on the optimisation of the output variables based on two methods. The first method is increasing the installed power mentioned before. Installing more power while the power load remains the same lowers the PEM FC´s load factor. The lower load factor increases the system efficiency of the PEM FC system and reduces fuel consumption. However, installing more power increases the cost, the weight, and the volume of the PEM FC. This chapter evaluates this trade-off. The second optimisation method is to increase the refuelling frequency displayed in figure 5.1. The

refuelling frequency is the number of times the skipper refuels the ship per trip. A refuelling frequency of one means the skipper fuels the ship once so, it can sail the entire trip range on this fuel tank. Increasing the frequency raises the number of times the ship needs to fuel, which increases the trip completion time. The bright side of increasing this frequency is that the fuel tank size reduces. Decreasing the fuel tank size lowers the storage cost and the storage impact on the ship design.

5.1 Fuel consumption

The fuel consumption is dependent on several other components of like the propulsion efficiency, the power demand and the system efficiency of the PEM FC. The validation of power prediction sub-model showed the ships' highest power demands to compare to other ships. These powers are the minimum installed powers of the PEM FC on the ships. This research uses them as the base value for increasing the installed power. One obtains these powers through the resistance approximation, ship speed, and propulsive efficiency. Table 5.1 shows the efficiency below.

Ship	Propeller	η_D LW				η_D HW			
		Upstream		Downstream		Upstream		Downstream	
		Trip 1	Trip 2	Trip 1	Trip 2	Trip 1	Trip 2	Trip 1	Trip 2
1	1.60 m, B4-100 P/D 0.70	0.39	0.38	0.41	0.43	0.47	0.44	0.49	0.49
2	1.85 m, B4-100 P/D 0.70	0.38	0.38	0.40	0.41	0.45	0.42	0.46	0.46
3	2×1.70 m, Ka5-75 P/D 1.20	0.54	0.54	0.56	0.57	0.59	0.57	0.60	0.60

Table 5.1: Average propulsion efficiency of the ships during the trips

Ship 3 has a better propulsion efficiency than ship 1 and 2. Due to the high required blade area ratio, this research had to fit ship 3 with two propellers. This decision resulted in a lower required blade ratio which allowed ship 3 to have propellers in nozzles. These propellers result in higher propulsion efficiencies in high propeller load conditions than open propellers. The propulsion efficiency among all ships is in general higher in HW condition compared to the LW condition. The increase in resistance results in higher blade loading, which results in lower propulsion efficiencies. LW and HW condition show the same findings in the efficiencies, in lower load (downstream) the ships have higher propulsion efficiencies than upstream sailing. The outcomes between trips are somewhat different. On average, trip 1 performs better upstream than trip 2, but worse downstream. This observation represents that the propeller load is on average higher for trip 2 than 1 upstream. This aspect relates similarly to the lower loads sailing downstream. These observations should show where the ships need more power and where the power demand is slightly less. The system efficiency of the PEM FC can also show this. Table 5.2 displays the average system efficiencies.

Ship	P_{FC} [kW]		η_{FC} LW				η_{FC} HW			
			Upstream		Downstream		Upstream		Downstream	
	Trip 1	Trip 2	Trip 1	Trip 2	Trip 1	Trip 2	Trip 1	Trip 2	Trip 1	Trip 2
1	689	1008	0.418	0.452	0.485	0.497	0.481	0.470	0.497	0.497
2	928	1497	0.417	0.466	0.479	0.497	0.472	0.469	0.497	0.497
3	808	1367	0.423	0.473	0.480	0.497	0.462	0.468	0.497	0.497

Table 5.2: Average system efficiency of PEM FC during the trips

When a PEM FC operates at a lower load, the system efficiency becomes higher. This is resembled in table 5.2. Downstream the load is lower, resulting in higher system efficiency,

while upstream the load is higher, resulting in lower system efficiency. The power loads during trip 2 result in higher system efficiencies on average. This effect occurs because the ship is outfitted with a large amount of power while it only needs this power for a relatively short time. The ships sailing trip 1 have power demands closer to the installed power, meaning higher loads on the FC and therefore lower system efficiencies. This characteristic is not the case in HW upstream. The power loads on the PEM FC are lower for trip 1 and higher for trip 2 in HW upstream. This research bases the minimum installed power on the highest power demand during the trips in either the high or low water depth situation. The calculation model bases the installed power for trip 1 on the LW power demand, while for trip 2, on the HW power demand. This aspect means the power loads are higher overall in their water depth situation. This high power load results in lower system efficiencies. The reason for the high power loads is due to extreme currents in two sections. These extreme currents result in large power demands. The power demand in LW is still high on this section but does not exceed that of the HW power. For trip 1, the LW power demand is higher due to strong shallow water effects. Although the current is higher in HW than LW, the power demand does not exceed those of the LW ones. Both the propulsion and the system efficiency should provide some grip in the upcoming subject to determine the ships' RFR.

The calculation model determines fuel consumption for the different installed powers through the trip modelling and fuel flow calculations. Figures 5.2 and 5.3 show the fuel consumption. The volume difference between liquid and compressed hydrogen fuel consumption occurs due to the difference in their storage densities. The ships consume the same amount in mass, but liquid hydrogen has a higher density resulting in lower volumetric fuel consumption.

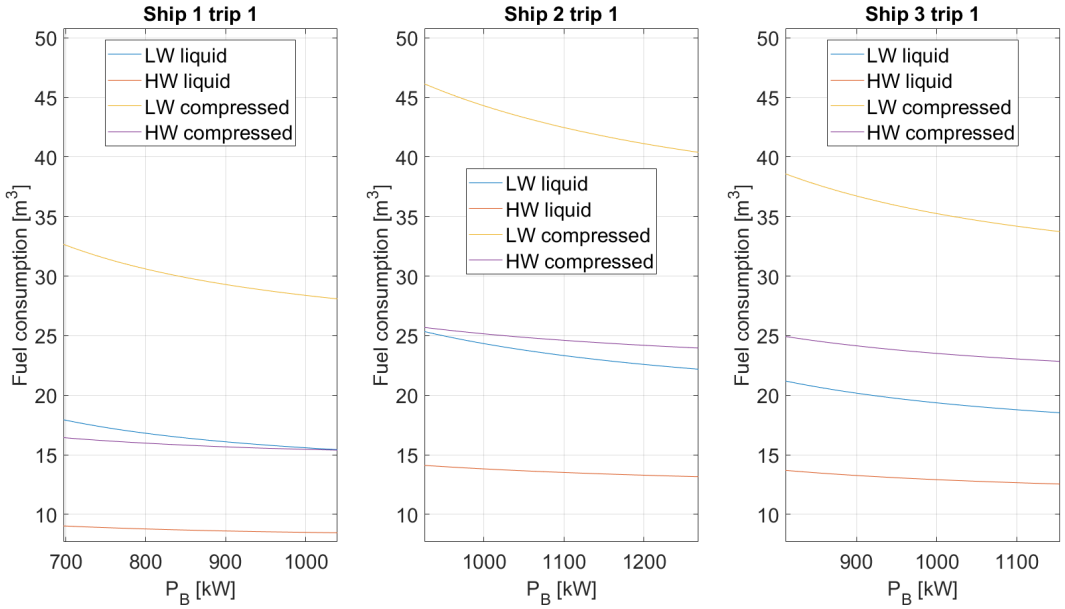

Figure 5.2: Trip 1: Fuel consumption versus Installed power

The results for trip 1 show different behaviour between the ships. The ships consume more fuel if the trip sailing in LW condition compared to the HW condition. However, the difference between LW and HW is more significant for ship 1 than the others. Ship 1 consumes initially about 90% more in LW than in HW. For ship 2 and 3 this is respectively 70 and 50 % more. The difference between LW and the HW condition of trip 1 becomes smaller when one installs more power. This observation means that the ship benefits more from installing more power in LW than in HW condition. It is also visible the figure, the fuel consumption in LW condition decreases faster than the fuel consumption in HW condition. The differences between the

ship happen because the power demand between the LW and HW differ. On top of this, the lower system efficiency in the LW condition than the higher system efficiency in HW condition strengthens this effect. This characteristic results in the differences in fuel consumption among the ships. The system efficiency for the ship is approximately 44% in LW and 48% in HW condition on average.

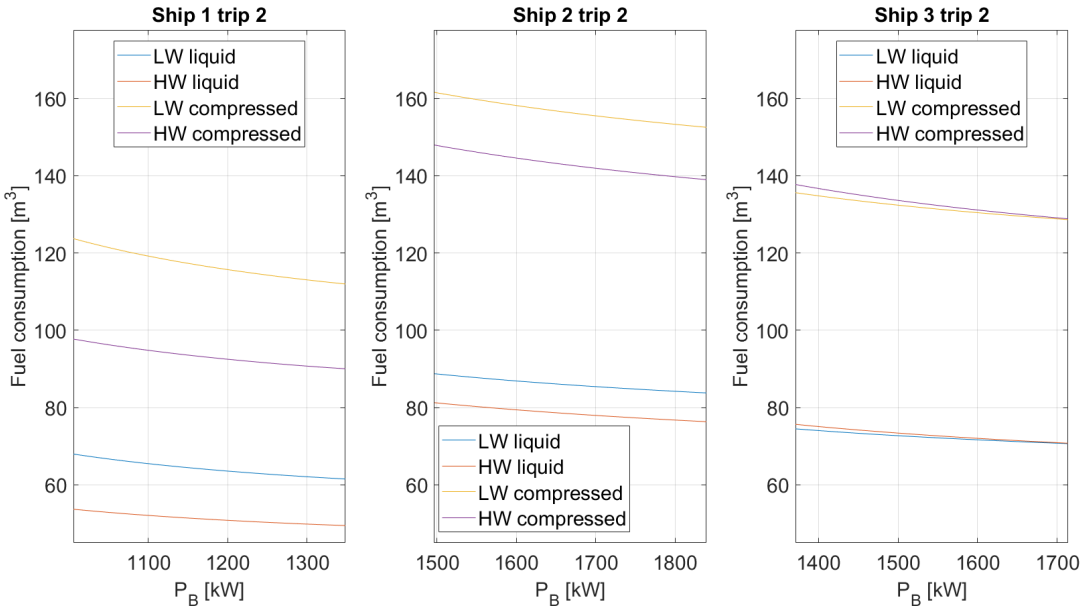

Figure 5.3: Trip 2: Fuel consumption versus Installed power

Figure 5.3 shows different characteristics between the ships and the fuel consumption in the various conditions compared to those found in trip 1. The difference between the HW and LW fuel consumption is smaller compared to trip 1. Ship 3 even has a fuel consumption in LW almost equal to the HW condition. Ship 3 seems to develop similar power demands in both conditions overall during trip 2, resulting in comparable system efficiencies and fuel consumption. Ship 1 and 2 do have different power demands between the LW and HW condition. The power demands strongly depend on the propulsive efficiencies. The efficiency of ship 1 and 2 are lower than ship 3. On top of this, the propulsive efficiencies of ship 1 and 2 decreases more in LW conditions.

The fuel consumption directly relates to the hydrogen storage size if the shipowner does not refuel more then once on the trip. As explained earlier, dividing the consumed fuel with the volume fraction of each storage option results in the storage size, which will impact the ship design. The consumed fuel affects the ships' total cost in two ways, the storage and fuel cost. The amount of hydrogen fuel present on the ship determines the storage cost, and it determines the fuel cost needed to complete the trip. Tables 3.1, and 3.2 shows the price of both cost components.

5.2 Total cost per trip

The fuel consumption is a first step in the total cost calculation, but the cost depends on many components. The total cost per trip depends on both capital costs and operational costs as tables 3.1 and 3.2 display. Increasing the minimum installed power results in different fuel consumption per trip. This is displayed in figures 5.2 and 5.3 already. It clearly shows the influence of installing more power to make the total fuel cell system run on more beneficial

system efficiencies. These beneficial efficiencies lower the fuel mass flow during the trip and eventually lead to lower fuel consumption. Although installing more power results in saving fuel and reduces fuel storage, it also means costs increase by installing more fuel cell stacks and installing a larger electric motor (assuming the electric motor can always exert the PEM FC's full power). Other cost components determine the total cost's magnitude aside the cost components that change due to the power increase. The investment cost for the ships is similar to the cost components shown in table 4.1. The difference between the trips and the speed versus range calculations resides in the minimum installed power that changes some investment costs. Table 5.3 shows these costs.

	Trip 1			Trip 2		
Part/system	Ship 1	Ship 2	Ship 3	Ship 1	Ship 2	Ship 3
The PEM FC system	193.000	260.000	226.000	282.000	419.000	383.000
The electric motor	304.000	409.000	344.000	464.000	693.000	624.000
The batteries	15.800	21.300	18.500	23.100	34.200	31.200
The gearbox	24.300	32.700	27.500	37.100	55.500	49.900
The propeller	36.500	49.100	82.600	55.700	83.200	150.000
The steering equipment	50.000	50.000	100.000	50.000	50.000	100.000
The hull (steel + yard)	2.500.000	3.800.000	4.890.000	2.500.000	3.800.000	4.890.000
Machinery	273.000	330.000	356.000	285.000	353.000	378.000
Investment without fuel storage	3.390.000	4.950.000	6.050.000	3.700.000	5.490.000	6.610.000
Investment conventional ship	3.090.000	4.560.000	5.760.000	3.170.000	4.700.000	5.900.000

Table 5.3: Investment cost of building components in Euros

Again, the ships' investment with the PEM FC installed is higher than the conventional ship. Table 5.4 shows the hydrogen storage cost. The range from minimum cost to maximum cost is relative to the installed power. At the minimum installed power, the storage cost is maximised.

		Trip 1		Trip 2	
	Ship	Min cost	Max cost	Min cost	Max cost
Liquid hydrogen	1	404.000	453.000	1.620.000	1.730.000
	2	574.000	634.000	2.200.000	2.290.000
	3	482.000	533.000	1.870.000	1.930.000
Compressed hydrogen	1	649.000	729.000	2.600.000	2.790.000
	2	922.000	1.020.000	3.540.000	3.670.000
	3	775.000	856.000	3.010.000	3.100.000

Table 5.4: Hydrogen storage cost in Euros

The storage cost is a significant investment cost and will increase the amortization and depreciation costs heavily. Increasing the installed power decreases the fuel consumption as it is shown in figures 5.2 and 5.3. This effect decreases the storage size and cost. Table 5.3 shows this result as the minimum per trip and storage option. The hydrogen fuel cost and other cost components will influence the most optimal installed power for the ships. So combining all the capital and operational cost components with the power variation of the ships results in figures 5.4 and 5.5.

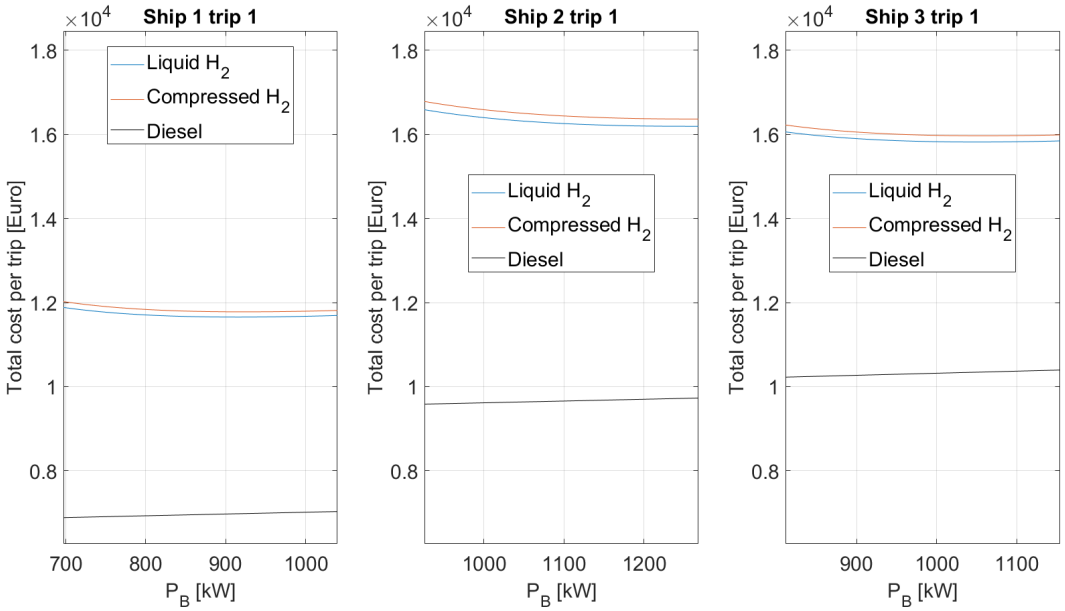

Figure 5.4: Trip 1: Total cost versus Installed power

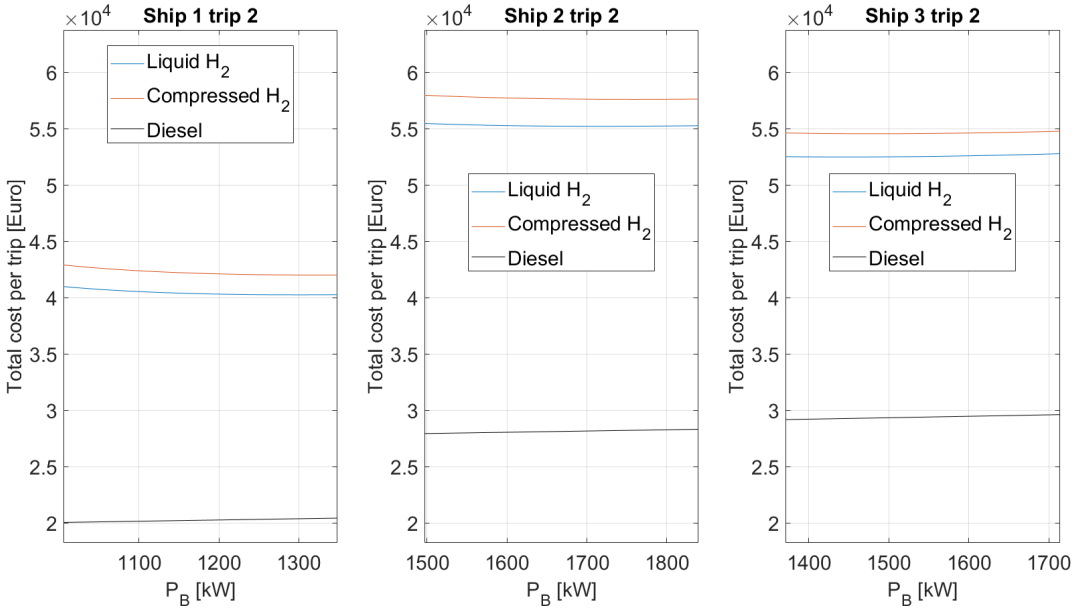

Figure 5.5: Trip 2: Total cost versus Installed power

The costs, shown in figures 5.4 and 5.5, are quite high comparing the hydrogen fuel options to the conventional diesel configuration. In both figures 5.4 and 5.5 the cost for the compressed hydrogen storage option has the highest cost per trip. The cost per trip for the diesel configuration increases linearly with the increasing installed power. The cost of the installed diesel engine becomes larger when more power is installed. Other factors do not change for the diesel configuration. The characteristics of the compressed and liquid hydrogen cost per trip across all ships are very similar to one another for trip 1. They seem to reach an optimum value at higher installed powers. It shows that the shipowner would gain in reducing the total cost per trip by installing more power. In the case of trip 2, the characteristics are less similar among the ships as well. Ship 1 and 2 continue to benefit from the power installed, especially ship 1. Ship 3 does benefit a little from increased installed power. However, it reaches an optimum for

the total cost per trip with only a small power increase, and then the cost per trip rises when one installs more power.

The compressed hydrogen storage option always leads to a higher cost per trip than the liquid hydrogen storage option and conventional diesel configuration. This difference occurs due to the cost of the compressed storage being larger than the other ones. In case for ship 1, 2 and 3 designed for trip 1, the cost increase for the compressed storage option is respectively 1.2, 1.2 and 1.1 percent and in the case for trip 2 respectively 4.8, 4.7 and 4.2 percent concerning the liquid storage option. The larger difference between the two storage options for trip 2 is due to the larger storage system that is needed. This research assumes the ships' fuel storages comply with the entire round trip's range plus a buffer. The required fuel storage is larger for trip 2 compared to trip 1, see figures 2.12 and 2.13, and this leads to a much larger storage system on board of the ships. Although the diesel engine en generators are taken out of the ship, they are replaced with an electric motor, fuel cell, and hydrogen storage system. These components raise costs. Also, the hydrogen fuel is much more expensive compared gas oil at the moment, which results in the significant increase in the cost of the liquid and compressed storage configurations compared to the conventional design.

This research made an overview and displayed the result in figure5.6 to have more insight into the total cost. The figure shows the cost division of ship 2 sailing trip 2.

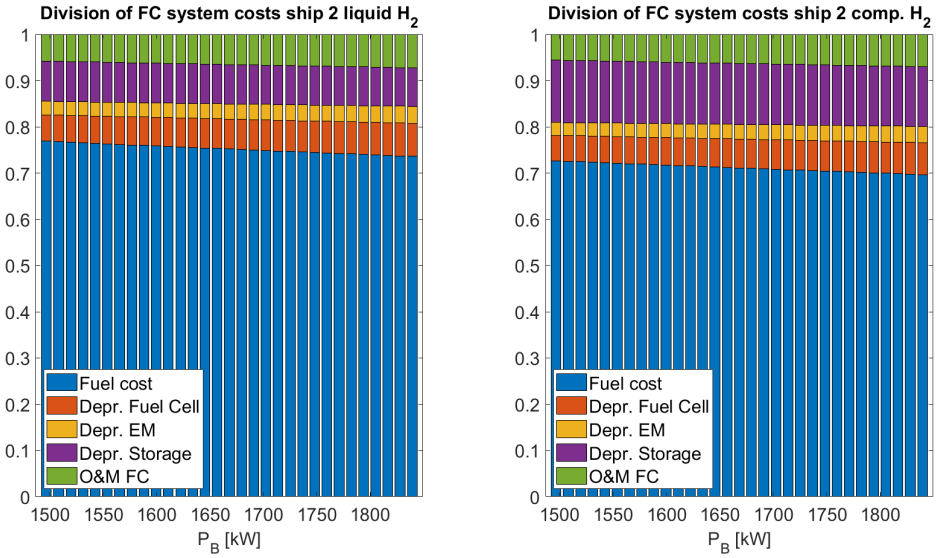

Figure 5.6: Ship 2: Cost division for various storage systems

The legend of the figures associates from the bottom to the top, so fuel cost on the bottom, operation and maintenance FC, afterwards crew cost, etc. The cost division in figure 5.6 shows a heavy dependency of the total cost on the fuel cost, the crew cost and the amortization cost. The configurations with hydrogen as fuel show a significant cost element in the depreciation of the storage units. The cost of the storage units is high due to the material cost and the labour cost. The sub-figures of the liquid and compressed storage systems of the ships show a decrease in the depreciation cost of the hydrogen storage and fuel cost with the increase of the power installed. On the contrary, the depreciation cost of the electric motor, FC's depreciation, and O&M cost of the FC system rise when one installs more power. As mentioned before, the fuel cost is a significant part resulting in higher costs for the hydrogen fuel configurations. This is visible in figure 5.6. Comparing it to the current gas oil prices for inland ships, the price for a kilogram of hydrogen is around ten times more than a kilogram gas oil.

5.3 Loss of cargo space

5.3.1 Bulk capacity

In terms of cargo space, the new system changes the mass and the volume requirements compared to the original inland ship design. Applying the two different storage options on the ship and assuming the ships' range to be equal to the round trip shows how much hydrogen fuel is required and how this affects the cargo hold in volume when the new system exceeds the conventional spaces. The method described in paragraph 3.2 and in paragraph 3.6 are applied to the trip and this results in figures 5.7 and 5.8.

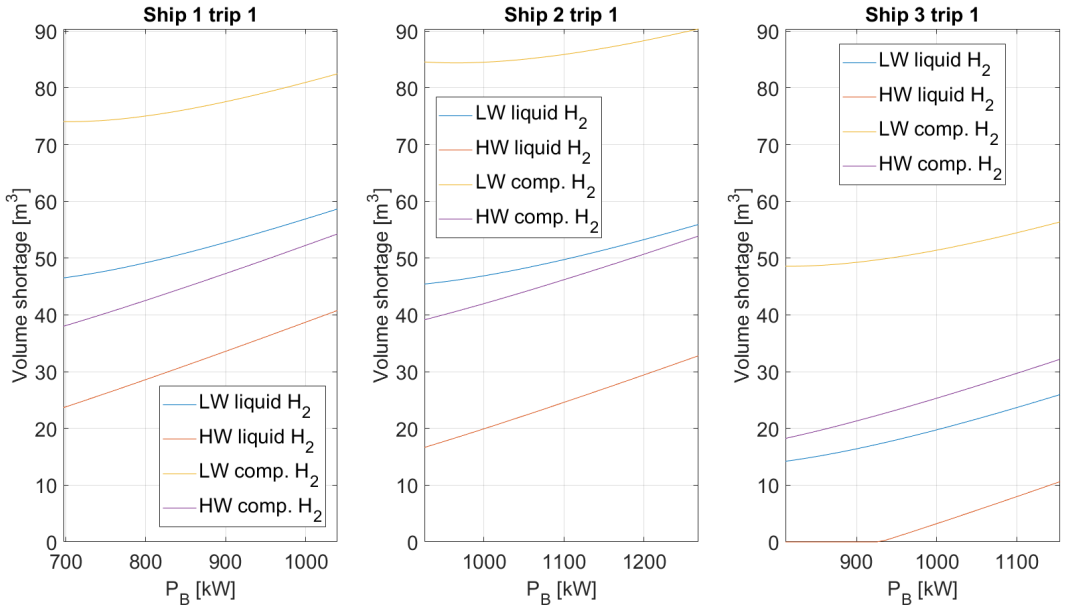

Figure 5.7: Trip 1: Cargo loss in volume versus Installed power

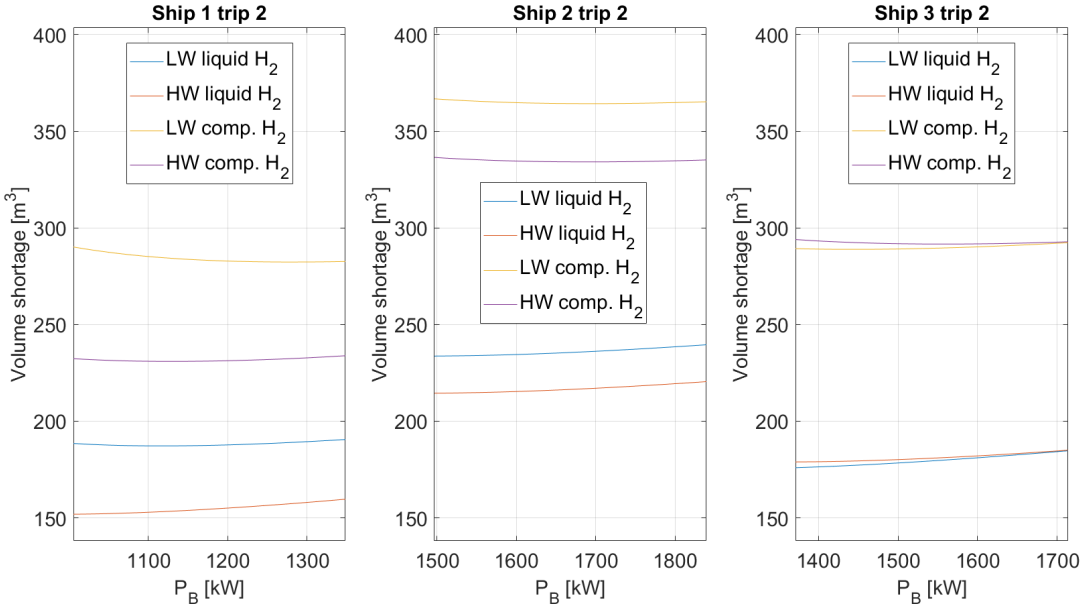

Figure 5.8: Trip 2: Cargo loss in volume versus Installed power

The volume needed to have sufficient storage capacity for the new system show different

characteristics between trip 1 and 2. In case of trip 1, there is a steep rise in volume shortage when the power increases. This rise occurs because increasing the power has too little effect on saving fuel and storage space while the PEM FC's volume raises faster. There is no gain obtained in increasing the installed power on the ships. The difference between the liquid and compressed storage options is due to the different hydrogen densities and storage unit volumes. The total storage system of liquid hydrogen requires a bit more space than the compressed hydrogen storage, but compressed hydrogen has a smaller density. The difference in the LW and HW conditions happens due to different power loads during the trip. This difference results in various hydrogen fuel consumption. The power demand is lower in the HW condition compared to the LW condition.

Trip 2 seems to differ in the volumetric shortage characteristic. The shortage in volume is much larger than trip 1, which should happen since the fuel consumption is much larger. Therefore, the fuel storage system is more extensive. Again the difference in the liquid and compressed storage is due to the different storage volumes and hydrogen densities. The power demand for the various conditions per ship results in diverse behaviour for the volume shortage versus the installed power. Ship 1 and 2 benefit in the reduction of the compressed storage for both LW and HW condition. For the liquid storage option, the inland ships do not gain anything when the installed power increases. The difference between LW and HW conditions per hydrogen storage system is again due to the power demand difference in each circumstance. The difference for ship 1 is more extensive between the LW and HW condition than the other ones. For ship 3, the LW and HW condition show almost the same volume shortage due to the similar fuel consumption. Ship 3 shows less increase in volume shortage for the HW condition because the power demand in this condition determines the minimal installed power. Therefore,e increasing the installed power strongly impacts the system efficiencies of the PEM FC on the sections with higher loads. This effect is not the case in the LW condition. Although the volume shortage is almost the same, indicated by the similar fuel space requirement in either LW or HW, the PEM FC already performs well in most sections. So, increasing the installed power has more effect in increasing the PEM FC's volume than reducing the fuel storage system.

5.3.2 Container capacity

The container capacity decreases because of the additional space required by the new system. Figure 5.7 shows an increase in volume when one installs more power. This characteristic means the amount of 20 ft dummy containers can only increase when one installs more power. The minimal required power installed shows the lost container capacity in this case. For liquid hydrogen, this would be three container spaces for all ships. When one equips these ships with the compressed hydrogen storage, all ships lose four container spaces initially. Although the volumes differ per ship, they all seem to fall in the same amount of dummy containers. These are the number of dummy containers outside of the ones already constructed for ships 2 and 3. If the corners were not present and not capable of stalling hydrogen, the inland ships would lose container capacity. Ships 2 and 3 would lose six and five for the compressed and both ships four for the liquid storage option containers spots. Figure 5.8 shows more extensive volume requirements for the ships, which results in more container capacity loss. The compressed hydrogen storage gives 12, 14, and 12 less container capacity for ship 1, 2, and 3. The liquid hydrogen storage shows 8, 10, and 8 less container capacity for ship 1, 2, and 3. The difference between the compressed and liquid storage numbers comes from the difference in the fuel density per storage and the storage density. Ship 3 has a better propulsive performance than the other two ships, which results in less loss in container capacity.

It is difficult to say how the container capacity reduction reflects itself in the RFR of container

ships. Inland ships that transport container are paid a block price for the trip itself or paid a daily rate when sailing one or multiple trips. Only in a brief period in the economic crisis, shipping companies paid inland ships in the container transport in the Netherlands in a freight rate per container. This way meant that shipping companies shifted all the risk on the skippers and ship owners themselves. Container inland ships sailing in daily rate conditions are also lifted from port payments and fuel cost because this is all paid for by the shipping company. How a shipping company deals with less capacity resides in the planning of container transport. This research translates the RFR to a unit of Euro per container per kilometre to compare the potential.

5.4 RFR

The larger mass of the new system and the larger volume requirement reflects the cargo space loss. This loss affects the ships' RFR for the transport of containers, heavy cargo, and voluminous cargo to cover the costs. Figures 5.9 and 5.10 show the RFR of the ships based on their tonnage capacities and kilometres sailed.

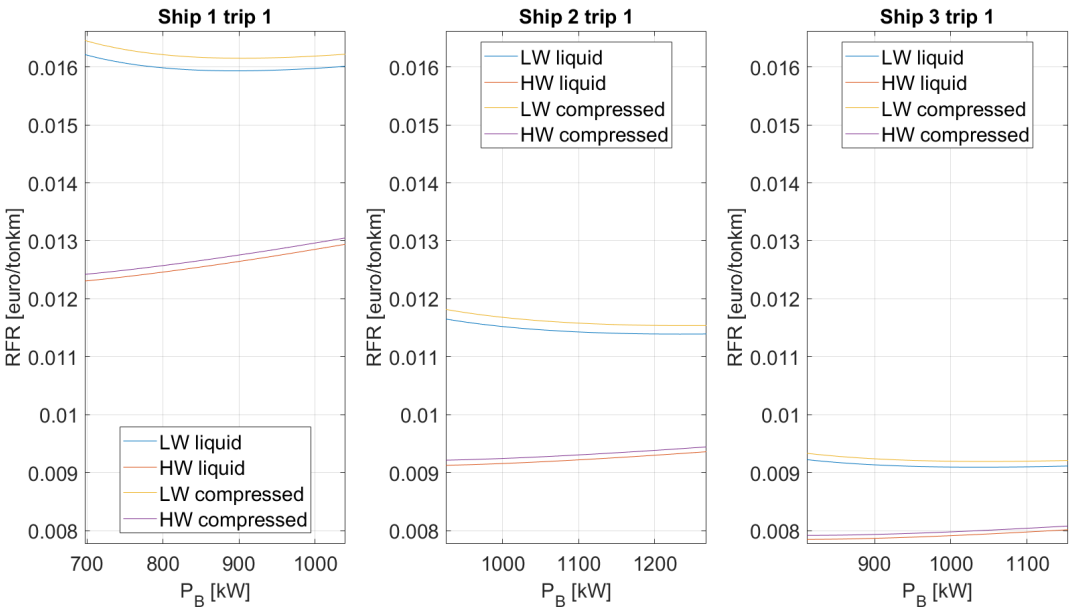

Figure 5.9: Trip 1: RFR versus Installed power

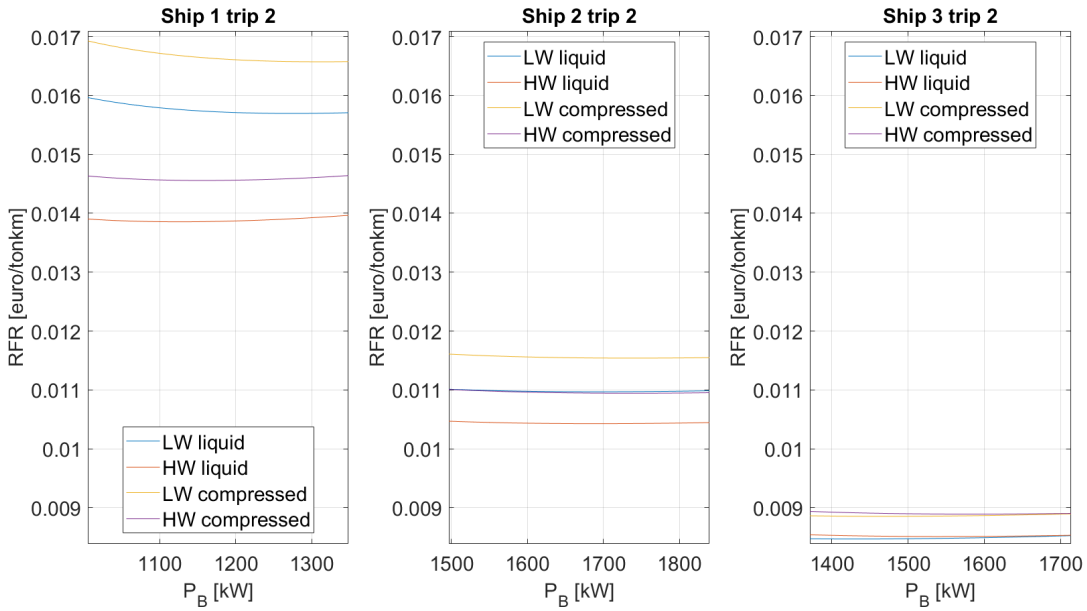

Figure 5.10: Trip 2: RFR versus Installed power

According to figures 5.9 and 5.10, the compressed hydrogen storage option is more expensive compared to the liquid storage option in each condition. Increasing the installed power has more influence for the inland ships sailing trip 1 than for trip 2 in LW condition. This difference happens because the power demand for trip 1 is closer to the minimal installed power. Therefore, they obtain a larger gain in increasing power to the increase system efficiency. In HW condition, there is small or no gain in installing more power on the inland ships. For trip 1, there is no reduction in the minimal RFR because installing more power will barely improve the system efficiency. Installing more power means increasing the system's mass, which lowers the tonnage capacity of the ships. In case of trip 2, there is some gain to be obtained in lowering the RFR. Here, it does help to install more power, reduce fuel capacity and thus storage. After a certain amount of power installed, the increasing mass of the system surpasses the lowering of the hydrogen fuel storage. In the LW condition, the dependency of the power increase on the inland ships reaches a clear optimum. For ship 1, this is about 25% power increase. The optimum for ship 2 occurs after a 27% increase in power and ship 3 after 21%. The RFR for the compressed hydrogen option is higher than the liquid one because the compressed storage's mass is larger. The more extensive mass results in lower tonnage capacity of the inland ships. The ships' RFRs are lower in the HW than in LW condition because they obtain better FC system efficiencies in HW condition. For a trip in the HW condition, the ships use less hydrogen fuel for trip 1. The is also true for ship 1 and 2 sailing trip 2. For ship 3 the same things happen as it was explained in paragraph 5.3 figure 5.8. Installing more power does also benefit when the ships sail trip 2. The ships reach an optimum for each condition and hydrogen storage option. Ship 1 benefits more in the RFR reduction than the other two ships when one increases the installed power. The mass reduction in hydrogen storage has more impact on ship 1. Installing more power makes it possible to save costs and create a more competitive RFR for the ship. Table 5.5 shows the decrease of the RFR per ton per kilometre.

Ship	Trip 1			Trip 2		
	1	2	3	1	2	3
liquid H_2 LW	1.7	2.2	1.4	1.7	0.4	0.0
liquid H_2 HW	0.0	0.0	0.0	0.3	0.4	0.3
Compressed H_2 LW	1.9	2.4	1.5	2.1	0.6	0.1
Compressed H_2 HW	0.0	0.0	0.0	0.5	0.6	0.5

Table 5.5: Possible decrease in percentage of RFR of ships by installing more power

Table 5.5 shows that ship 1 can reduce the RFR mainly in the LW condition for both trips. It does not benefit from the increase in power for trip 1 and only a little for 2 in the HW condition. Ship 2 and 3 can mainly benefit from the power increase for trip 1 in the LW condition, but a little in the two trip conditions for the second trip.

5.5 refuelling frequency

The refuelling frequency is an interesting variable in the design of a ship with hydrogen fuel. The refuelling frequency shows how often the skipper needs to refuel the ship because of an empty fuel tank. The shipowner does not want to lose cargo space and tonnage capacity. When the refuelling frequency increases, the fuel storage capacity is reduced, including the ship's range. So, increasing the refuelling frequency reduces the hydrogen storage size, decreases storage costs and decreases cargo space losses. However, it increases the completion time of the trip due to the extra refuel stop. This research assumes the skipper needs 2 hours of extra time to moor the ship and attach the refuel lines. Figure 5.11 shows the RFR for ship 2 sailing trip 1 with liquid H_2.

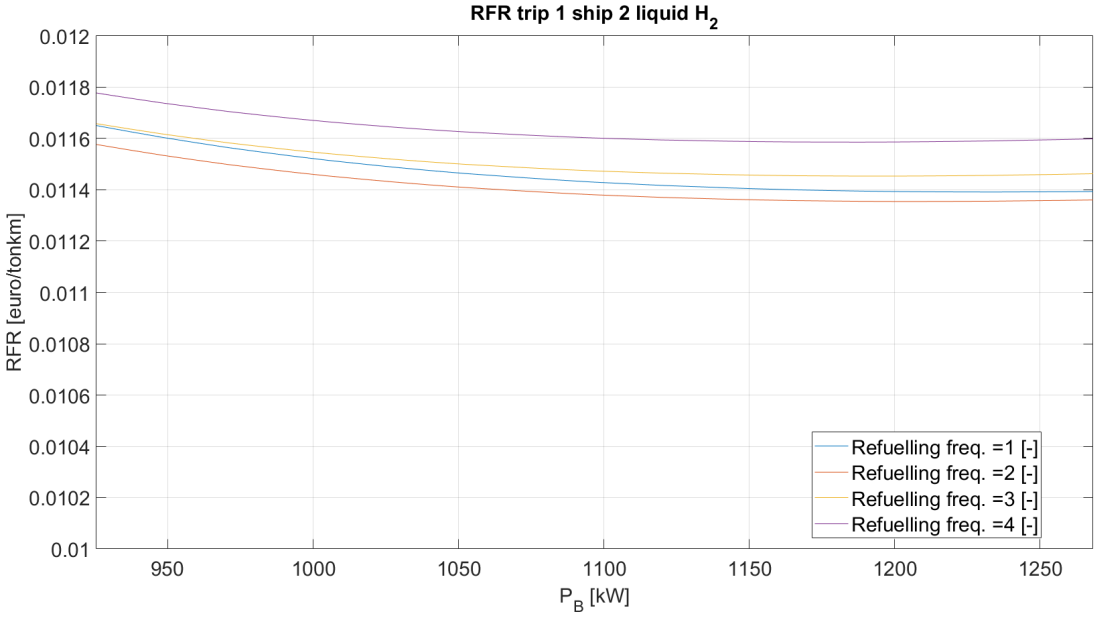

Figure 5.11: Trip 1, Ship 2 with liquid H_2: RFR per ton per kilometre versus Installed power

Figure 5.11 shows a decrease and increase of the RFR when the calculation model varies the refuelling frequency. The refuelling frequency of 1 displays the original strategy, where the shipowner fuels the ship once to sail the entire round trip. The graphs show that for both hydrogen storage options, a refuelling frequency of 2 decreases the RFR while the refuelling frequency of 3 increases the RFR relative to lower refuelling frequencies. The ships do not gain

much when the refuelling frequency increases for short trip distances because the hydrogen storage system is not as drastic in size as it would be for longer ranges. The new system installed on a ship sailing only short distances has less effect on the ship's performance than sailing longer distances. Ship 3 does not benefit a lot from the increase in refuel frequency. The RFR of ship 3 compared to 1 and 2 shows that the RFR's minimum happens earlier when the refuelling frequency increases. This effect occurs because ship 3 has relatively less hydrogen storage due to a better propulsion performance, which results in less benefit from decreasing the storage size. Trip 2 should show different results in the refuelling frequency increase. Figure 5.12 shows the RFR for ship 2 sailing trip 2 for compressed H_2.

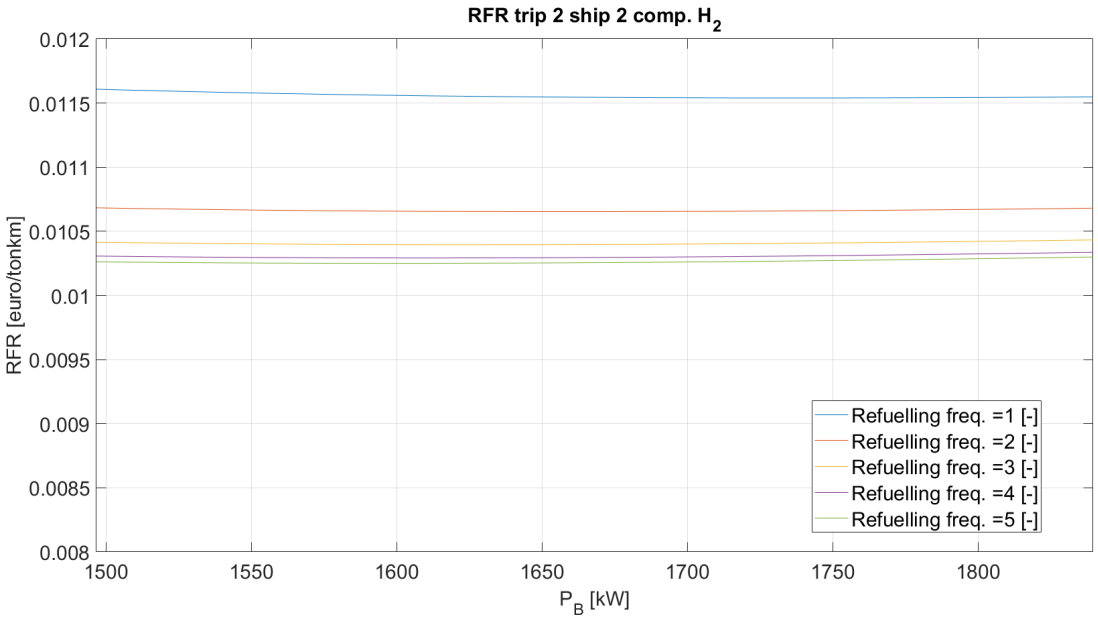

Figure 5.12: Trip 2, Ship 2 with compressed H_2: RFR per ton per kilometre versus Installed power

Figure 5.12 shows that the ship benefits from increasing the refuelling frequency up to 5, which means that the storage is 20% of the original size. The refuelling frequency of 5 does result in a better RFR, but the decrease of the RFR becomes less. There is a limit to the refuelling frequency increase because the trip's completion time becomes too large. For the range of trip 2, the refuelling frequency shows more effective in decreasing the RFR. This effect happens since the hydrogen storage size is much larger compared to trip 1. The reduction of the storage size is larger, which results in larger reductions in the depreciation cost of the storage units. Also, the weight of the storage system becomes lower, which results in less tonnage capacity losses. Figures 5.13 and 5.14 show how the RFR behaves as a functions of the refuelling frequency for respectively trip 1 and trip 2. For these figures, the calculation model uses the optimal installed power to determine the ships' optimal RFR. The model determines the optimal installed power by checking which installed power the RFR becomes the lowest at a refuelling frequency of 1.

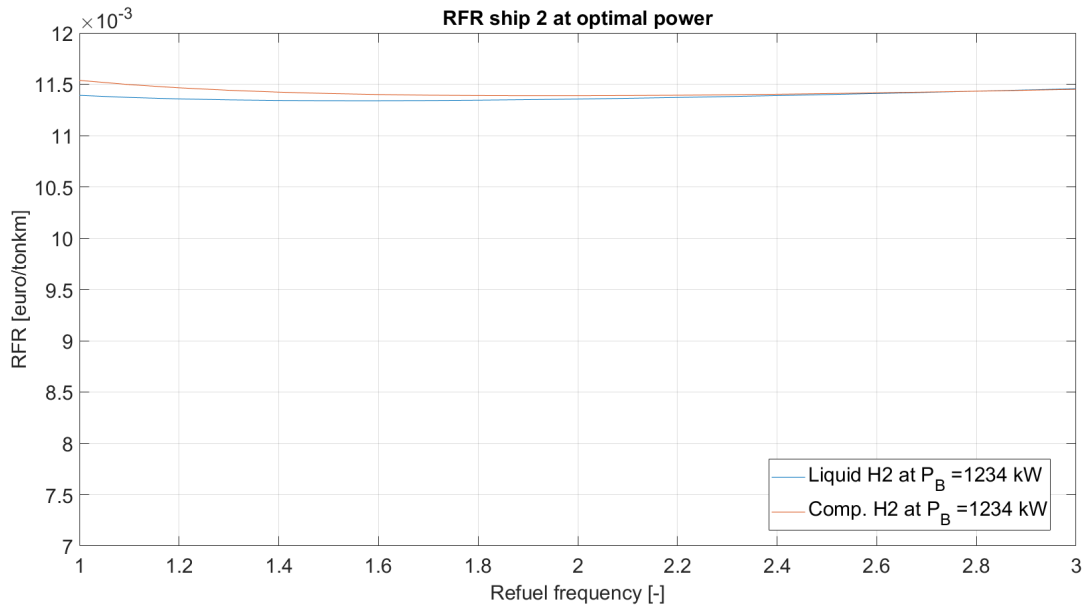

Figure 5.13: Trip 1, Ship 2: RFR per ton per kilometre versus the refuel frequency

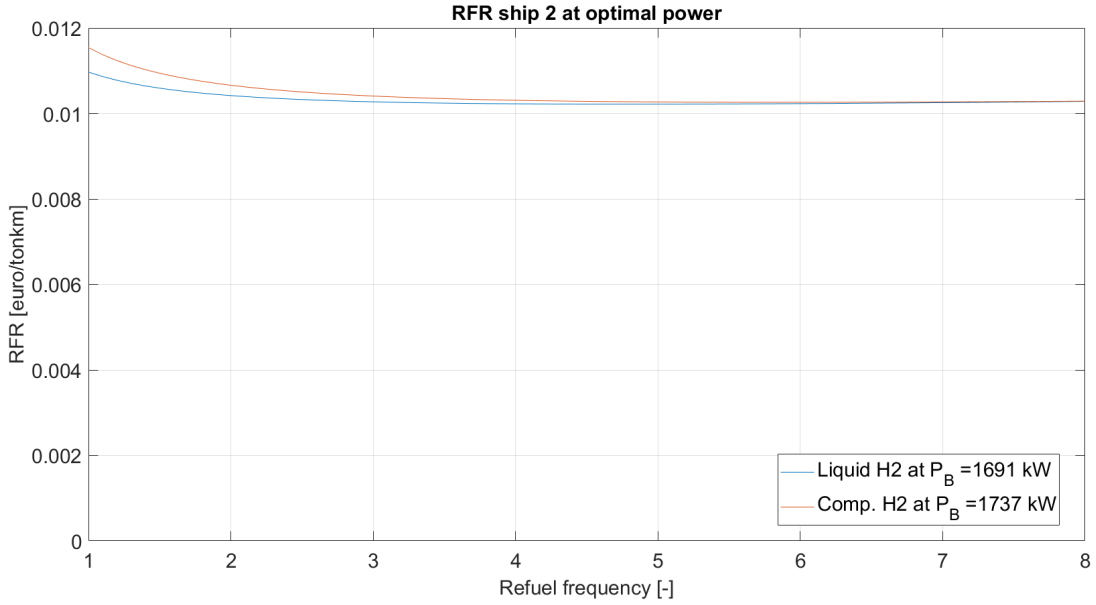

Figure 5.14: Trip 2, Ship 2: RFR per ton per kilometre versus the refuel frequency

If the time per trip becomes higher, the cost per trip becomes more extensive, which is also visible in the figures. Due to the short trip duration of trip 1, this effect is more significant. The time to refuel is not proportional to the sailing time but fixed. So it has more impact on short trip distances compared to large trip distances. Earlier is noticed that ship 3 has slightly different behaviour in the RFR versus the refuelling frequency compared to the others. Ship 3 has a better propulsion performance, which leads to smaller hydrogen storage relative to its ship size and so, it benefits less from the increase of the refuelling frequency. Ship 1 and 2 reach their respective minimum RFR at a higher refuelling frequency compared to ship 3. This feature is also different between the compressed hydrogen and liquid hydrogen. The compressed hydrogen storage allows more reduction in the RFR compared to the liquid hydrogen. As mentioned before, the storage of compressed hydrogen at 700 bar is more expensive than liquid

hydrogen storage units. The storage weight is also more extensive than the liquid hydrogen, so reducing the storage size shows more effectiveness for the compressed hydrogen case.

5.6 Conclusions

This paragraph shows how the ships would perform on trips. It has worked its way up to determine the influence of a PEM FC system with hydrogen storage on the RFR of the inland ships. This research implemented two options to see how one could save costs from the expensive PEM FC with hydrogen storage and how the RFR could be improved:

1. Increasing the installed power.
2. Increasing the refuel frequency.

Each option is capable of lowering the RFR per ton per km. Table 5.5 presents the reduction in the RFR by increasing power. It shows that increasing the installed power is mainly beneficial for the short trip. Only ship 1 benefits from increasing the installed power for longer ranges. The second option, increasing the refuelling frequency, has more potential in reducing the RFR. The refuel frequency shows that there is a limit to increasing the refuelling frequency. Despite the limit, a small reduction in the RFR is still possible for trip 1. Trip 2 shows a more significant decrease in the RFR.

The combination of the two options can show an optimal solution for the new system. For longer ranges, it is more beneficial to increase the refuelling frequency instead of installing more power. When the range is already short for a ship, it can decrease the cost slightly. Increasing the power and refuelling frequency can deliver a RFR lower than installing the minimum required power and fuel for the whole round trip. Table 5.6 shows the percentage of reduction in the ships' RFR when the refuelling frequency increases at the most optimal installed power.

		Ship		
H_2 Storage option	Trip	1	2	3
Liquid	1	0.6	0.5	0.2
Compressed	1	1.5	1.3	0.8
Liquid	2	7.7	6.8	5.5
Compressed	2	12.2	11.1	9.2

Table 5.6: RFR reduction in percentage due to increasing the refuel frequency

Table 5.6 shows that after optimising the installed power, there is still room for improving the ships' RFR. Trip 1 allows less improvement of the RFR compared to trip 2 because the trip distance is short. Compressed hydrogen shows more significant reductions in the RFR than liquid hydrogen, as noticed earlier. For every case, ship 3 benefits less from increasing the refuelling frequency compared to the other ships.

Ship size and propulsion arrangement also influence the decision of installing more power or increasing refuel frequency slightly. For ship 1 installing more power, it seems that installing more power can always result in a lower RFR per ton per kilometre, while ship 2 and 3 do not benefit much or nothing at higher refuel frequencies. Table 5.7 shows the ships' best RFRs when both savings methods are combined.

	Trip 1						Trip 2					
	Ship 1		Ship 2		Ship 3		Ship 1		Ship 2		Ship 3	
	RFR	Rf	RFR	Rf	RFR	Rf	RFR	Rf	RFR	Rf	RFR	Rf
liquid H_2 LW	15.84	1.60	11.34	1.60	9.08	1.40	14.49	5.00	10.22	4.80	8.00	4.20
Compressed H_2 LW	15.91	2.00	11.39	1.90	9.12	1.70	14.55	6.20	10.26	5.90	8.04	5.20
liquid H_2 HW	12.65	1.10	9.33	1.20	7.94	1.10	13.03	4.40	9.77	4.60	8.05	4.30
Compressed H_2 HW	12.72	1.40	9.38	1.50	7.98	1.40	13.12	5.40	9.81	5.60	8.08	5.30

Table 5.7: Optimised RFR (10^{-3} euro/tonkm) for both the refuel frequency and the installed power

According to the calculations for the optimised RFR, the compressed hydrogen storage is always slightly more costly compared to the liquid hydrogen for the ships. The RFRs do come very close to each other when the ships optimised in the refuelling frequency. Still, the liquid hydrogen storage with an optimised installed power and refuel frequency seems to be the best option to install on a ship with a PEM FC system. Although the RFR of the compressed hydrogen option reduces more significantly, it is still slightly more expensive.

Chapter 6

Conclusion & Recommendation

This research was conducted to find the influence of a PEM FC system running on hydrogen on the inland ships' performance. This Thesis measured the performance of inland ships with the RFR in various ways. This research used a generic approach with varying ship speed and range on a fixed water depth to evaluate the PEM FC system. Also, this research presented two cases to determine inland ships' performances. It performed calculations on three inland ships with different ships on bulk carrying and container carrying inland ship types.

This chapter contains the conclusions and recommendations of this Thesis. The first paragraph summarises the conclusions drawn earlier for both the general overview and the trip case, whereas the second one suggests recommendations for future research.

6.1 Conclusion

The research question of this Thesis reads: How does an inland ship with a PEM FC system running on hydrogen perform in terms of the required freight rate? The following two sections provide the answer to this question.

6.1.1 General

In the general overview in chapter 4, the ship speed and the ship range were varied for a ship with a PEM FC system running on hydrogen. This approach shed light on the triangular relation mentioned in the introduction and on the influence the new system has on the inland ships' RFRs. The results showed that the required hydrogen storage size is much larger in volume compared to conventional diesel. As diesel can easily reside in steel tanks of all kinds of shapes, the hydrogen is more voluminous by its storage density. The hydrogen storage units take up space as well. The mass and volume of the new system show a decrease in cargo-carrying capacity. Aside from the hydrogen storage that uses extra weight and space, the PEM FC with all auxiliary systems is also quite a large unit in weight and volume.

The cost overview showed that a large portion of the total cost is the hydrogen fuel cost, especially at higher ship speeds where the fuel consumption is much higher. The hydrogen fuel price has a large effect on the ships' RFR and optimal ship speed from an economic perspective. Therefore, the hydrogen fuel price has a strong influence on the competitive position of these ships. The range's impact on the RFR is smaller than that of the ship speed. At higher ship speeds, the effect of range becomes stronger. This effect happens due to the higher power demand and the lower system efficiencies of the PEM FCs. The assumed values for the different parameters result in an optimal ship speed of approximately 10 km/h. The optimal ship speed for ships with a PEM FC system is roughly 1.5 km/h lower than a conventional one.

The comparison of the two storage options showed that based on the assumptions made, the liquid hydrogen would be a better option in terms of the RFR of the ships. The cost of compressed hydrogen is higher compared to liquid hydrogen. This cost difference results in higher RFRs for the compressed hydrogen. When the difference between the storage prices becomes small, the performance in RFR becomes similar. At high ship speeds with similar storage prices, the compressed hydrogen would outperform the liquid hydrogen at short ranges, while for longer ranges the liquid hydrogen becomes a better option. The optimal ship speed of the ships imposes problems when they need to deliver cargo sailing upstream. If the current is strong and the ships sail at the optimal ship speed, the cargo reaches its destination in a very long time compared to actual cargo shipping times. The optimal ship speed is reachable sailing downstream.

This section provides the inland ship's performance in a generalised case looking at the research question. The PEM FC ships' performance is lower than that of a conventional ship. The optimal ship speed is lower while the required freight rate is higher than diesel-fuelled ships. The new system is also heavier and more voluminous, meaning the ship always loses cargo capacity. These losses can become more extensive when the ship speed and range increase. The PEM FC ship's competitiveness becomes much better when the hydrogen, PEM FC, and storage system price becomes lower. The case evaluation adds more content to this answer.

6.1.2 Trip case

In addition to the conclusions from the general overview, the trip cases show various as well. The trip cases created are two round trips, Rotterdam to Duisburg and Rotterdam to Basel. This research has evaluated two methods to save costs and improve the RFR of the ships. These options are:

1. Increasing the installed power to lower the load on the PEM FC system. The boost in power increases the system efficiency and lowers the fuel consumption of the inland ships.
2. Increasing the refuelling frequency to decrease the storage size of the hydrogen tanks. This method lowers the costs, while it increases the average time to complete the trip.

Both options show that they are capable of lowering the RFR of the inland ships. It showed that a small increase in the installed power could save some costs. The short trip showed the most gain in the RFR of the inland ships by at least 1% in LW conditions. The long trip allowed only little improvement in increasing the installed power. Ship 1 could raise its performance in LW condition by at least 1%, while ship 2 improves the only 0.1% while ship 3 has even lower improvements than ship 2.

The refuelling frequency showed more decrease in the RFR, so a more significant improvement in the inland ships' performance. The gain is more extensive for the compressed hydrogen than liquid hydrogen option. The compressed option results in more costs than the liquid hydrogen option. Extra refuelling results in a closer gap between the two options in terms of RFR. The decrease of the RFR is smaller for the short trip compared to the long one. This decrease makes sense since a more extensive and costly storage system gains a lot more cost reduction than a small and cheaper storage system. For the short trip, an inland ship might be able to reduce the RFR by approximately 0.4% for the liquid hydrogen option and 1.2% for the compressed hydrogen option. The long trip shows that a reduction of 6.7% and 10.8% of the RFR for respectively the liquid and compressed hydrogen option might be obtainable. The difference between the RFRs of the two fuel options becomes small. Still, hydrogen fuel is the better option after optimising for the refuelling frequency and power.

The trip case outcomes finalize the answer to the research question. The general conclusion confirmed that the inland ships' performance is lower with the PEM FC system than with a

conventional diesel engine. The case evaluation shows that the PEM FC ships can improve their competitive position on the market by installing more power and increasing the refuelling frequency. These aspects lower the required freight rates meaning the inland ships' performance becomes better.

6.2 Recommendation

This research has evaluated how a PEM FC system running on hydrogen impacts the inland ship's RFR. Two types of hydrogen storage are evaluated on three inland ships, each with different dimensions. This research looked into dry bulk type inland ships, which are bulk carrying and container carrying ships. The ships are evaluated under the assumption of sailing at their design draught in shallow water conditions. These reasons show that certain aspects of this research could use follow-up research. For example, tankers are also part of the total inland ship fleet. This section will discuss the recommendations for future research.

One of the limits in this research is that it does not consider all different hydrogen storage options. The liquid and compressed under 700 bar storage options were chosen, based on having one of the higher densities that hydrogen can obtain. A lot of research is performed in determining other storage options, for example, solid hydrogen carriers. One of these options might prove very beneficial for inland ships, regarding cost, safety, and ease of use. So considering other hydrogen storage options for inland ships and comparing them to each other is a recommendation for future research.

Another recommendation is to perform a more in-depth design analysis. The design assumptions in this research should represent the proper volume and mass assumptions of the new system. However, this research gave little attention to placing the components into the ships. One could create a better understanding of the implications of these systems through an in-depth design analysis. The PEM FC system consists of the cell stacks and auxiliary system. One could place these components more optimally if research investigates the inland ship lay-out and shape more thoroughly. This thorough study could save space and have less impact on the cargo hold.

As this research performs the calculations, shallow water is considered in speed limitations and ship resistance increase, not limiting the draught and freight carried. Low water depth occurs regularly in inland shipping. So, ship owners are often limited in the amount of cargo they can transport. The inland ships' performance in extremely low water depths with a PEM FC installation provides more information on the subject. If a model can calculate the performance in various water depths, one could perform analysis on events of different water depths throughout time. This approach can show more on the average RFR the inland ship could obtain for sailing particular trajectories and how the PEM FC installation plays a part.

Dry bulk inland ships cover the majority of the Dutch inland ship fleet. This characteristic does not mean that the PEM FC installation is not an option for other inland ship types, such as tankers. One could discover a different solution for these inland ship types than the two suggested in this research, installing more power and increasing the refuelling frequency. Also, the inland ship dimensions in this research cover only a few inland ship dimensions. This limitation suggests looking into a larger spectrum of ship types and dimensions.

Acknowledgements

At the start of my Thesis, the idea crossed my mind to analyse the combination of alternative fuels with inland ships on a design and performance basis. Struggling through the first weeks showed me the difficulty in making a proper Plan of Approach on this subject. My Plan of Approach was reviewed by my supervisor, Robert Hekkenberg, and master coordinator, Peter de Vos. They consulted me on the option to alter the course of my Thesis approach slightly. Mr Hekkenberg and Mr de Vos had allowed me to change the method from a broad design perspective to a more mathematical in-depth one on the subject. I am grateful that I was given this opportunity by my supervisor and master coordinator to choose an approach that suited me more in skill and perspective.

I want to thank my supervisor in particular for keeping me on track and focused during my Thesis. I often dove in too deep in certain aspects of my research. Mr Hekkenberg asked me the right questions to keep me from getting caught up in matters beyond this Thesis' scope. Thank you for your consultation and support during the strange time in which I completed my master Thesis. I want to thank Mr Lindert van Biert for providing me with insight into the PEM FC system and help understand its characteristics. You have given me great support, which allowed me to set up a proper calculation model for a PEM FC system. I would also like to thank Dr Ir. R. Hekkenberg, Dr Ir. L.van Biert, and Dr V. Reppa for taking the time to read this report and review my Thesis.

I like to thank Peter Bout from the company AirProducts for providing me with some insight into hydrogen refuelling and Jogchum Bruinsma from the company Nedstack for providing information on one of their PEM FC systems.

I would also like to express my gratitude towards my family, friends, and girlfriend for supporting me in this turbulent time. It has been a rough year during these lockdowns and additional regulations due to Covid-19. Also, my appreciation goes out to my relatives and friends from the inland ship sector. You have provided me with practical knowledge and meaningful discussion regarding my subject.

References

Abma, D., Verbeek, R., Kelderman, B., Hoogvelt, B., & Quispel, M. (2018). *Standardized model and cost/benefit assessment for right-size engines and hybrid configurations* (Tech. Rep.). TNO.

Barbir, F. (2013). Chapter three - fuel cell electrochemistry. In F. Barbir (Ed.), *Pem fuel cells (second edition)* (Second Edition ed., p. 33 - 72). Boston: Academic Press. Retrieved from http://www.sciencedirect.com/science/article/pii/B9780123877109000035 doi: https://doi.org/10.1016/B978-0-12-387710-9.00003-5

Barnes, M. (2003). *Practical variable speed drives and power electronics.* Elsevier Science. Retrieved from https://books.google.nl/books?id=LxW9F9WCixcC

Binnenvaartkennis. (2020). *Aflaaddiepte rijn - vuistregels.* Retrieved from https://www.binnenvaartkennis.nl/aflaad-diepte-rijn/

CCNR. (2019, June). *Plenaire voorjaarszitting 2019 van de ccr.* Retrieved from https://www.ccr-zkr.org/files/documents/cpresse/cp20190607nl.pdf

Collins, L. (2020). *A wake-up call on green hydrogen: the amount of wind and solar needed is immense.* Retrieved from https://www.rechargenews.com/transition/a-wake-up-call-on-green-hydrogen-the-amount-of-wind-and-solar-needed-is-immense/2-1-776481

Danser. (n.d.). *Eiger lng refit.* Retrieved 2020 November 25, from https://www.danser.nl/nl-nl/Vloot/Eiger-LNG-Refit

Geest, W. v. d., & Menist, M. (2019, July 10). *Op weg naar een klimaatneutrale binnenvaart per 2050* (Tech. Rep.). Panteia.

G&R, S. B. (2007). *Mission.*

Hassel, E. V. (2011). Developing a small barge convoy system to reactivate the use of the small inland waterway network..

Hekkenberg, R. G. (2013). *Inland ships for efficient transport chains* (Doctoral dissertation, Delft University of Technology). doi: https://doi.org/10.4233/uuid:f2ead20f-80b5-4d92-818f-7586c7b85f76

Hekkenberg, R. G., Dorsser, C. v., & Schweighofer, J. (2017). Modelling sailing time and cost for inland waterway transport. *European Journal of Transport and Infrastructure Research*, 508-529.

IMO. (2019). *Greenhouse gas emission.* Retrieved from http://www.imo.org/en/OurWork/Environment/PollutionPrevention/AirPollution/Pages/GHG-Emissions.aspx

IVR. (2018). *Samenstellign nederlandse vloot.* Retrieved from https://binnenvaartcijfers.nl/samenstelling-nederlandse-vloot/

Klein Woud, H. J., & Stapersma, D. (2012). *Design of propulsion and electric power generations systems.*

Lipman, T. E., Edwards, J. L., & Kammen, D. M. (2004). Fuel cell system economics: comparing the costs of generating power with stationary and motor vehicle pem fuel cell systems. *Energy Policy*, *32*(1), 101 - 125. Retrieved from http://www.sciencedirect.com/science/article/pii/S0301421502002860 doi: https://doi.org/10.1016/S0301-4215(02)00286-0

Nedstack. (2019, November). *Nedstack fcs 13-xxl pem fuel cell stack.*

Oosterveld, M. W. C. (1970). *Wake adapted ducted propellers* (Unpublished doctoral dissertation). Technische Hogeschool Delft.

Oosterveld, M. W. C., & van Oossanen, P. (1975). Further computer-analyzed data of the wageningen b-screw series. *International shipbuilding progress*, *22*(251), 251–262.

Paster, M., Ahluwalia, R., Berry, G., Elgowainy, A., Lasher, S., McKenney, K., & Gardiner, M. (2011). Hydrogen storage technology options for fuel cell vehicles: Well-to-wheel costs, energy efficiencies, and greenhouse gas emissions. *International Journal of Hydrogen Energy*, *36*(22), 14534 - 14551. Retrieved from http://www.sciencedirect.com/science/article/pii/S0360319911017162 (Fuel Cell Technologies: FUCETECH 2009) doi: https://doi.org/10.1016/j.ijhydene.2011.07.056

Pompée, P.-J. (2015). About modelling inland vessels resistance and propulsion and interaction vessel-waterway key parameters driving restricted/shallow water effects. *Proceeding of Smart Rivers 2015*.

Rabbani, R. A. (2013). *Dynamic performance of a pem fuel cell system* (Unpublished doctoral dissertation). Technical University of Denmark.

Rivard, E., Trudeau, M., & Zaghib, K. (2019). Hydrogen storage for mobility: A review. *Materials*, *12*(12), 1973.

Smit, M. (2014). Towards 40 000 hours of operation for nedstack's fcs xxl pem fuel cell stacks. *Fuel Cells Bulletin*, *2014*(8), 12 - 15. Retrieved from `http://www.sciencedirect.com/science/article/pii/S146428591470238X` doi: https://doi.org/10.1016/S1464-2859(14)70238-X

Tirnovan, R., & Giurgea, S. (2012). Efficiency improvement of a pemfc power source by optimization of the air management. *International Journal of Hydrogen Energy*, *37*(9), 7745–7756.

Tronstad, T., Åstrand, H. H., Haugom, G. P., & Langfeldt, L. (2017). Study on the use of fuel cells in shipping. *European Maritime Safety Agency*.

van Biert, L., Godjevac, M., Visser, K., & Aravind, P. (2016). A review of fuel cell systems for maritime applications. *Journal of Power Sources*, *327*, 345 - 364. Retrieved from `http://www.sciencedirect.com/science/article/pii/S0378775316308631` doi: https://doi.org/10.1016/j.jpowsour.2016.07.007

Zhang, Y., Lundblad, A., Campana, P. E., & Yan, J. (2016). Comparative study of battery storage and hydrogen storage to increase photovoltaic self-sufficiency in a residential building of sweden. *Energy Procedia*, *103*, 268 - 273. Retrieved from `http://www.sciencedirect.com/science/article/pii/S1876610216314941` (Renewable Energy Integration with Mini/Microgrid – Proceedings of REM2016) doi: https://doi.org/10.1016/j.egypro.2016.11.284

Zigic, B. (2007). *Banana carrier design* (Tech. Rep.).

Appendix A

Propeller curves

In this chapter of the Appendix the remaining propeller curves of the Wageningen B-series and the Kaplan series are given.

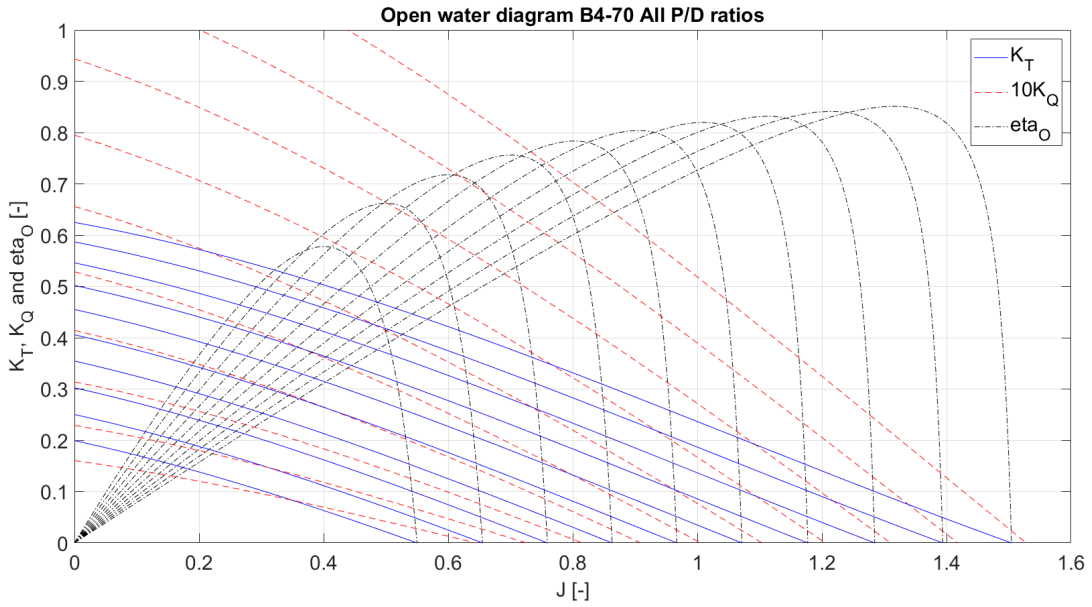

Figure A.1: Wageningen B4-70

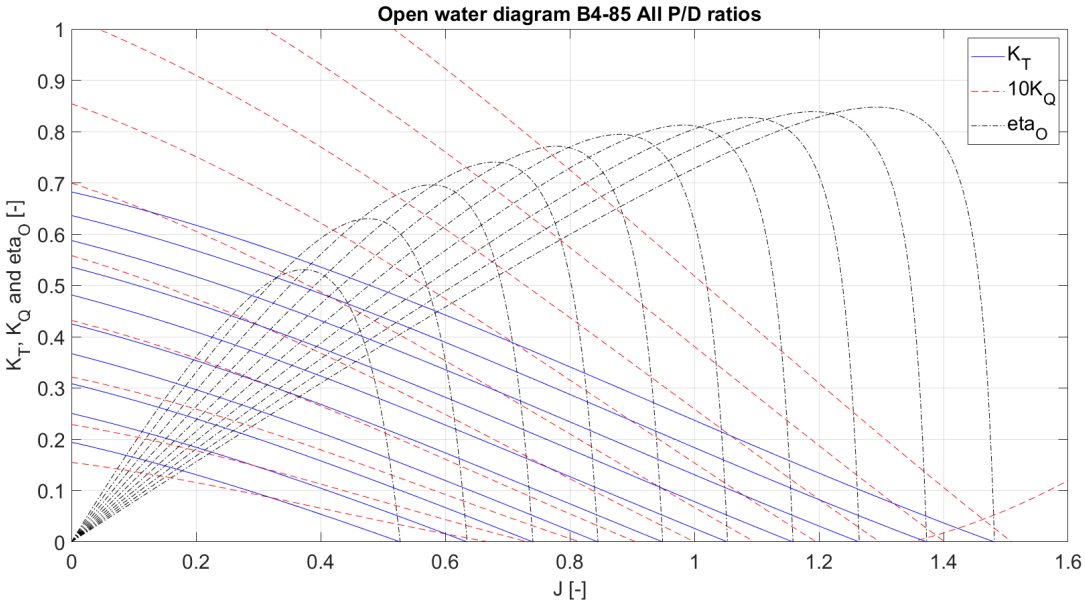

Figure A.2: Wageningen B4-85

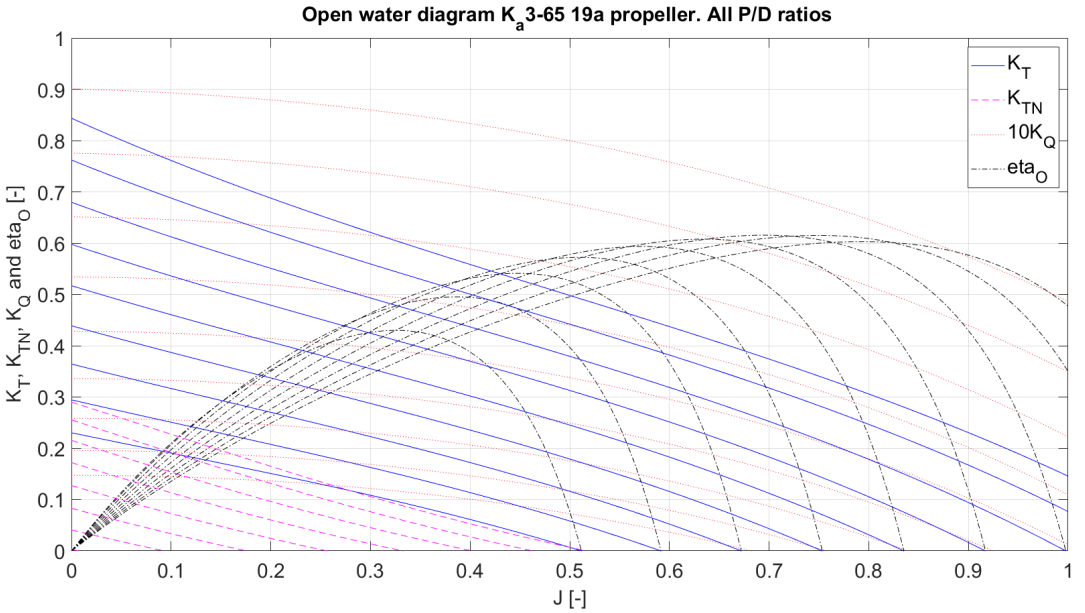

Figure A.3: Wageningen K_a3-65

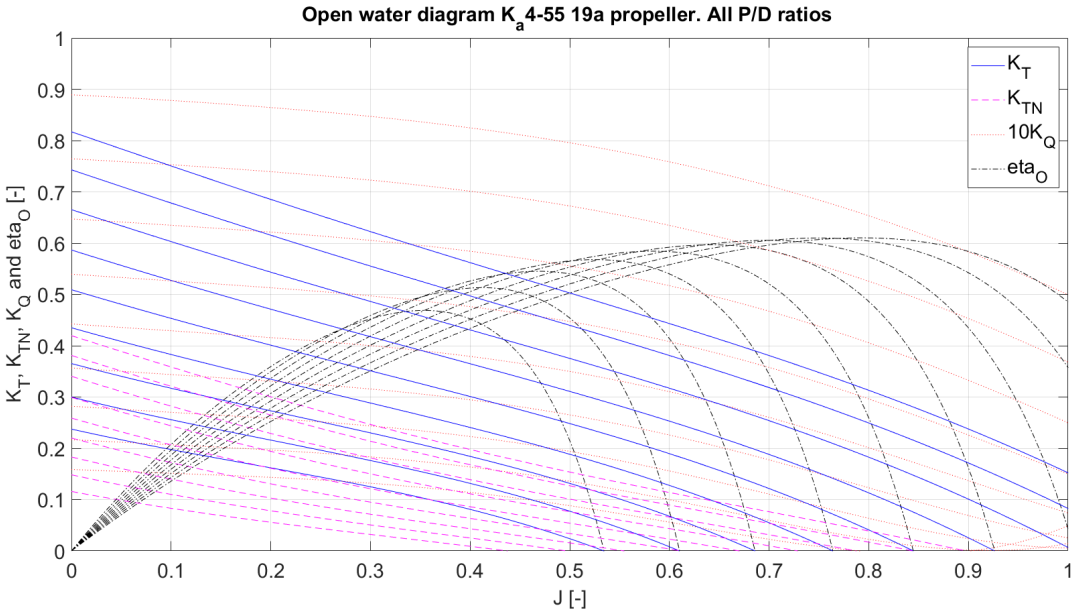

Figure A.4: Wageningen K_a4-55

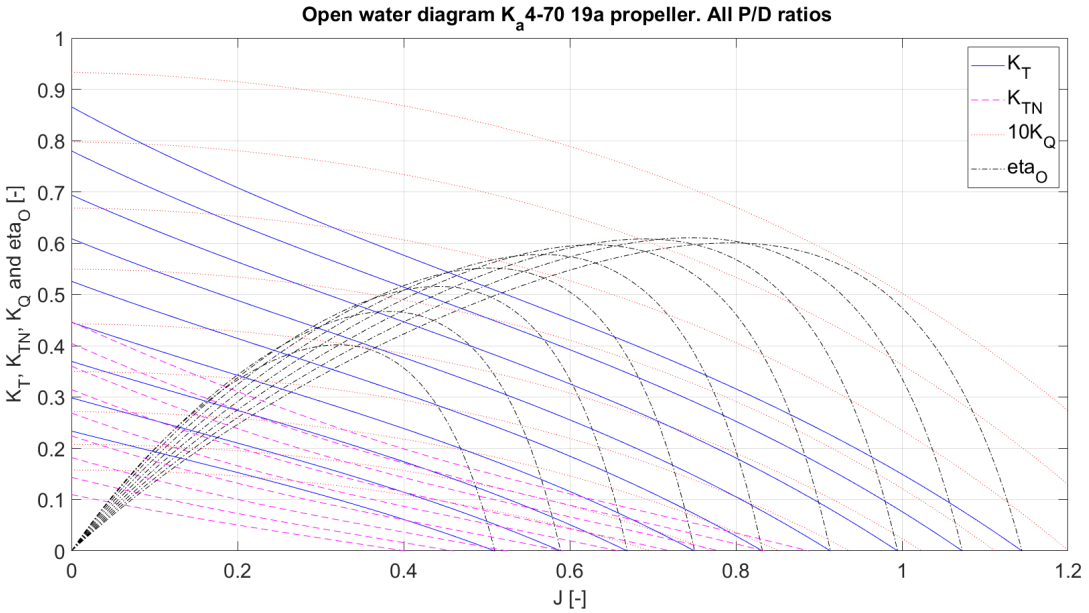

Figure A.5: Wageningen K_a4-70

Appendix B

River characteristics

Section	**Length section** [km]	**LW Current** [km/h]	**LW depth** [m]	**HW current** [km/h]	**HW depth** [m]
Nieuwe Maas	24	0	10	0	12
Noord	9	0	5	0	10
Beneden-Merwede	15	-1.5	5	-2	10
Waal	98	-4	3.98	-5	9.06
Millingen - Duisburg	87	-5	3.75	-7	8.83

Table B.1: River section characteristics trip 1, ship1 (Hekkenberg et al., 2017)

Section	**Length section** [km]	**LW Current** [km/h]	**LW depth** [m]	**HW current** [km/h]	**HW depth** [m]
Nieuwe Maas	24	0	10	0	12
Noord	9	0	5	0	10
Beneden-Merwede	15	-1.5	5	-2	10
Waal	98	-4	4.58	-5	9.06
Millingen - Duisburg	87	-5	4.35	-7	8.83

Table B.2: River section characteristics trip 1, ship 2 and 3 (Hekkenberg et al., 2017)

Section	**Length section** [km]	**LW Current** [km/h]	**LW depth** [m]	**HW current** [km/h]	**HW depth** [m]
Nieuwe Maas	24	0	10	0	12
Noord	9	0	6	0	10
Beneden-Merwede	15	-1.5	6	-2	10
Waal	98	-4	4.56	-5	9.06
Millingen - Duisburg	87	-5	4.33	-7	8.83
Duisburg - Keulen	92	-5	4.1	-7	8.83
Keulen - Koblenz	102	-6	3.84	-8.75	8.79
Koblenz - St. Goar	29	-7	3.84	-10.5	7.61
St. Goar - Bingen	29	-8	3.75	-12.55	6.7
Bingen - Mannheim	103	-5	4.08	-7	7.03
Mannheim - Karlsruhe	65	-6	4.08	-8	7.03
Karlsruhe - Iffezheim	26	-6	4.14	-8	7.09
Iffezheim - Kembs	160	-4	5.35	-6	8.3
Kembs - Basel	4	-5	4.52	-7	7.47

Table B.3: River section characteristic trip 2, ship 1 (Hekkenberg et al., 2017)

Appendix C

Propulsion efficiency

To following table shows a general overview of the development of the propulsion efficiency of the ships. In general the propulsion efficiency decreases in condition where the propeller suffers more load. This is shown in the table for lower water depths and higher ship speeds.

	h/T	v_{ship} [km/h]											
	$[m]$	9	10	11	12	13	14	15	16	17	18	19	20
Ship 1	3	0.489	0.491	0.491	0.488	0.483	0.477	0.466	0.454	0.439	0.423	0.406	0.388
	2.5	0.486	0.486	0.486	0.482	0.476	0.466	0.453	0.437	0.420	0.402	0.383	0.364
	2	0.477	0.476	0.471	0.465	0.454	0.442	0.426	0.407	0.386	0.366	0.345	0.325
	1.5	0.457	0.451	0.442	0.429	0.415	0.396	0.377	0.354	0.332	0.307	0.284	0.259
	1.2	0.437	0.426	0.412	0.396	0.378	0.358	0.337	0.314	0.287	0.261	0.236	0.214
Ship 2	3	0.464	0.466	0.467	0.466	0.464	0.461	0.457	0.450	0.441	0.430	0.416	0.403
	2.5	0.461	0.463	0.463	0.463	0.460	0.455	0.447	0.438	0.425	0.412	0.396	0.382
	2	0.453	0.453	0.452	0.449	0.442	0.435	0.424	0.411	0.396	0.380	0.364	0.346
	1.5	0.436	0.433	0.427	0.419	0.408	0.396	0.380	0.364	0.348	0.328	0.309	0.289
	1.2	0.420	0.412	0.403	0.390	0.376	0.361	0.343	0.327	0.307	0.287	0.266	0.244
Ship 3	3	0.605	0.605	0.605	0.604	0.603	0.600	0.597	0.592	0.586	0.577	0.568	0.557
	2.5	0.603	0.604	0.603	0.602	0.600	0.597	0.592	0.585	0.576	0.566	0.554	0.541
	2	0.599	0.599	0.597	0.595	0.591	0.586	0.578	0.568	0.556	0.542	0.527	0.510
	1.5	0.590	0.588	0.583	0.577	0.570	0.559	0.547	0.531	0.514	0.495	0.473	0.451
	1.2	0.580	0.575	0.567	0.558	0.545	0.531	0.514	0.495	0.474	0.451	0.425	0.398

Table C.1: Propulsion efficiency in shallow water

Appendix D

Speed vs. Range graphs

Figures D.2, D.1, D.4, and D.3 show the container capacity relations of ship 1 and 3.

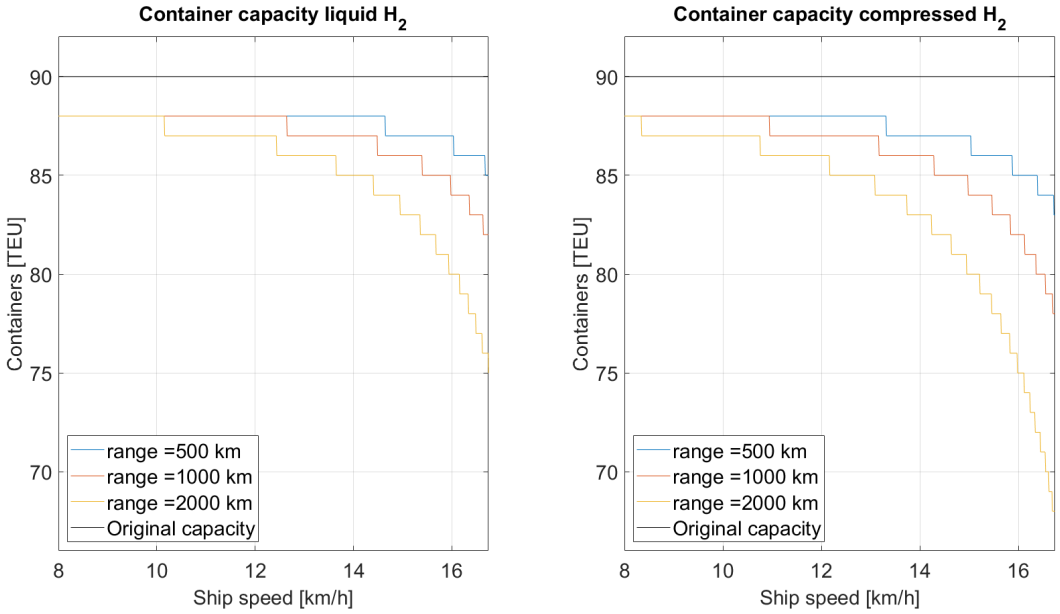

Figure D.1: Container capacity ship 1 versus ship speed

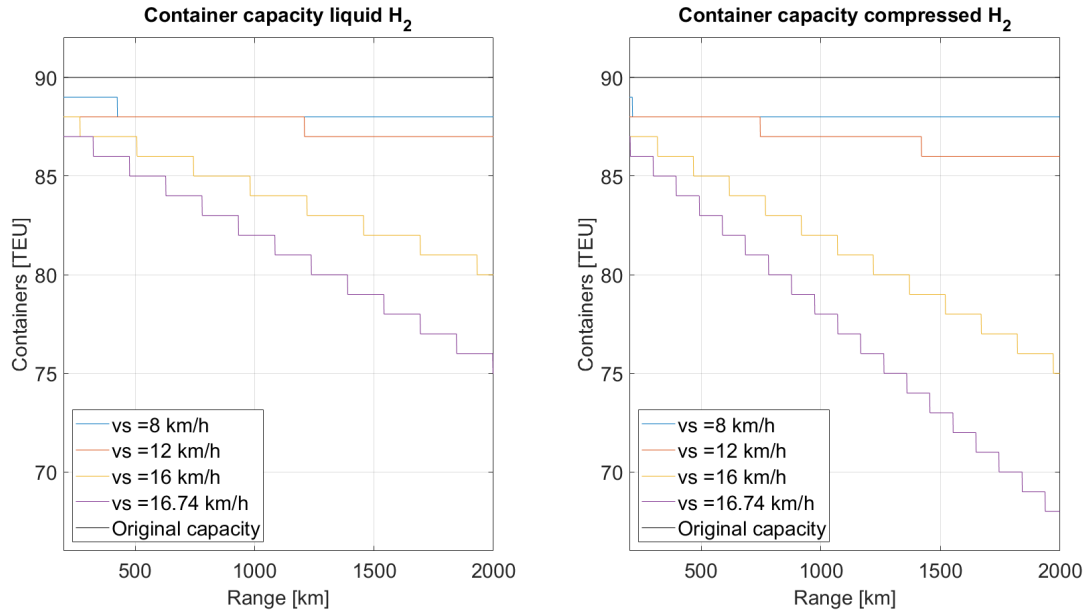

Figure D.2: Container capacity ship 1 versus range

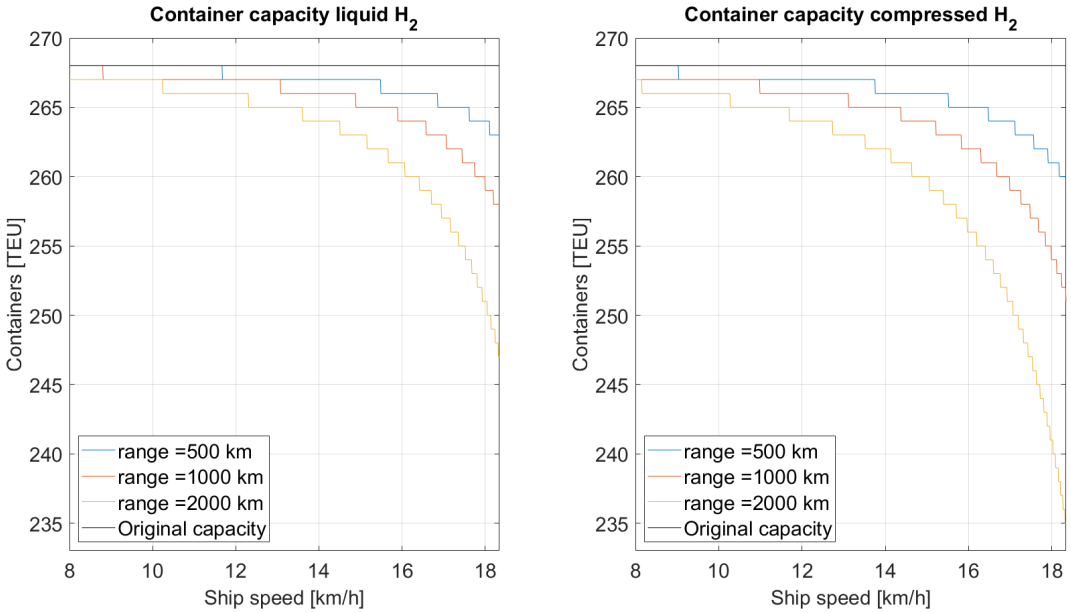

Figure D.3: Container capacity ship 3 versus ship speed

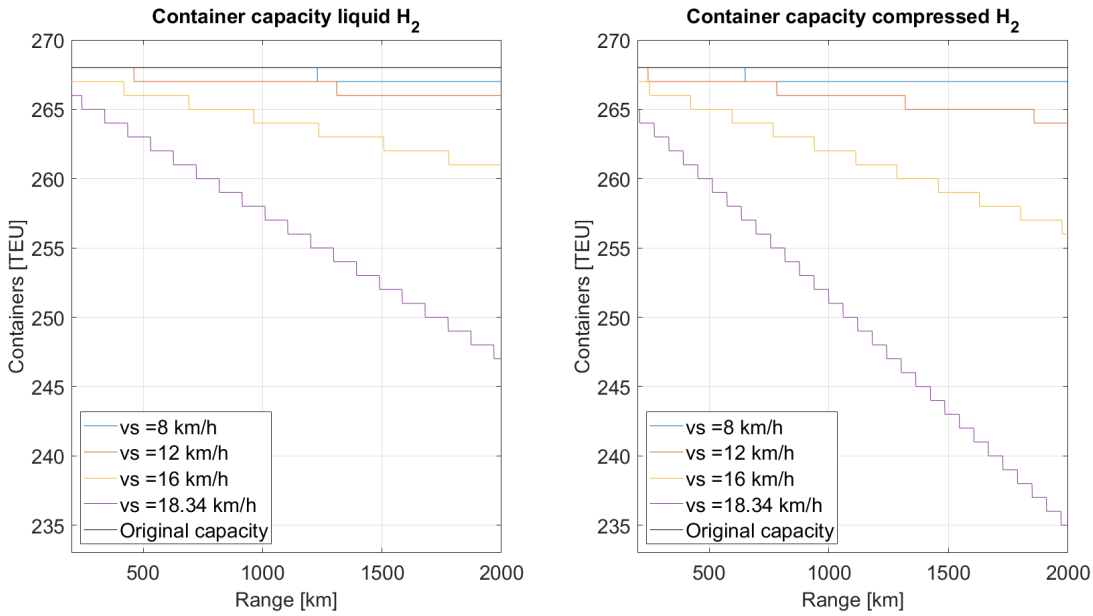

Figure D.4: Container capacity ship 3 versus range

Figures D.5, D.6, D.7, and D.8 show the RFRs of ship 1 and 3.

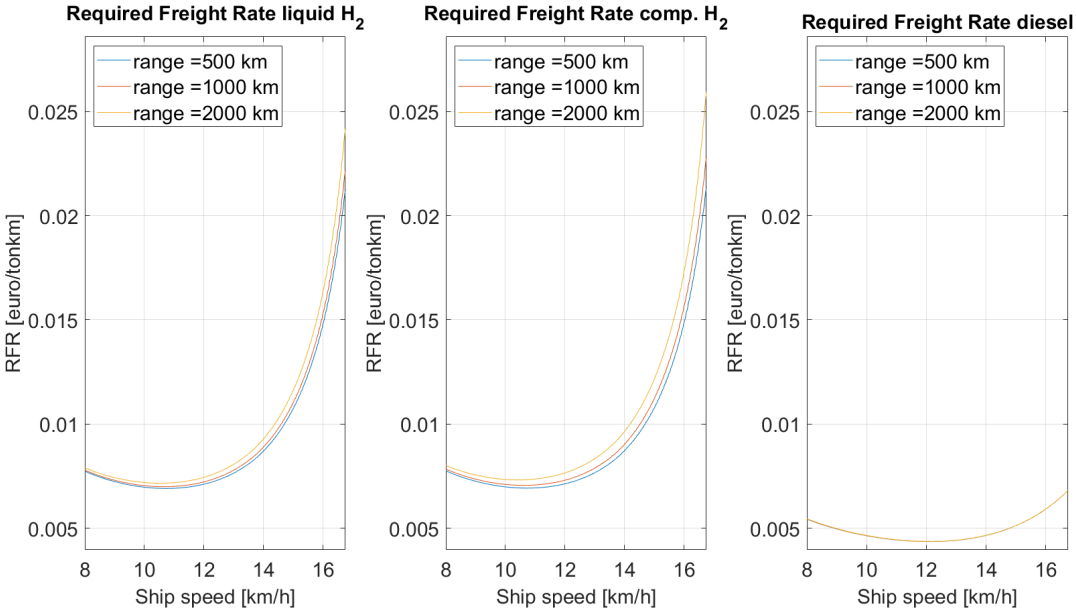

Figure D.5: Container capacity ship 1 versus ship speed

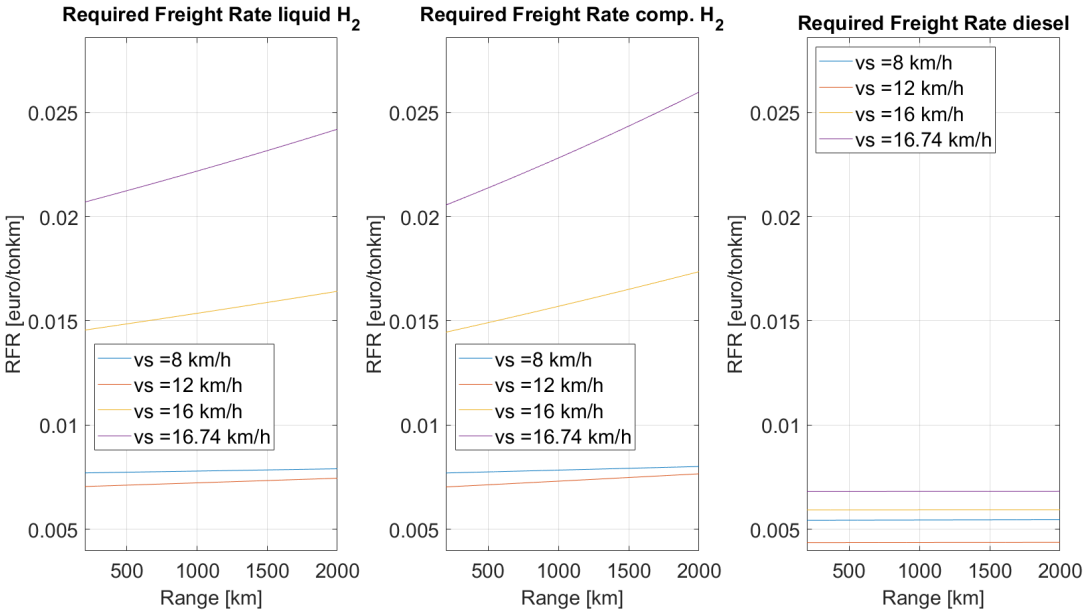

Figure D.6: Container capacity ship 1 versus range

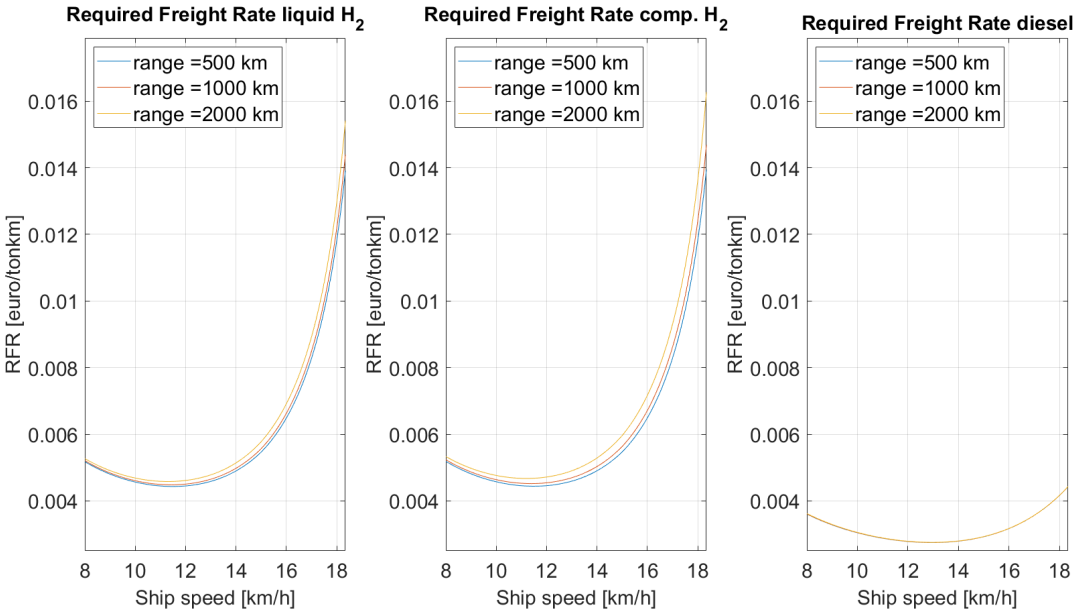

Figure D.7: Container capacity ship 3 versus ship speed

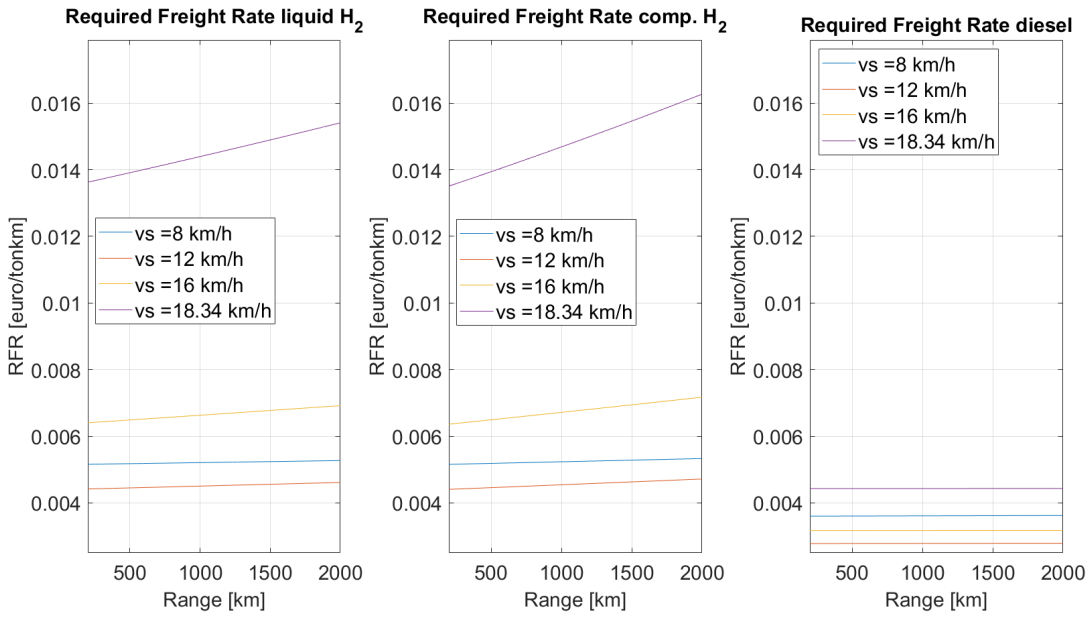

Figure D.8: Container capacity ship 1 versus range

Figures D.9 and D.10 show the relative cost of the different cost components at a range of 1100 km.

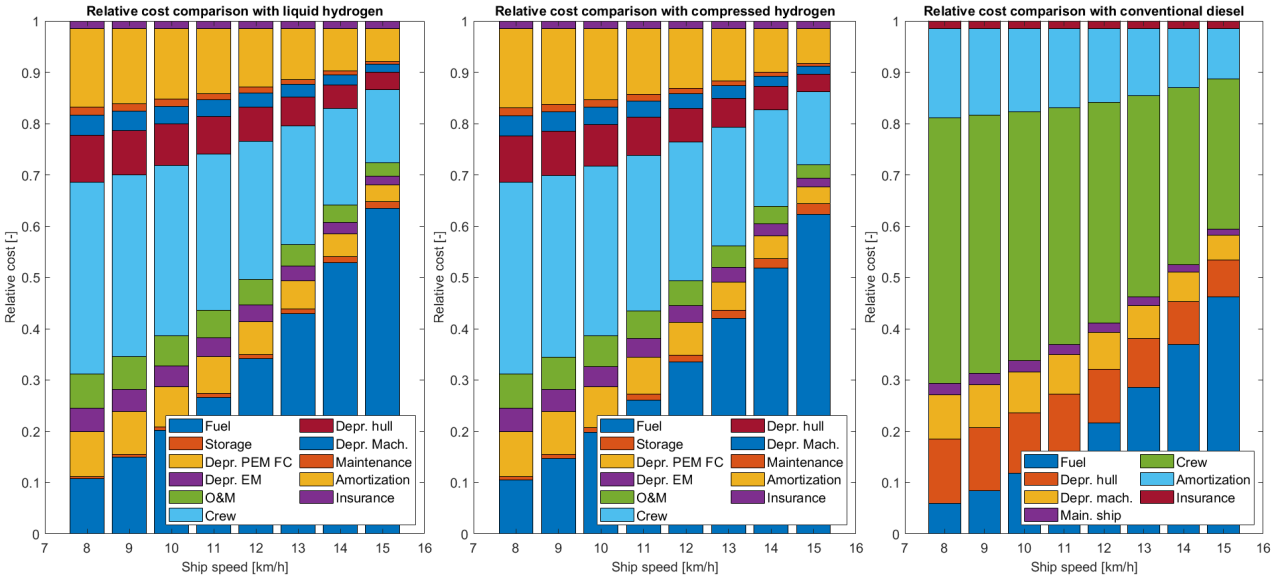

Figure D.9: Relative cost of cost components for ship 1

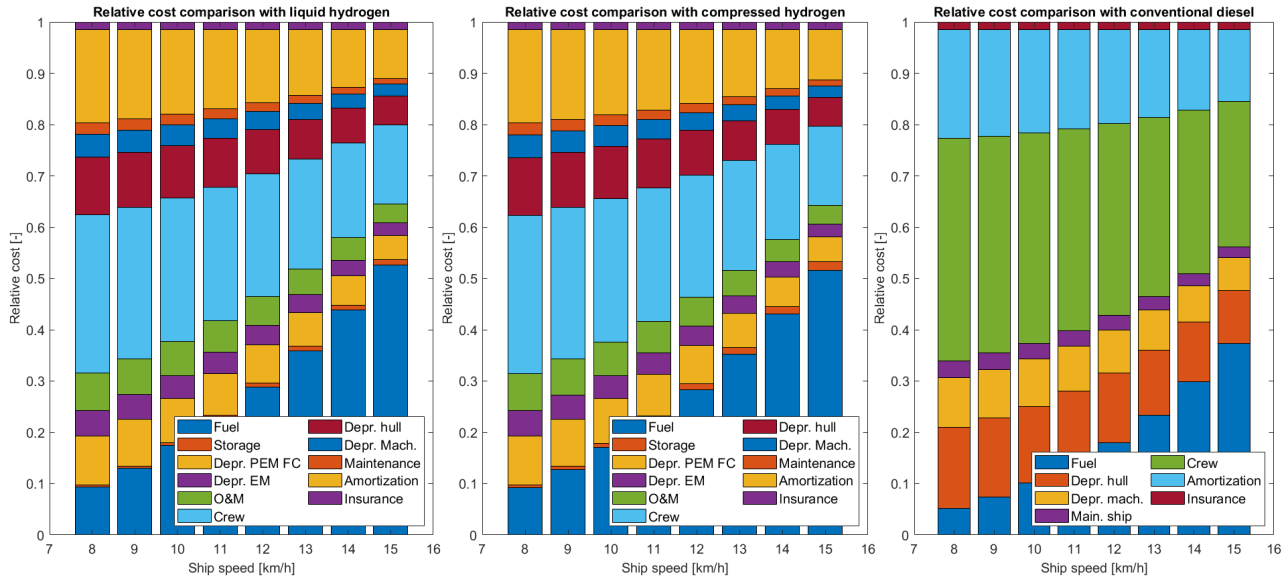

Figure D.10: Relative cost of cost components for ship 3

Figures D.11, D.12, D.13 show the relation of the cargo space capacity versus the ship's range and figures D.14, D.15 and D.16 show the relation of the cargo capacity versus the ship speed.

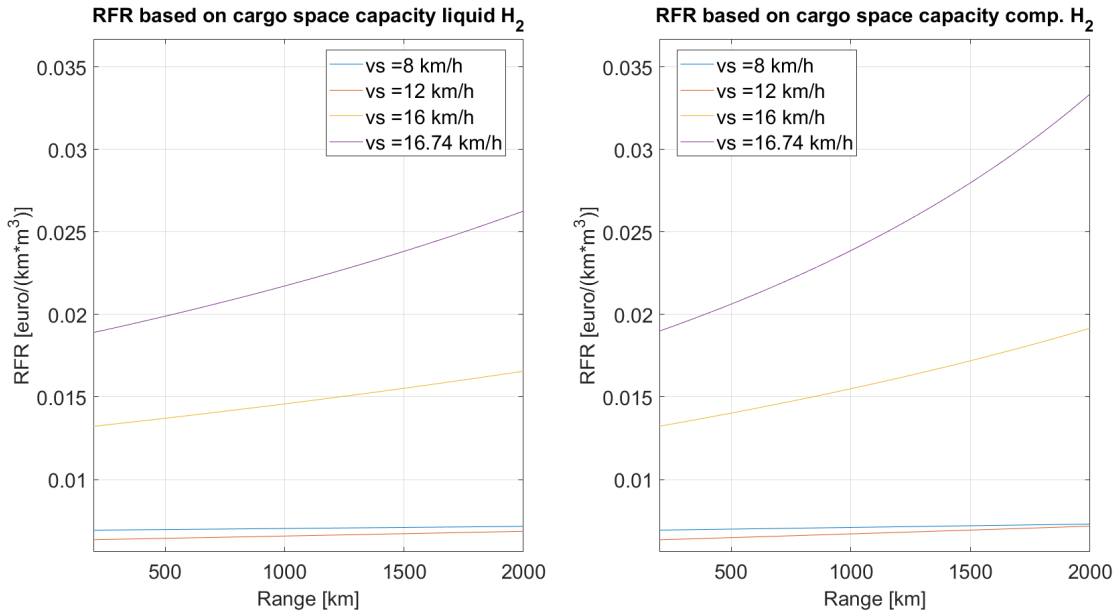

Figure D.11: RFR per cubic meter per km versus range for ship 1

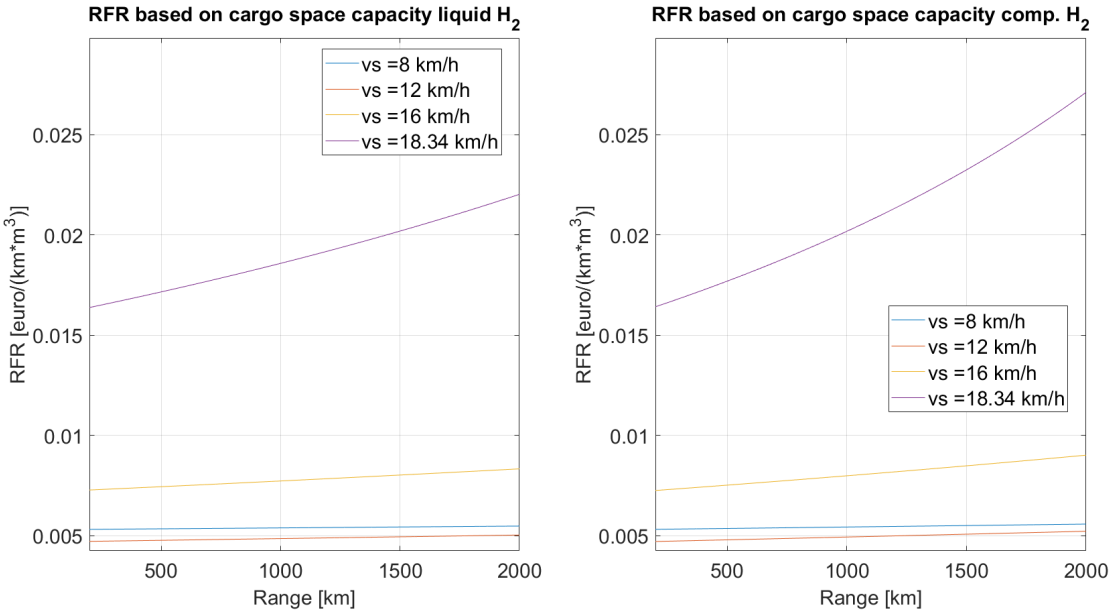

Figure D.12: RFR per cubic meter per km versus range for ship 2

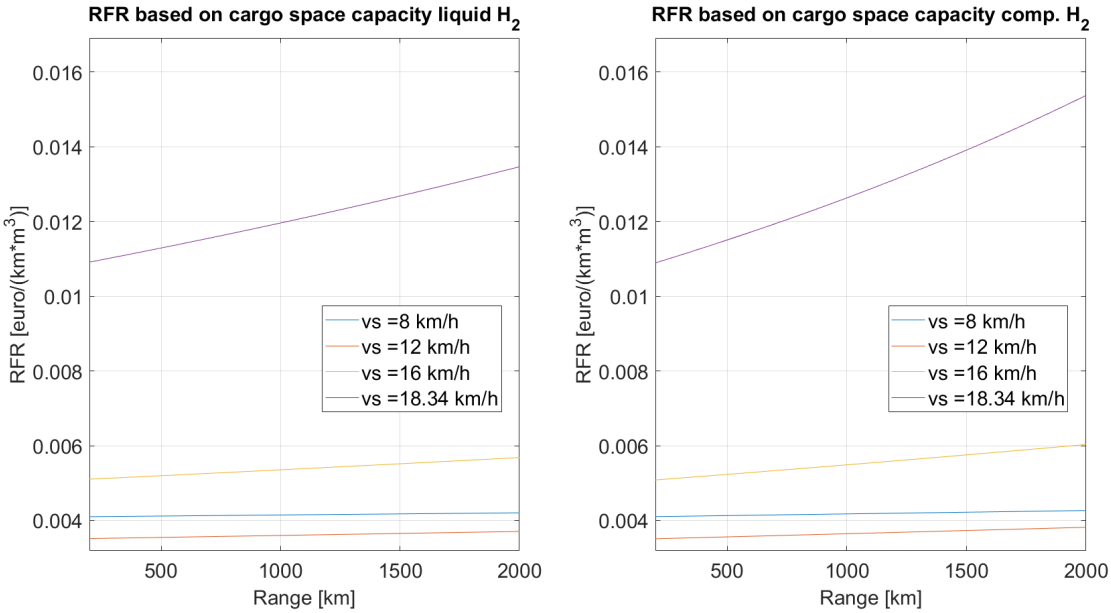

Figure D.13: RFR per cubic meter per km versus range for ship 3

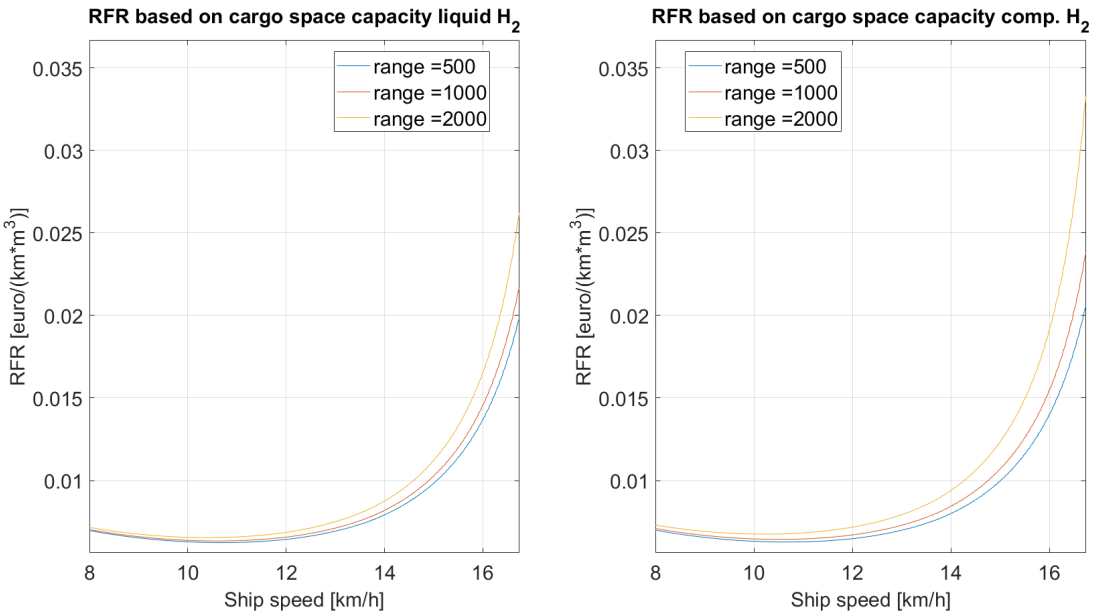

Figure D.14: RFR per cubic meter per km versus ship speed for ship 1

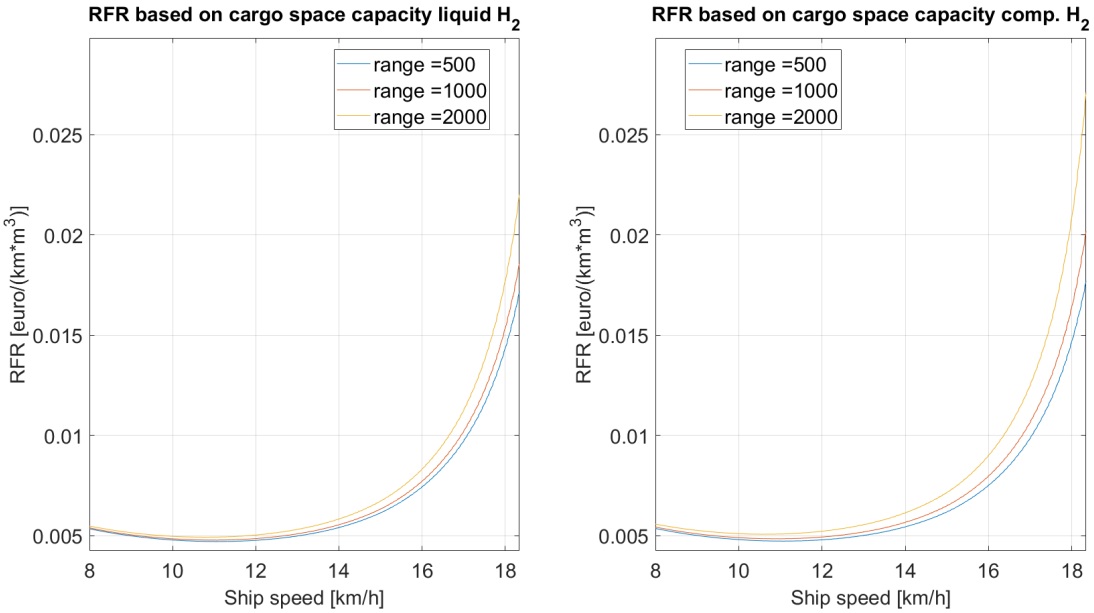

Figure D.15: RFR per cubic meter per km versus ship speed for ship 2

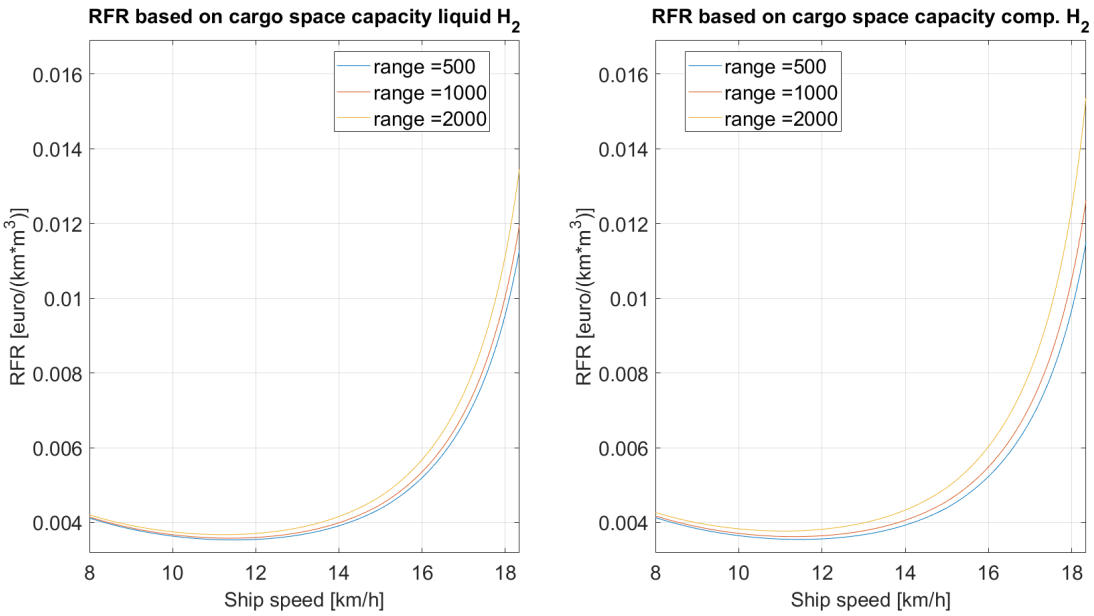

Figure D.16: RFR per cubic meter per km versus ship speed for ship 3

The following figures show more on the RFR of the ships based on container capacity. Figures D.17, D.18 and D.19 show the RFR based on the container capacity as a function of the range of the ships and figures D.20, D.21 and D.22 show the RFR based on the container capacity as a function of the ship speed.

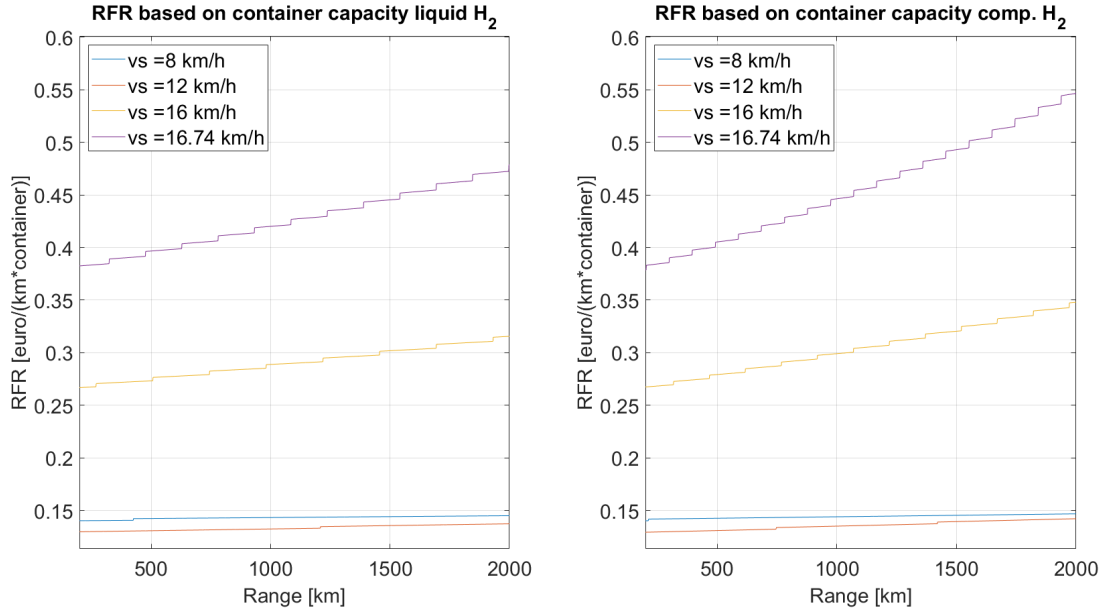

Figure D.17: RFR per container per km versus range for ship 1

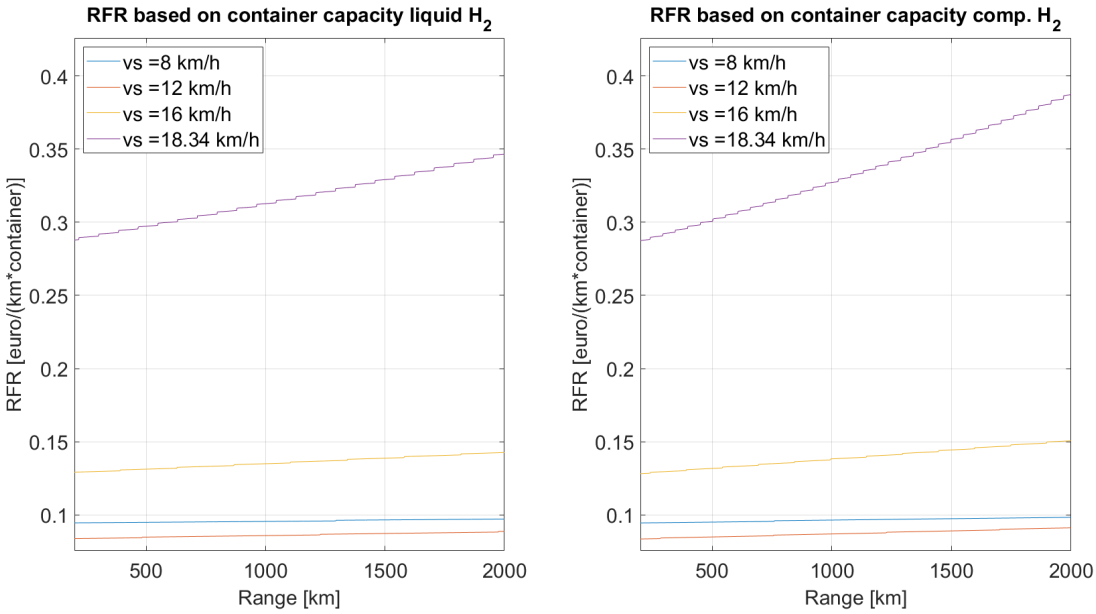

Figure D.18: RFR per container per km versus range for ship 2

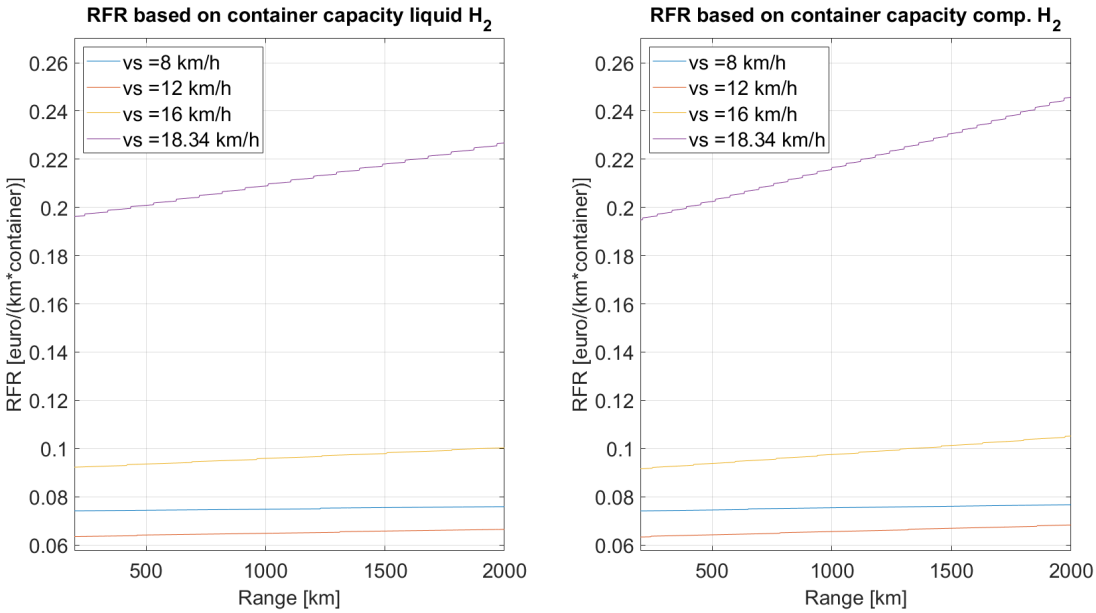

Figure D.19: RFR per container per km versus range for ship 3

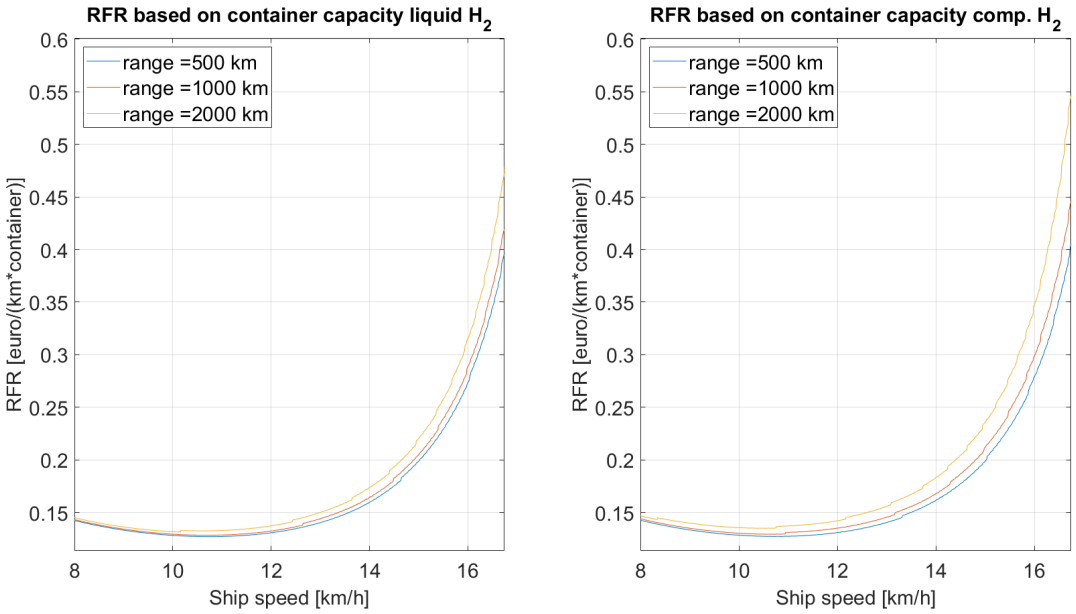

Figure D.20: RFR per container per km versus ship speed for ship 1

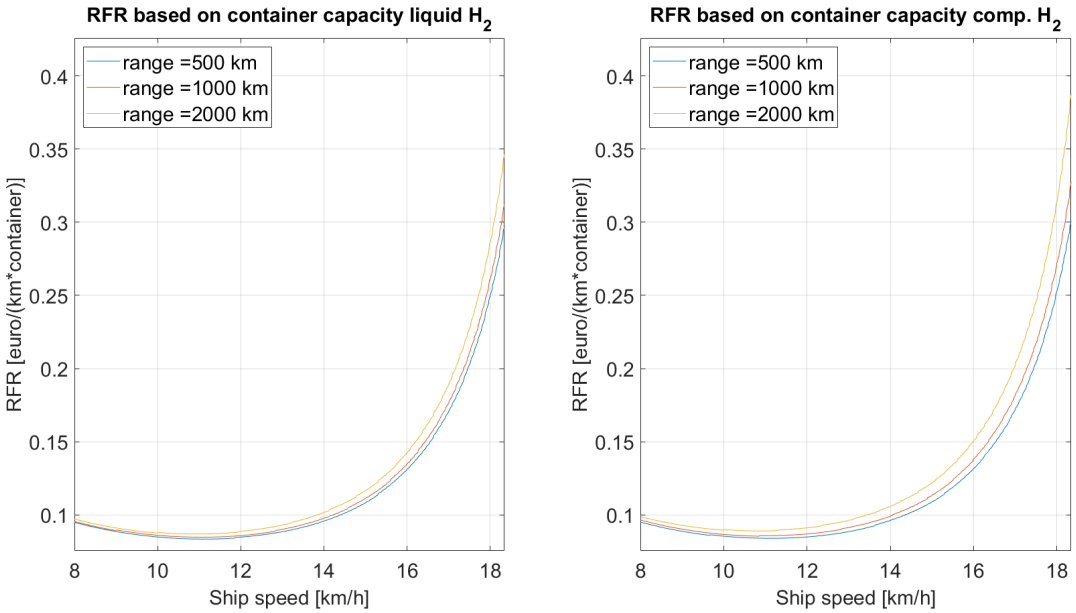

Figure D.21: RFR per container per km versus ship speed for ship 2

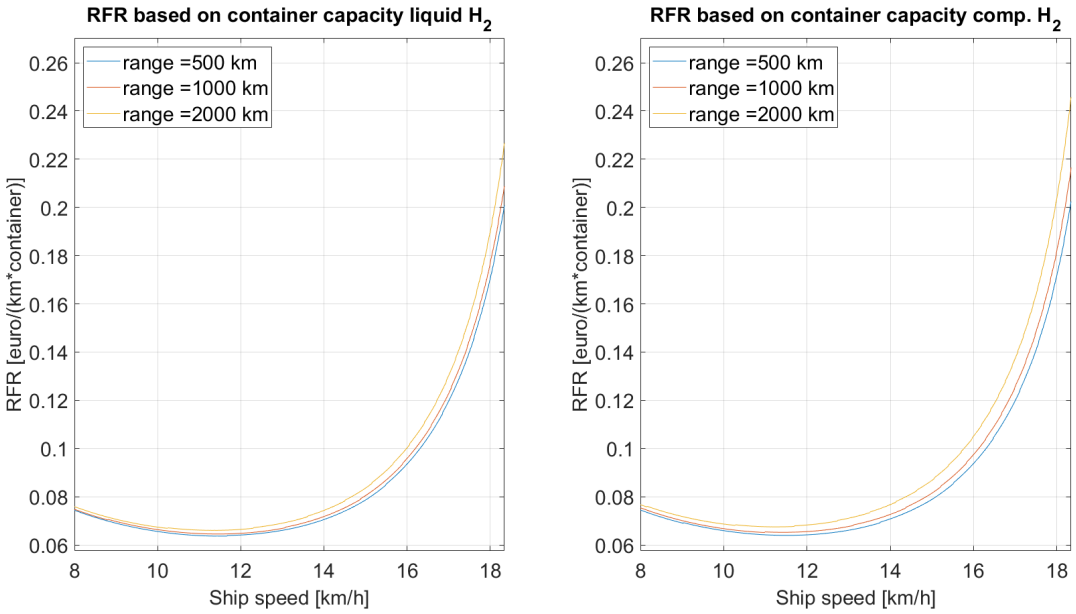

Figure D.22: RFR per container per km versus ship speed for ship 3